STATIC AND DYNAMIC STATE ESTIMATION METHODS FOR ELECTRIC POWER SYSTEMS

by

Christian Kow Gharban, B.Sc. (Eng.), Kumasi

A thesis submitted for the degree of
Doctor of Philosophy in Engineering of
the University of London and for the Diploma
of Membership of the Imperial College

DEPARTMENT OF ELECTRICAL ENGINEERING
IMPERIAL COLLEGE OF SCIENCE AND TECHNOLOGY
UNIVERSITY OF LONDON
LONDON S.W.7 2AZ

March, 1979

ABSTRACT

Title of thesis: STATIC AND DYNAMIC STATE ESTIMATION METHODS FOR ELECTRIC POWER SYSTEMS

Name of author : CHRISTIAN KOW GHARBAN

Since the measurement and telemetering equipment in an electric power system is always subject to random and systematic instrument and phenomenon errors, the raw measurement information is obviously unsatisfactory for assessing the system's behaviour, state and performance. This has led to the approximate determination of the power system's response variables by processing the real-time measurement variables with computer algorithms called state estimators. The type of estimation scheme applicable depends on the assumed system model, linear or non-linear, and the system operating conditions, static or dynamic. Because of the multi-faceted nature of the power system state estimation problem, linear and non-linear static and dynamic estimation techniques are studied in this thesis.

Two basic static estimation approaches have been adopted in this thesis namely, linear and non-linear weighted least squares methods. A fast decoupled estimator (FDE) that improves the characteristics of the non-linear method has been proposed, tested and shown to be computationally as efficient as the linear AEP method.

In the dynamic operating mode, a linear decentralised estimation scheme based on Kalman filtering techniques is described and tested using a two-area load frequency control power system model. In the non-linear case, the invariant imbedding procedure is used to derive the state variables of a non-linear synchronous machine power system model by processing a set of noisy generator measurements.

ACKNOWLEDGMENTS

I am especially indebted to Dr B.J. Cory, B.Sc.(Eng.), D.Sc., A.C.G.I., C.Eng., F.I.E.E., Reader in Electrical Engineering, Imperial College, without whose supervision, constant guidance and encouragement this work could not have been completed.

I also gratefully acknowledge the enormous debt I owe all my colleagues of the Power Systems Laboratory, Imperial College, particularly Messrs A. Indurwa, D. Olguin and E. Vaheedi, for the many useful and stimulating discussions we had about several aspects of this project.

My very special thanks go to the Association of Commonwealth Universities for the award of a Commonwealth Academic Staff Scholarship and to the University of Science and Technology, Kumasi, Ghana, for the financial assistance they provided during the last three months of this work.

Finally I wish to extend my sincere appreciation to my wife, Doris, who for long hours patiently and painstakingly typed the manuscript.

To my wife

my brother

Nyame ntsi ye mmpa aba

And to the blessed memory of my
beloved parents

CONTENTS

LIST OF FIGURES

Figure

LIST OF TABLES

Table

CHAPTER I

INTRODUCTION

The past few decades have witnessed a tremendous and rapid growth in the size and complexity of power systems. The increased complexity has intensified the search for better and sophisticated monitoring and control schemes to effect a more reliable, secure and efficient operation. At present because of the heavy dependence of the society on electrical energy, interruptions of power supply to consumers is almost completely intolerable; as it is also necessary to achieve a certain quality of supply, that is, to maintain system voltage levels and frequency within stipulated statutory limits the operational security requirements of power systems are indeed higher than ever before.

The stringent operational requirements of power systems have led to the design and on-line implementation of data processing and system monitoring schemes to provide reliable data bases that are essential for security and economy related functions. Appropriate control decisions required for reliable and secure operation necessitates prior knowledge of the existing system operating conditions, best described in terms of the system state vector. In general, the state vector of any system is defined as the minimum number of variables (state variables) a knowledge of which ensures a complete description of the system behaviour. Initially, therefore, the prescription of adequate control actions must proceed via the provision of the system state vector. The state vector is best obtained by processing system measurement information with a suite of computer algorithms called state estimators. A power system may be considered to possess two distinct modes of operation, a static operating regime where the system is assumed to remain in a quasi-steady

state over short time periods with sudden transitions in between the intervals, and a dynamical operating state that recognises the fact that because a power system is in reality a conglomeration of several dynamical units (such as synchronous machines) and because of the continously changing load demand patterns, it never really attains a true steady state operating condition. For these reasons, two classes of estimators are readily identifiable, namely static estimators and dynamic estimators.

1.1 Static state estimation

A large number of control centre installations for real-time power system monitoring and control are being undertaken world-wide. There are about 80 such centres in service or planned (50 of these in the Western World) which have as a minimum Automatic Generation Control and System Security Monitoring[1]. Static State Estimation techniques are used in eleven of the control centres with this number continually increasing. Because any control centre which has system security as one of its prime concerns ought to possess an on-line state estimation capability, most new control centre design contracts and specifications include the provision of a state estimation facility. It is anticipated that by the late 1980 about three dozen on-line static state estimators will be operational, mostly in the U.S.

In many present power systems applications, static state estimation is performed by on-line computer algorithms which derive the static state variables as the complex network busbar voltages. The complex busbar voltages at all the network nodes constitute an appropriate set of state variables because once these have been determined both metered and un-metered bulk transmission network variables of interest may be calculated.

A set of imperfect but redundant measurements is taken and optimally fitted to the actual real-time measurements to produce the state vector consistent with the network Kirchoff's law. The measurements can include the bulk electrical transmission network variables, node power injections, branch power flows and voltage magnitudes. Static state estimation may be classified into two main categories:

i. Linear Weighted Least Squares (LWLS) Estimators
Dopazo et al.[2-7] at American Electric Power Service (AEP) derived a linear model for estimation purposes by considering only line power flow measurements. Through a transformation they obtained a simple linear weighted least squares (LWLS) estimator, called the AEP or Line-Only Method, which is extremely fast, efficient and requires modest computer storage space. The disadvantage of this method is that it is approximate and restricts the measurements to branch power flows only.

ii. Generalized Weighted Least Squares (GWLS) Estimators
Schweppe and co-workers[8-13] at MIT did not rely on a transformation to simplify the non-linear estimation problem. Rather they applied a Newton's type technique to solve the estimation problem by accepting all types of system measurements. This yielded a generalized weighted least squares estimator (GWLS) providing a sounder mathematical basis. The method possesses the disadvantage that it is characterised by high dimensionality and rather long solution times.

For on-line implementation, a technique that leads to short execution times and requires small computer core memory is desirable. It is therefore necessary to evaluate the competitiveness of the LWLS and GWLS

techniques, in particular their solution times and core requirements. In an attempt to improve the computational properties of the GWLS method so as to make it as efficient as the AEP method, algorithmic enhancement procedures have been adopted by several subsequent investigators leading to a host of decoupled estimators[14-18]. Because it is essential to assess how reliable these modified estimators are, a Fast Decoupled Estimator, FDE, is proposed and its computational characteristics evaluated through simulation tests in this thesis.

1.2 Dynamic state estimation

Power system disturbances caused by load fluctuations result in changes in tie-line power and system frequency, necessitating some form of load frequency control (LFC). These and other disturbances also lead to a distortion of the operation of synchronous machines, requiring a corrective control strategy. Modern control theory provides design techniques which lead to significant improvements in the control of dynamical systems. The application of these techniques to improve the LFC and the transient stability of power systems has received a great deal of attention in the literature [20,22]. Unfortunately the implementation of these control policies requires the knowledge of the entire system dynamic state which is in general not directly accessible or measurable. The need is therefore felt for the development of dynamic estimators which reconstruct the necessary system states from the system outputs available by direct measurements.

As the power system LFC problem is representable by systems of linear differential equations, linear Kalman filtering techniques may be directly utilised to generate the system state estimates. However, for a multi-area power system the system equations are very highly

dimensional; hence the implementation of a single, large dimensional Kalman filter [23] is unsuitable for on-line purposes. Decentralised dynamical estimation schemes are therefore considered in this thesis for a multi-area LFC power system model.

For transient stability augmentation of power systems, the synchronous machines are normally represented by sets of non-linear state-dependent differential equations. The non-linearity and state dependence led Arumugan [24] to derive a continuous linear observer for the synchronous machine by linearising the machine equations and applying the linear observer theory directly to obtain the synchronous machine states. Takata et al. [25] retained the non-linearity and designed an iterative sequential observer for estimating the machine state variables. Both techniques did not account for the inevitable presence of metering equipment errors. To account for both system non-linearities and measurement noise, the invariant-imbedding technique [26-28] has been used in this thesis to derive estimates of the synchronous machine states from a set of noisy system measurements.

1.3 Contents of thesis

This thesis concerns the development and evaluation of computer based state estimation schemes suitable for the on-line monitoring functions of power systems in both the static and dynamic regions. Chapters II, III and IV cover the area of static state estimation whilst Chapters V and VI consider the dynamical problem.

Chapter II describes the application of linear weighted least squares estimation (LWLS) concepts to derive the AEP or Line-Only static state estimator. Sparsity techniques are employed in the algorithms and the computational characteristics of the method assessed. Simulation results with

four different test systems are reported.

In Chapter III the non-linear static power system state estimation problem is studied using generalized weighted least squares (GWLS) techniques. A fast decoupled estimator (FDE) is derived to enhance the computational properties of the GWLS method. The basic GWLS method and the FDE as well as a P-δ, Q-E estimator are all studied with the same four test systems as in Chapter II. It is shown that the FDE is much faster than the GWLS estimator.

Chapter IV addresses the problem of detection and identification of grossly erroneous input measurement information in static state estimation. Statistically based detection and identification methods are described and used in all the tests performed with the LWLS, GWLS and FDE state estimators. It is shown that the FDE is reliable in detection and identification schemes, despite the approximations made in its derivation.

Chapter V deals with estimation of states of a LFC power system model. It is shown that for a multi-area system a completely decentralised estimator produces degenerate state estimates, unless each decentralised estimator is provided with supplementary signals from other areas. The decentralisation leads to low storage requirements and minimal information exchange between the areas.

In Chapter VI the invariant imbedding technique is adopted to derive a non linear dynamical state estimator for a single machine infinite busbar power system. Simulation results confirm the viability of the method, which recognises system non-linearities as well as instrumentation noise.

Chapter VII presents the discussions and conclusions reached and offers directions for future research. The principal contributions offered by this thesis are believed to be:-

i. A detailed analysis of the linear and non-linear weighted least squares techniques and their direct application to static power systems state estimation.

ii. The development and testing of a Fast Decoupled Estimator derived from the concepts of a conventional fast decoupled load flow routine.

iii. The evaluation of the computational characteristics of the AEP, GWLS, (P-δ, Q-E) and FDE state estimators.

iv. The design and testing of a decentralised dynamical estimation scheme for a multi-area power system load frequency control model.

v. The application of the invariant imbedding technique to estimate the states of a non-linear single machine infinite busbar power system.

CHAPTER II

APPLICATION OF LINEAR WEIGHTED LEAST SQUARES (LWLS) TO STATIC POWER SYSTEMS STATE ESTIMATION

2.1 Introduction

Conceptually static power system state estimation methods are closely related to conventional load flow computations but performed with real-time data. The objective of estimation is to derive an approximation to the network voltage profile by processing a redundant but noisy set of power system measurements. The problem is inherently non-linear and various solution approaches may hence be adopted[29]. When the LWLS technique is used, a method known as the AEP or Line-Only (LO) algorithm (first proposed by Messrs Dopazo et al[3,4,30-33])results. The method's popularity stems from its simplicity which is obtained by restricting the measurements to only complex branch power flows on a network tree of the power system with at least one reference voltage magnitude measurement. Measurement redundancy may be increased by metering co-tree branch power flows as well. The full-fledged method is then realised through an algebraic non-linear transformation that converts the non-linear problem into a linear one and leads ultimately to the solution of basic network equations. Naturally it has been criticised for rejecting other types of measurement variables such as node power injections [40,41]. Subsequent investigators [30-34] have successfully modified it to handle other types of measurements although this modification has degraded the basic attractive properties of the original version.

Since the AEP method is computationally the fastest available technique with the least computer storage requirements, it was chosen

for general investigation with the view of serving as a reference for comparing more optimal but slow, high storage techniques like the GWLS approach and its associated approximate forms of "Constant-Gain", "P-δ, Q-E Decoupled Estimator" and "Fast-Decoupled-Estimator". In particular the reliability of the estimates, the speed of the estimation technique and the numerical solution technique used are all described and investigated.

2.2 Description of the state and measurement vectors

2.2.1 Static state vector $\underline{x}$

The n-dimensional static state vector $\underline{x}$ of an electric power system is defined as the vector whose components are the complex voltages of all the network nodes, because once these are known all other bulk transmission variables of interest such as complex power injections and complex branch power flows are easily computable. For an N-node network where the N-th node is prescribed as the reference, $\underline{x}$ is described as follows:

Let $V_i \triangleq e_i + jf_i$

$$\triangleq E_i \angle \delta_i \qquad i = 1,2,\ldots,N$$

denote the complex busbar voltages at all the nodes. Then:

$$\underline{x}^T = (e_1, e_2, \ldots, e_N, f_1, f_2, \ldots, f_{N-1})$$

$$= (E_1, E_2, \ldots, E_N, \delta_1, \delta_2, \ldots \delta_{N-1})$$

$$= (x_1, x_2, \ldots, x_n)$$

where $n = 2N-1$

2.2.2 Measurement vector $\underline{z}_m$ and measurement errors $\underline{v}$

An exact description of the current operating state of a power system is normally extracted from measurement information derived from the

system. Since it is practically impossible to directly access and measure the state vector $\underline{x}$, its value is inferred from the noise-corrupted system observation vector $\underline{z}_m$. $\underline{Z}_m$ is generally a non-linear vector function of $\underline{x}$.

$$\underline{z}_m = \underline{h}(\underline{x}) + \underline{v} \qquad (2.2.1)$$

where:

$\underline{h}(\underline{x})$ is a deterministic vector that relates each measured variable and the true-but-unknown state $\underline{x}$, whilst $\underline{v}$ is a stochastic disturbance noise vector that accounts for metering and telemetering errors. The dimension m of $\underline{z}_m$ depends on the type and number of variables that are telemetered to the on-line computer. In the most general case, $\underline{z}_m$ is composed as follows:

i. Complex node power injection measurements at all nodes

$P_i + jQ_i \qquad i = 1,2,\ldots,N$

ii. Complex line power flow measurements at all ends of transmission lines and transformers

$S_j = P_{ik} + jQ_{ik} \quad i,k = 1,2,\ldots,N; \quad j = 1,2,\ldots,2L$

$i \neq k$

where L = total number of lines in the network

iii. Voltage magnitude measurements at all nodes

$E_i = (e_i^2 + f_i^2)^{\frac{1}{2}} \quad i = 1,2,\ldots,N$

$\underline{Z}_m$ may therefore be described symbolically by:

$\underline{z}_m = (\underline{P}_i, \underline{Q}_i, \underline{P}_{ik}, \underline{Q}_{ik}, \underline{E}_i)$

where the components are also symbolic vectors that describe the type of measured variables. The maximum dimension of $\underline{z}_m$ is thus $3N+4L$. With the transmission lines modelled by linear, lumped RLC π-sections as in Fig. 2.1 and the parameters $z_{ik} = R_{ik} + jX_{ik}, y_{ik} = jYS_{ik}$

all assumed known, the equations for $\underline{h}(\underline{x})$ are:

$$P_i = e_i \sum_{k=1}^{N} (e_k G_{ik} - f_k B_{ik}) + f_i \sum_{k=1}^{N} (f_k G_{ik} + e_k B_{ik})$$

$$Q_i = f_i \sum_{k=1}^{N} (e_k G_{ik} - f_k B_{ik}) - e_i \sum_{k=1}^{N} (f_k G_{ik} + e_k B_{ik})$$

$$P_{ik} = -G_{ik}\left[e_i(e_i - e_k) + f_i(f_i - f_k)\right] + B_{ik}\left[e_i(f_i - f_k) - f_i(e_i - e_k)\right]$$

$$Q_{ik} = B_{ik}\left[e_i(e_i - e_k) + f_i(f_i - f_k)\right] + G_{ik}\left[e_i(f_i - f_k) - f_i(e_i - e_k)\right] - (e_i^2 + f_i^2) YS_{ik}$$

$$E_i = (e_i^2 + f_i^2)^{\frac{1}{2}}$$

where $G_{ik} + jB_{ik}$ is the i-k^{th} element of the network bus-admittance matrix.

The measurement errors $\underline{v}$ evolve from several independent but completely random processes; by virtue of the Central Limit Theorem of statistics[36,37] it is therefore reasonable to postulate a zero mean Gaussian distribution for $\underline{v}$. If the errors $\underline{v}$ are further assumed to be uncorrelated in pairs with an (mxm)-dimensional diagonal covariance matrix R, then:

$$E(\underline{v}) = \underline{0} \qquad (2.2.2)$$

$$\mathrm{Cov}(\underline{v}) \triangleq E(\underline{v}\,\underline{v}^T) = R \qquad (2.2.3)$$

$$\underline{v} \sim N(\underline{0}, R)$$

$$\sigma_{vj}^2 = R_{jj} \qquad j = 1,2,\ldots,m \qquad (2.2.4)$$

where σ_{vj}^2 is the variance of the j-th measurement error and reflects its precision and accuracy.

2.3 The AEP or Line-Only (LO) algorithm

2.3.1 Review of the method

The method is based on determining the least-squares values of the complex busbar voltages $\underline{x}$, that minimise the quadratic performance index $J(\underline{x})$ [29] given by:

$$J(\underline{x}) = (\underline{S}_m - \underline{S}_t)^T R^{-1} (\underline{S}_m - \underline{S}_t)^* \qquad (2.3.1)$$

where:

$\underline{S}_m$ is the vector of complex branch power flow measurements

$\underline{S}_t$ is the vector of the true-but-unknown value of $\underline{S}_m$

R is the measurement error covariance matrix

subject to the observation equation constraint

$$\underline{S}_m = \underline{S}_t + \underline{V}$$

The mathematical expressions for the complex branch power flows from node i to node k evaluated at i are:

$$S_{t,j} = S_{t,ik} = x_i \frac{(x_i - x_k)^*}{z_j^*} + |x_i|^2 y_j \qquad (2.3.2)$$

$$S_{m,j} = S_{m,ik} = x_i \frac{(x_i - x_k)^*}{z_j^*} + |x_i|^2 y_j + v_j \qquad (2.3.3)$$

where v_j is the error associated with the measurement $S_{m,j}$. Since these expressions are complex and non-linear in $\underline{x}$, $J(\underline{x})$ cannot be minimised directly. The AEP or LO technique avoids this difficulty by transforming each $S_{m,j}$ into an equivalent measured longitudinal line element voltage $V_{m,j}$ (see Fig. 2.1). From equation (2.3.3) the true-but-unknown branch voltage $V_{t,j}$ is:

$$V_{t,j} \triangleq x_i - x_k = z_j \left(\frac{S_{m,j}^*}{x_i^*} - y_j x_i \right) - \frac{z_j}{x_i^*} v_j \qquad (2.3.4)$$

However, because $S_{m,j}$ is the actual measured variable, the first

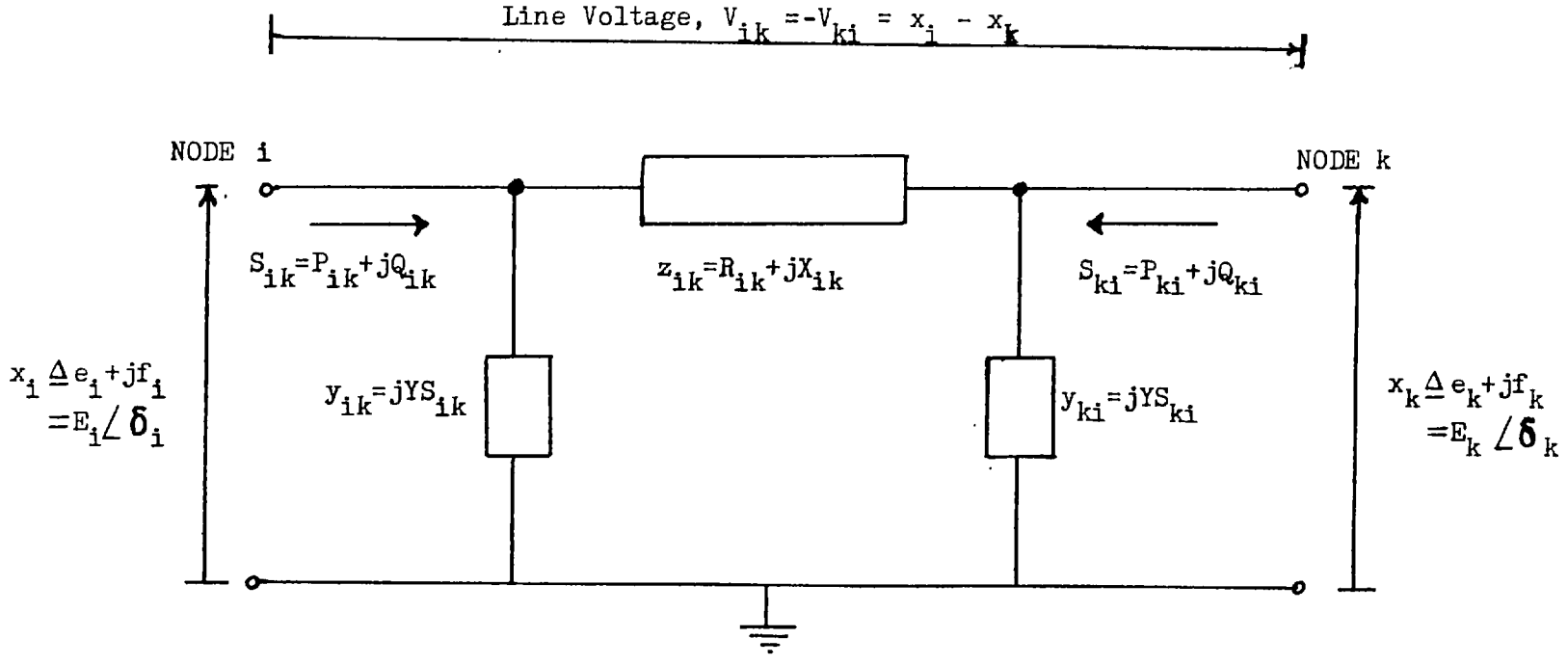

FIGURE 2.1: LINE MODEL, π-SECTION NETWORK ELEMENT

expression on the right-hand-side of equation (2.3.4) is equivalent to a noise-corrupted branch voltage measurement $V_{m,j}$. Hence:

$$V_{m,j} \triangleq z_j \left(\frac{S^*_{m,j}}{x_i^*} - y_j x_i \right) = V_{t,j} + \frac{z_j}{x_i^*} v_j \qquad (2.3.5)$$

The derived measured branch voltage is thus the sum of its true value and an associated transformed measurement error $\varepsilon_j = \frac{z_j}{x_i^*} v_j$.

Additionally, the definition of $V_{t,j}$ leads to the linear vector relationship:

$$\underline{V}_t = B\underline{x} \qquad (2.3.6)$$

where B is the measured line-node-incidence matrix which has exactly two non-zero elements per row [4,40]. The final measurement equation is thus:

$$\underline{V}_m = \underline{V}_t + \underline{\varepsilon} \qquad (2.3.7)$$

The transformed errors $\underline{\varepsilon}$ have the statistics:

$$E(\varepsilon_j) = \frac{z_j}{x_i^*} E(v_j) = 0 \qquad (2.3.8)$$

$$\text{Var}(\varepsilon_j) \triangleq E(\varepsilon_j \varepsilon_j^*) = \frac{|z_j|^2}{|x_i|^2} E(v_j v_j^*)$$

$$= \frac{|z_j|^2}{|x_i|^2} \sigma^2_{vj} \qquad (2.3.9)$$

A similarly transformed LWLS objective function may now be defined for the linear observation equation (2.3.7)

$$J(\underline{x}) = (\underline{V}_m - \underline{V}_t)^T D (\underline{V}_m - \underline{V}_t)^* \qquad (2.3.20)$$

where D is now the inverse of the (mxm)-dimensional diagonal covariance matrix of $\underline{\varepsilon}$ and:

$$D^{-1}_{jj} = \frac{|z_j|^2}{|x_i|^2} \sigma^2_{vj} \qquad j = 1,2,\ldots,m \qquad (2.3.11)$$

To determine D^{-1}, the values of x_i ought to be known. The best approximation is x_i = 1.0 pu (nominal); using this value of x_i increases the measurement uncertainty $\underline{\varepsilon}$ as well as its covariance. On this account the LO method does not possess statistically optimal properties.

The LWLS technique (Appendix A) may now be applied in a direct fashion to yield the linear estimation equation:

$$(B^TDB)\underline{x} = B^TD\underline{V}_m \qquad (2.3.12)$$

Because the matrix B^TDB is singular when only line power flow measurements are considered, at least one voltage magnitude measurement must be taken at the reference bus, giving $\underline{V}_t$ in partitioned form as:

$$\underline{V}_t = (C\,\vdots\,A)\begin{pmatrix} x_{ref} \\ \cdots \\ \underline{x} \end{pmatrix} = Cx_{ref} + A\underline{x} \qquad (2.3.13)$$

where x_{ref} is the reference voltage magnitude and $\underline{x}$ is now a reduced state vector of dimension n-1. The resultant estimation equation is then:

$$(A^TDA)\underline{x} = A^TD(\underline{V}_m - Cx_{ref}) \qquad (2.3.14)$$

As $\underline{V}_m$ is actually state-dependent (equation 2.3.5), equation (2.3.14) only generates approximations for $\underline{x}$ iteratively. The converged solution $\hat{\underline{x}}_{i+1}$ of the iterative scheme:

$$(A^TDA)\hat{\underline{x}}_{i+1} = \left[A^TD(\underline{V}_m - Cx_{ref})\right]_i \qquad (2.3.15)$$

is then the complex busbar voltage state estimate $\hat{\underline{x}}$, where i denotes the i-th iteration stage.

2.3.2 Properties of the Gain-matrix A^TDA

In consonance with LWLS estimation theory, matrix $G = A^TDA$ is called the Gain-matrix. G has precisely the same topology and pattern of non-zero elements as the corresponding network bus admittance matrix. Because D is almost constant as it depends on $|x_i|^2$ (at x_i = 1.0 pu) G is consequently also constant, iteratively invariant and real. Solutions for the real and imaginary components of $\underline{x}$ are therefore completely decoupled. Very simple rules may hence be employed to construct G directly [30] without performing the obviously time consuming matrix operations its definition suggests. Since G is almost fixed for a given metering configuration, the AEP technique is intrinsically a "Constant-Gain" algorithm [29]. The following attractive properties of G are easily identifiable:

i. Diagonally dominant and positive definite

ii. Real and iteratively invariant

iii. Symmetric and extremely sparse

These properties make the solution of equation (2.3.15) particularly amenable to sparse matrix oriented direct methods [42-45]. Of the three basic direct methods for solving systems of linear equations [42-45] namely, Triangular Factorisation, Product Form of Inverse and Bi-Factorisation, the Bi-Factorisation technique [44] is best for coefficient matrices that possess the enumerated properties of G. This method was thus adopted to solve the LO estimation problem. The algorithmic iterative solution procedure is shown in the flow chart of Fig. 2.2 and described as follows:

1. Set iteration count, i=0

2. Initialise all voltages, $\underline{\hat{x}}_i$ = 1.0+j0.0 pu; derive D and then

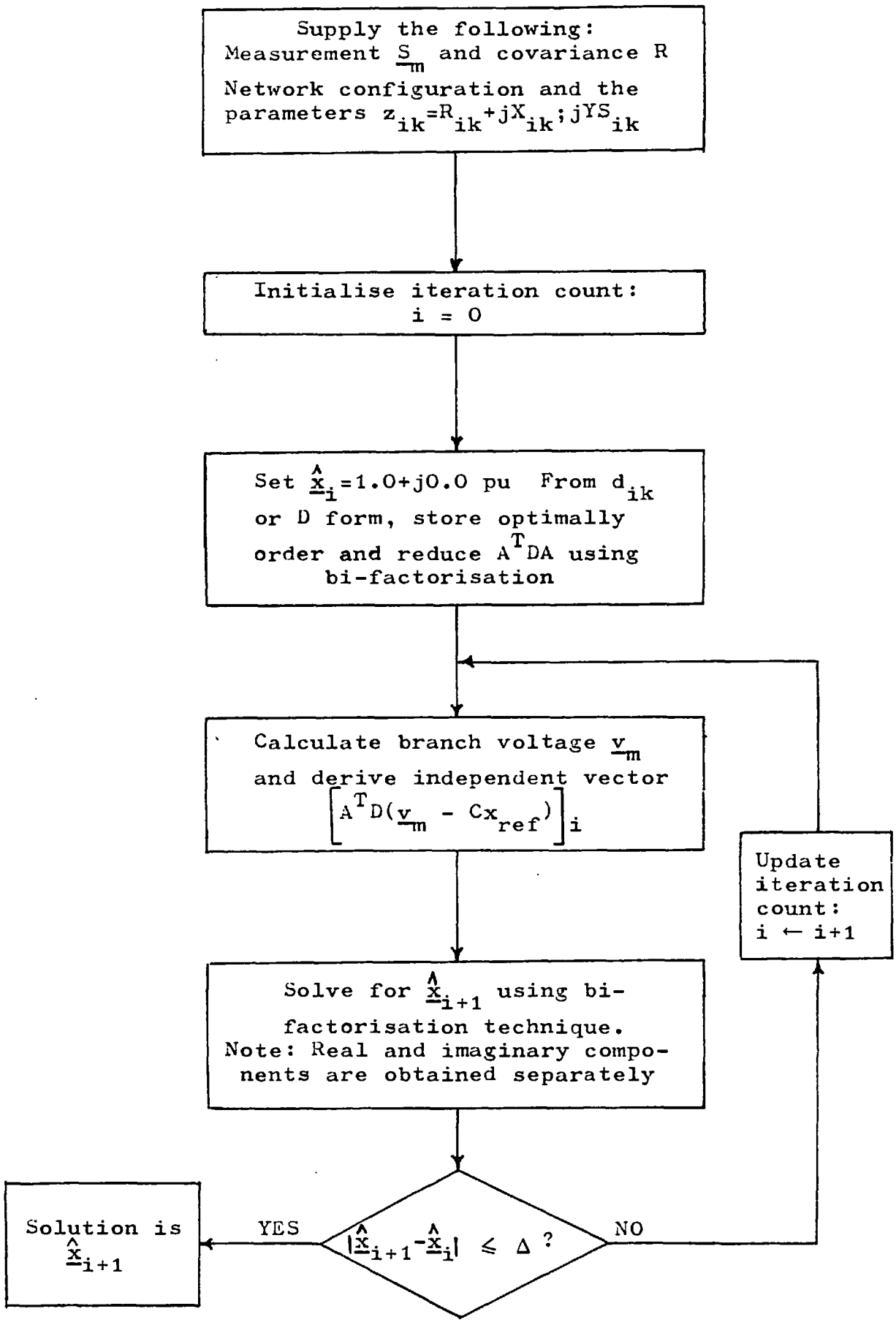

FIGURE 2.2: SOLUTION FLOW CHART OF AEP METHOD

automatically generate $G = A^T DA$ in sparse form.

3. Optimally order G and reduce it by bi-factorisation
4. Derive the equivalent branch voltages $\underline{V}_m$ with the current value of $\underline{\hat{x}}_i$ and then form the independent right-hand-side vector $\left[A^T D(\underline{V}_m - C\underline{x}_{ref})\right]_i$
5. Solve for $\underline{\hat{x}}_{i+1}$ in decoupled form from equation (2.3.15)
6. Check for convergence, that is $|\underline{\hat{x}}_{i+1} - \underline{\hat{x}}_i| \leq \Delta$ for all the components of $\underline{x}$. A rectangular voltage tolerance $\Delta = 5.0 \times 10^{-6}$ is usually sufficient [34].
7. If converged, output $\underline{\hat{x}} = \underline{\hat{x}}_{i+1}$; otherwise advance iteration count by 1 i.e. i = i+1 and return to step 4.

2.3.3 Interpretation of estimates

It is extremely essential to check the reliability of the state estimates $\underline{\hat{x}}$. To establish this reliability is to perform statistical tests of hypothesis [37-39, 46] to confirm whether or not the residuals $\underline{r} = \underline{V}_m - \underline{\hat{V}}$ and $\underline{R} = \underline{S}_m - \underline{\hat{S}}$ are actually attributable to normal errors of observation drawn from the postulated Gaussian probability distribution for $\underline{\varepsilon}$ and $\underline{V}$ respectively. In any LWLS estimation scheme, the best statistical test index for the preliminary hypothesis test is the post-estimation performance index $J(\underline{\hat{x}})$. Under the distributional assumptions for $\underline{V}$, $J(\underline{\hat{x}})$ has the following properties (Appendix A, Table A.1).

$E\left[J(\underline{\hat{x}})\right] = df(=m-n)$

$J(\underline{\hat{x}})$ is chi-square distributed

$J(\underline{\hat{x}})$ must therefore obey the probability statement:

$$PR\left[J(\underline{\hat{x}}) \leq \chi^2_{df,\alpha}\right] = \alpha$$

where $\chi^2_{df,\alpha}$ is the value of the chi-square distribution at df degrees of freedom and a probability of confidence equal to α. Should $J(\hat{\underline{x}})$ be unusually greater than its tabulated chi-square threshold value- $\chi^2_{df,\alpha}$ (obtained from statistical distribution tables [36]) the estimates $\hat{\underline{x}}$ are deemed unreliable. This procedure for ascertaining the reliability of $\hat{\underline{x}}$ is known as DETECTION [47-49]. The $J(\hat{\underline{x}})$-test also illustrates the crucial part played by redundancy in enhancing the effectiveness of the test. For example, at zero redundancy df = m-n = 0 and $J(\hat{\underline{x}})$ is identically zero, rendering it ineffective as a hypothesis test statistic.

Once $\hat{\underline{x}}$ has passed the detection test, the a-posteriori covariance of the residuals $\underline{x}-\hat{\underline{x}}$, $\underline{V}_t-\hat{\underline{V}}$, $\underline{V}_m-\hat{\underline{V}}$, $\underline{S}_t-\hat{\underline{S}}$, $\underline{S}_m-\hat{\underline{S}}$ may all be calculated to give an intuitive feeling for the degree to which the various variables have been well determined. The statistics of these residuals may be shown to be [49] (Appendix A).

$$E(\underline{x}-\hat{\underline{x}}) = \underline{0}$$

$$\mathrm{Cov}(\underline{x}-\hat{\underline{x}}) = \Sigma_x^A = \left(A^T D A\right)^{-1}$$

$$E(\underline{V}_t-\hat{\underline{V}}) = \underline{0}$$

$$\mathrm{Cov}(\underline{V}_t-\hat{\underline{V}}) = \Sigma_v^A = A \Sigma_x^A A^T$$

$$E(\underline{V}_m-\hat{\underline{V}}) = \underline{0}$$

$$\mathrm{Cov}(\underline{V}_m-\hat{\underline{V}}) = \Sigma_r^A = D^{-1} - A \Sigma_x^A A^T$$

$$E(\underline{S}_t-\hat{\underline{S}}) = \underline{0}$$

$$\mathrm{Cov}(\underline{S}_t-\hat{\underline{S}}) = \Sigma_s^A = \left[(\Sigma_v^A)_{jj} \frac{|x_i|^2}{|z_j|^2} \right] \qquad j = 1,2,\ldots,m$$

$$E(\underline{S}_m-\hat{\underline{S}}) = \underline{0}$$

$$\mathrm{Cov}(\underline{S}_m-\hat{\underline{S}}) = \Sigma_R^A = \left[(\Sigma_r^A)_{jj} \frac{|x_i|^2}{|z_j|^2} \right] \qquad j = 1,2,\ldots,m$$

Given these statistical properties the limits $CL_1(\cdot)$ and $CL_2(\cdot)$, called CONFIDENCE INTERVALS [36,46], within which the true-but-unknown values of the variables are likely to be found at a probability of confidence α may be constructed. The normalised unit random variates f_i, g_j and h_j are all student's t-distributed because they are normalised on their a-posteriori variances, where:

$$f_i = \frac{x_i - \hat{x}_i}{\sqrt{\Sigma^A_{x_{ii}}}} \quad ; \quad g_j = \frac{V_{tj} - \hat{V}_j}{\sqrt{\Sigma^A_{v_{jj}}}} \quad ; \quad h_j = \frac{S_{tj} - \hat{S}_j}{\sqrt{\Sigma^A_{s_{jj}}}}$$

But f_i, g_j, h_j all satisfy the probability law:

$$Pr(-t_{df,\frac{1+\alpha}{2}} < f_i \text{ or } g_j \text{ or } h_j < t_{df,\frac{1+\alpha}{2}}) = \alpha$$

where $t_{df,\frac{1+\alpha}{2}}$ is the tabulated value of the t-distribution at df degrees of freedom and $\frac{1+\alpha}{2}$ probability of confidence. The substitution of f_i into this probability law therefore yields:

$$Pr\left(\hat{x}_i - t_{df,\frac{1+\alpha}{2}} \sqrt{\Sigma^A_{x_{ii}}} < x_i < \hat{x}_i + t_{df,\frac{1+\alpha}{2}} \sqrt{\Sigma^A_{x_{ii}}}\right) = \alpha$$

The lower and upper inequality limits define an α % confidence interval for x_i, as:

$$CL_1(x_i) = \hat{x}_i - t_{df,\frac{1+\alpha}{2}} \sqrt{\Sigma^A_{x_{ii}}}$$

$$CL_2(x_i) = \hat{x}_i + t_{df,\frac{1+\alpha}{2}} \sqrt{\Sigma^A_{x_{ii}}}$$

In a similar way, the limits for V_{tj} and S_{tj} may be constructed.

2.4 Off-Line computer simulations of AEP state estimator and discussion of results

For a preliminary evaluation of the AEP technique, its feasibility and statistical properties were investigated by implementing the general simulation procedure depicted in the flow chart of Fig. 2.3. Four basic standard test networks were employed for the algorithmic tests, namely:

1. 5-NODES, 7-LINES system [50]
2. 10-NODES, 13-LINES system [51]
3. 14-NODES, 20-LINES system [51]
4. 23-NODES, 30-LINES system [52]

The parameters as well as the true load flow conditions of these test systems are detailed in Tables A.3.1 to A. 3.8 of Appendix A . These algorithmic tests were conducted in order to investigate the performance of the AEP State Estimator under various conditions. For each of the test systems, four different meter location configurations (Figs. 2.5 to 2.19) yielding various degrees of measurement redundancy were used. The P,Q meters are represented by black spots (•) located at the end of the line where the complex branch flow power measurement is taken.

Initially the network voltage profile, $\underline{x} = \underline{e}+j\underline{f}$, and the load flow conditions, $\underline{Z}_{ik} = \underline{P}_{ik}+j\underline{Q}_{ik}$, obtained from a conventional Newton-Raphson Load-Flow program [51,52] for each network were generated and assumed to be the true values. To simulate the real-time complex branch flow power measurements, the complex measurement errors, $\underline{V}_{ik} = \underline{V}_{P_{ik}} + j\,\underline{V}_{Q_{ik}}$ were derived from a pseudo-gaussian random number generator assuming that the error components, $\underline{V}_{P_{ik}}$ and $\underline{V}_{Q_{ik}}$ due to real power flow $\underline{P}_{ik}$ and reactive power flow $\underline{Q}_{ik}$ both have known measurement error standard deviations equal to 2% of their assumed true load flow values. That is,

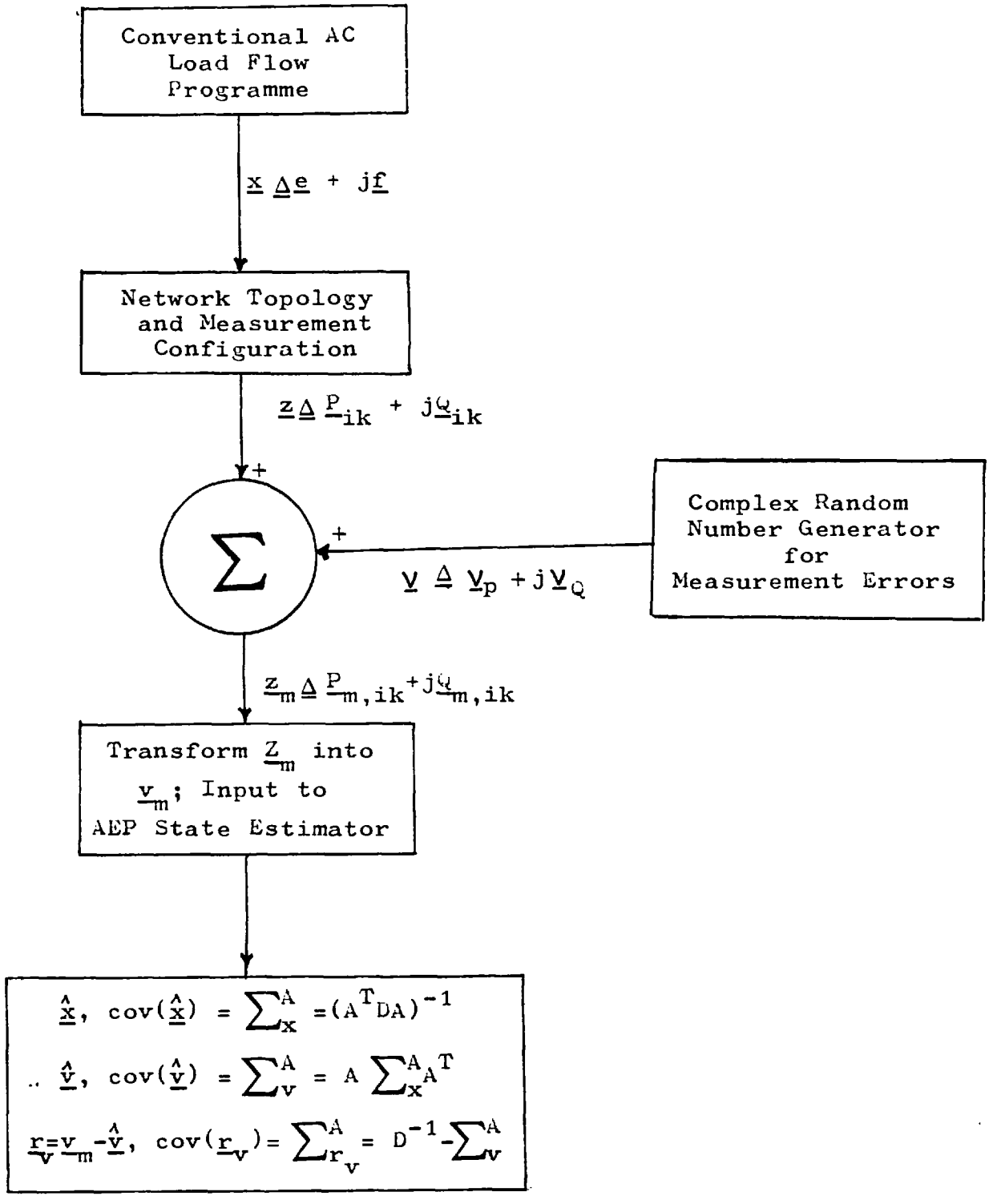

FIGURE 2.3: BLOCK DIAGRAM OF ESTIMATION SIMULATION PROCESS

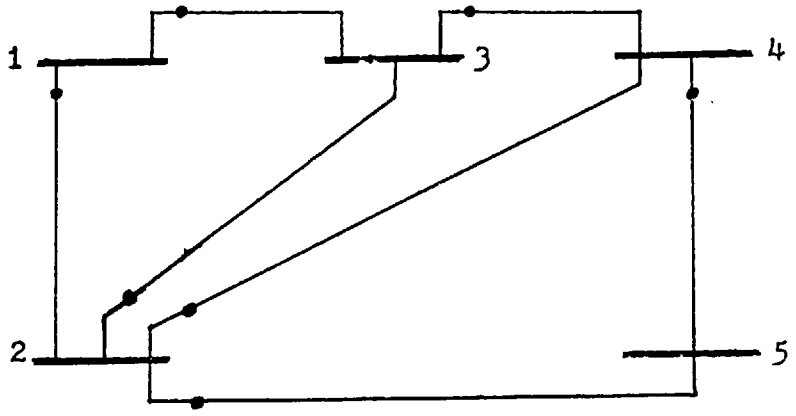

FIGURE 2.4: 7 - COMPLEX BRANCH POWER FLOW MEASUREMENTS ON 5-NODES, 7-LINES NETWORK

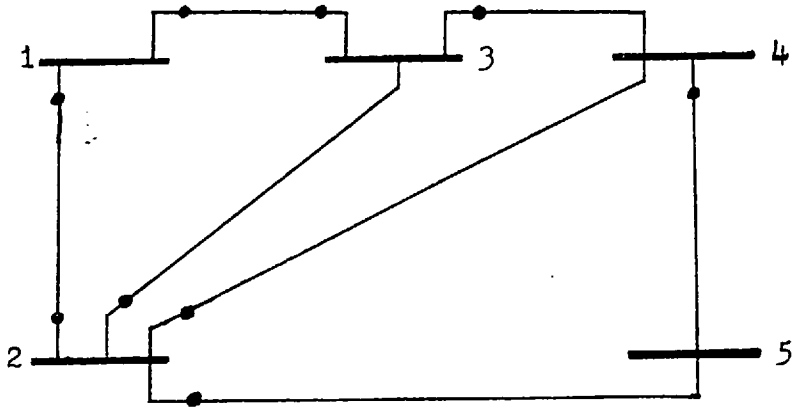

FIGURE 2.5: 9 - COMPLEX BRANCH POWER FLOW MEASUREMENTS ON 5-NODES, 7-LINES NETWORK

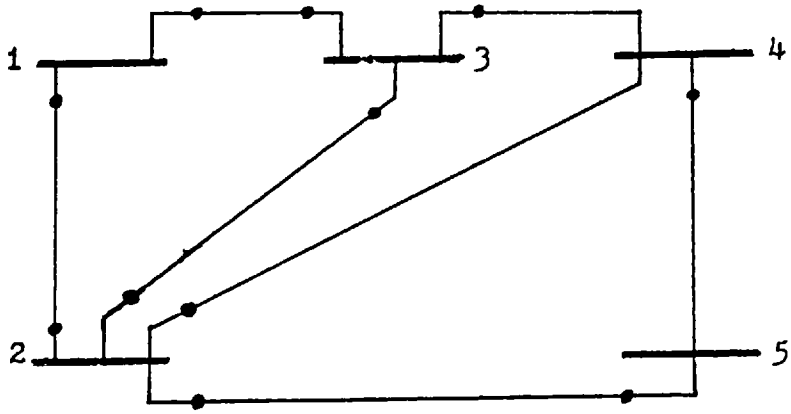

FIGURE 2.6: 11 - COMPLEX BRANCH POWER FLOW MEASUREMENTS ON 5-NODES, 7-LINES NETWORK

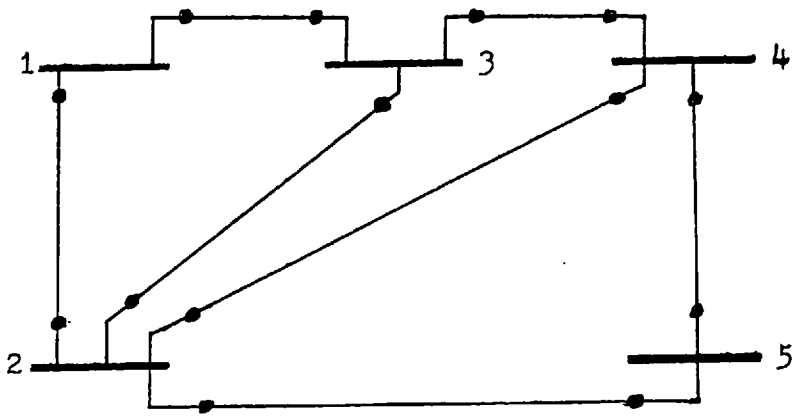

FIGURE 2.7: 14- COMPLEX BRANCH POWER FLOW MEASUREMENTS ON 5-NODES, 7-LINES NETWORK

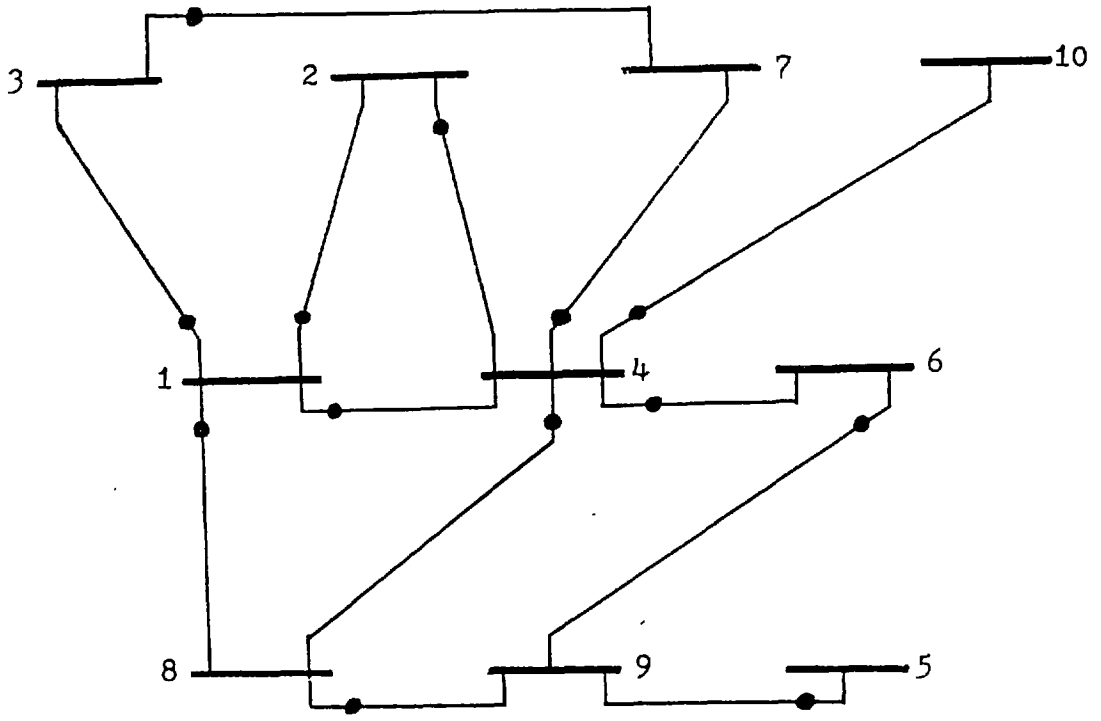

FIGURE 2.8: 13 - COMPLEX BRANCH POWER FLOW MEASUREMENTS ON 10-NODES, 13-LINES NETWORK

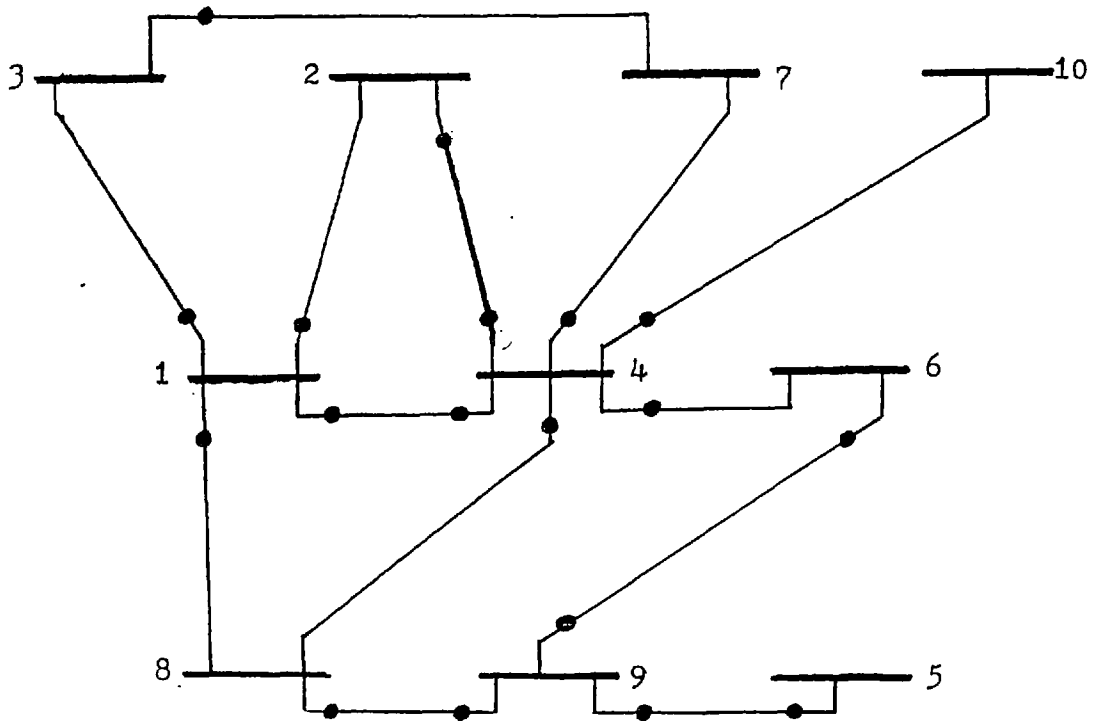

FIGURE 2.9: 18- COMPLEX BRANCH POWER FLOW MEASUREMENTS ON 10-NODES, 13-LINES NETWORK

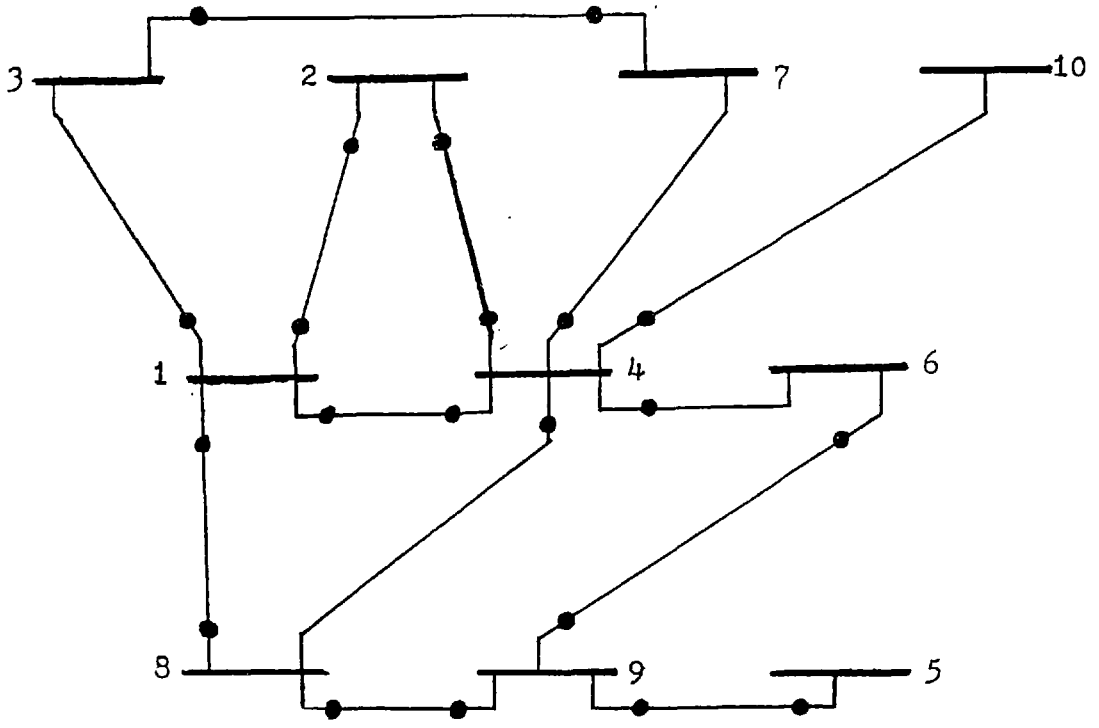

FIGURE 2.10: 21 - COMPLEX BRANCH POWER FLOW MEASUREMENTS ON 10-NODES, 13-LINES NETWORK

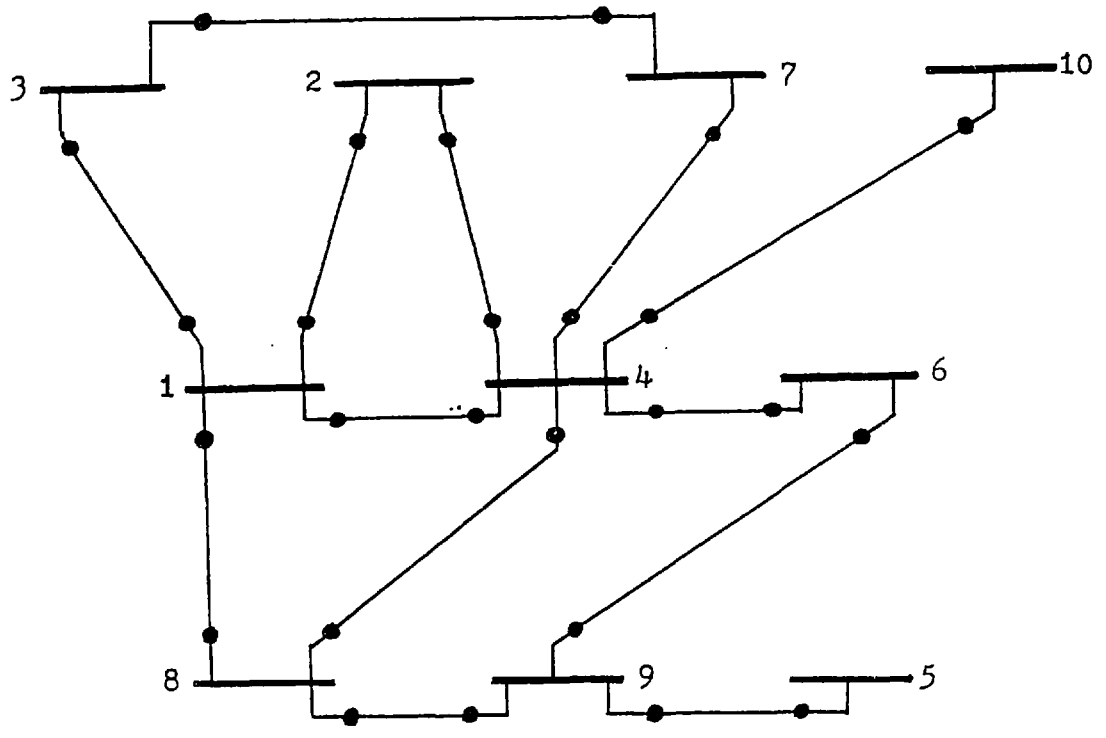

FIGURE 2.11: 26 - COMPLEX BRANCH POWER FLOW MEASUREMENTS ON 10-NODES, 13-LINES NETWORK

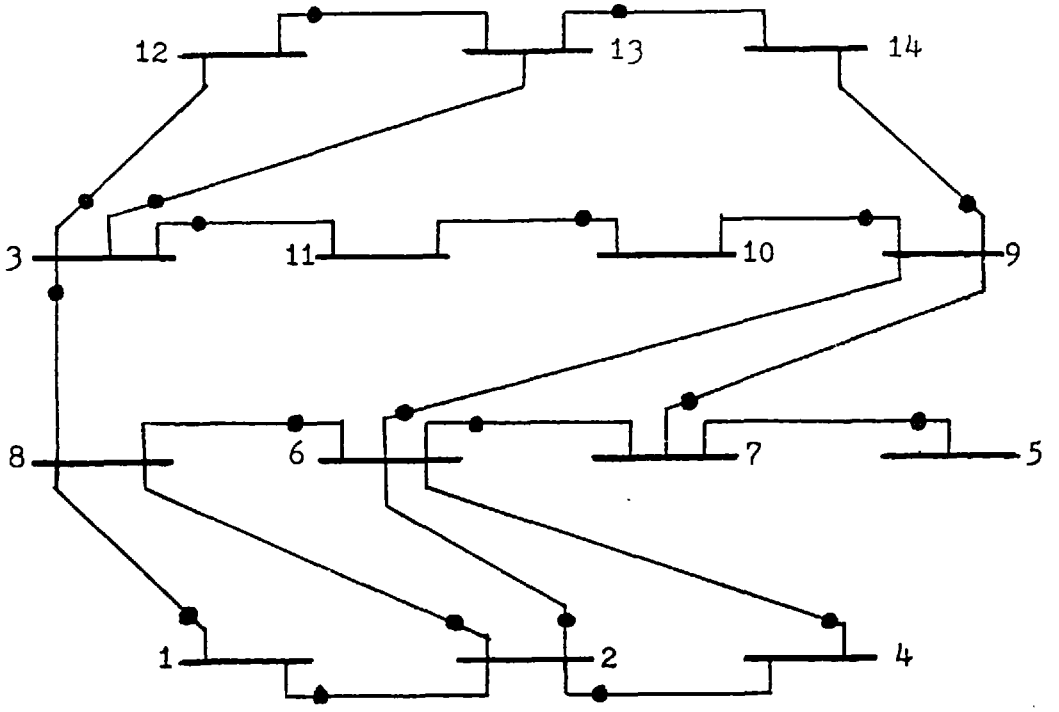

FIGURE 2.12: 20 - COMPLEX BRANCH POWER FLOW MEASUREMENTS ON 14-NODES, 20-LINES NETWORK

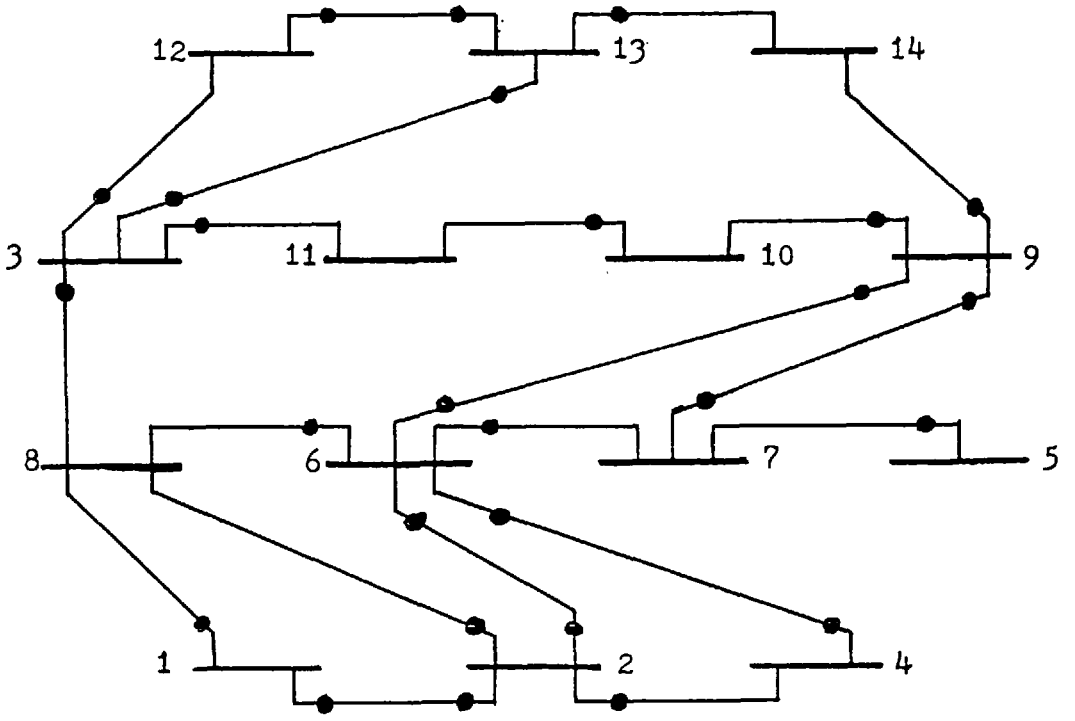

FIGURE 2.13: 27 - COMPLEX BRANCH POWER FLOW MEASUREMENTS ON 14-NODES, 20-LINES NETWORK

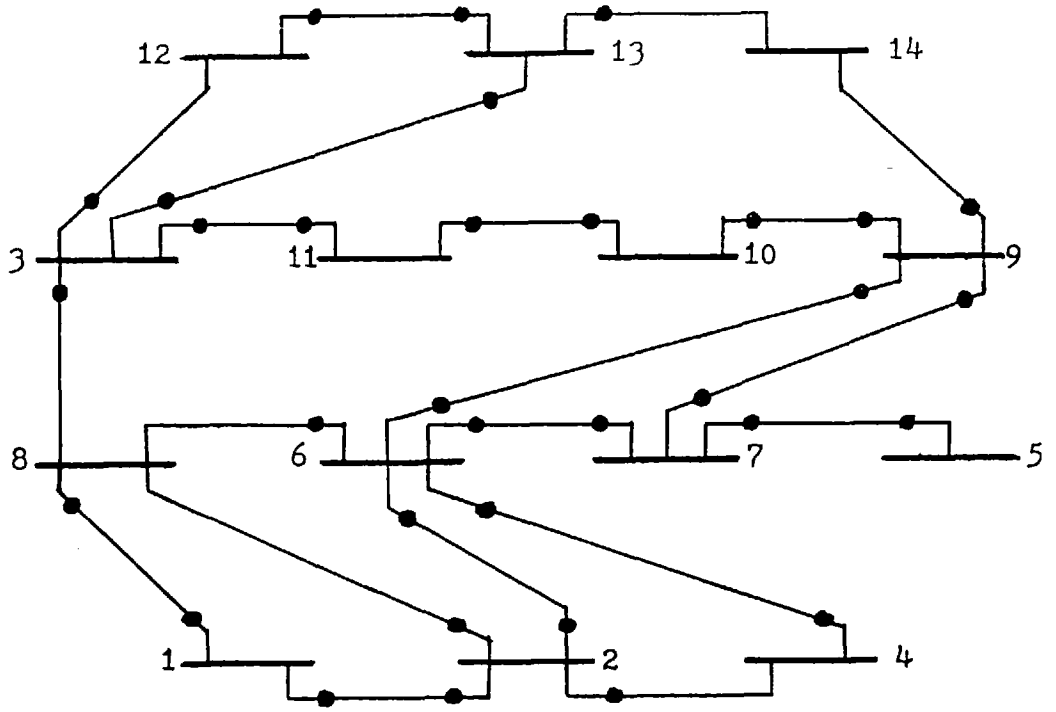

FIGURE 2.14: 33 - COMPLEX BRANCH POWER FLOW MEASUREMENTS ON 14-NODES, 20-LINES NETWORK

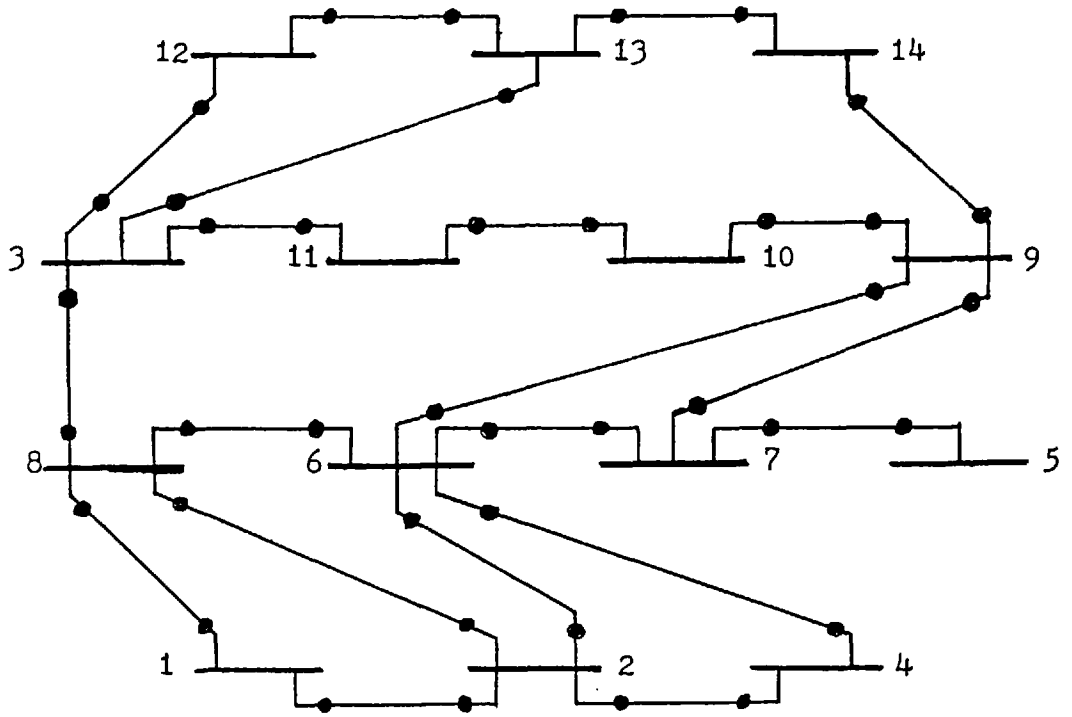

FIGURE 2.15: 40 - COMPLEX BRANCH POWER FLOW MEASUREMENTS ON 14-NODES, 20-LINES NETWORK

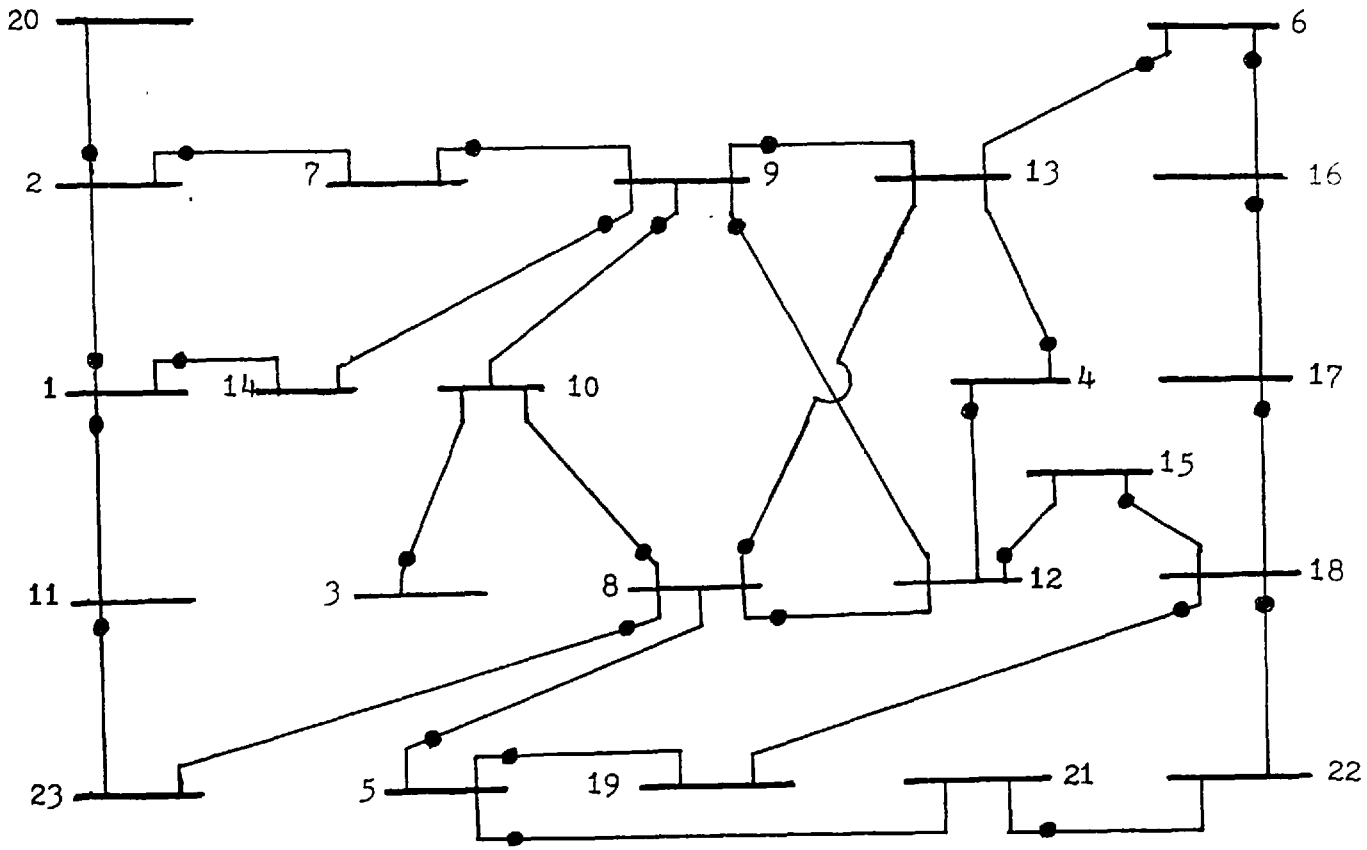

FIGURE 2.16: 30- COMPLEX BRANCH POWER FLOW MEASUREMENTS ON 23-NODES, 30-LINES NETWORK

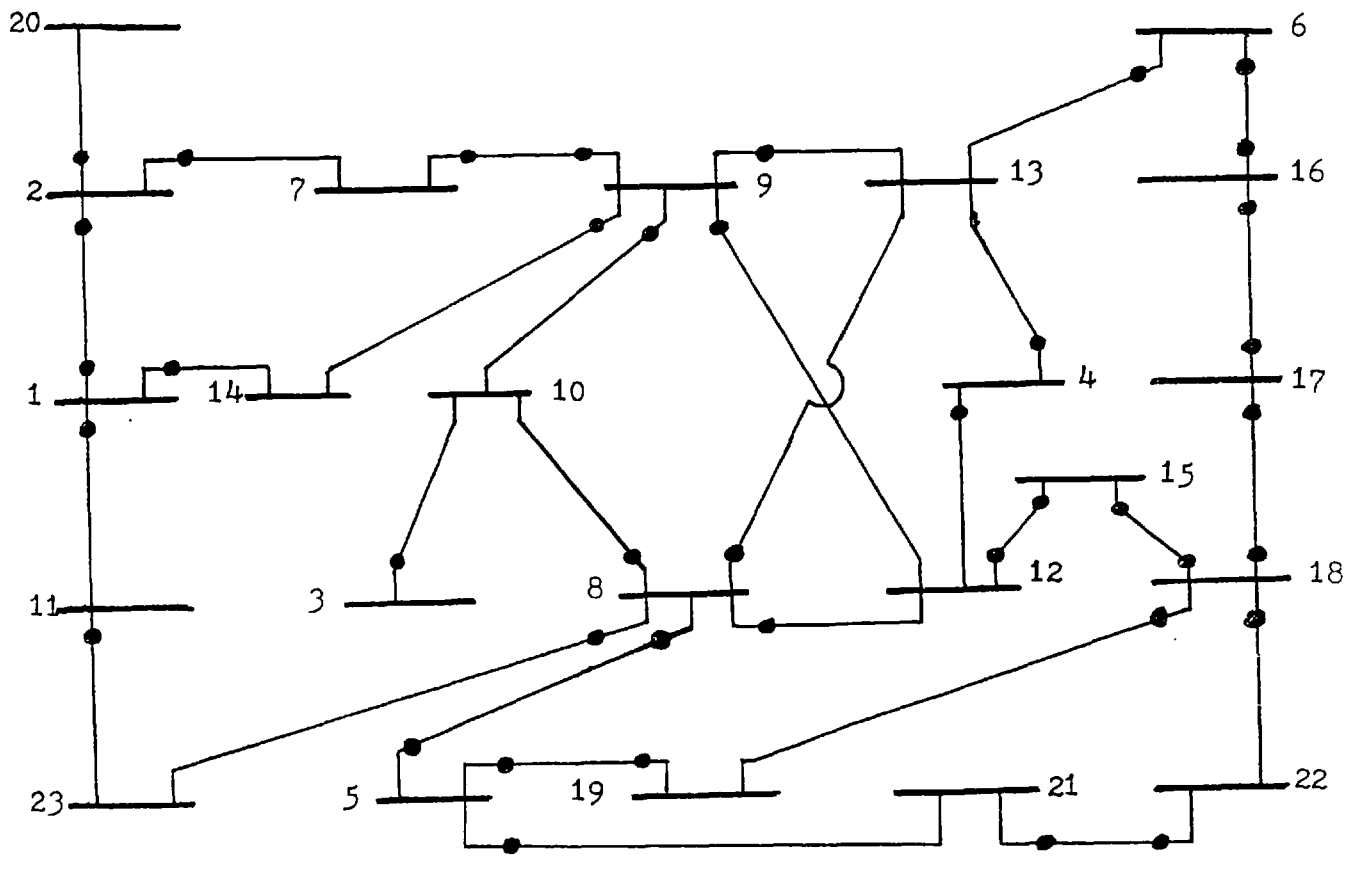

FIGURE 2.17: 40 - COMPLEX BRANCH POWER FLOW MEASUREMENTS ON 23-NODES, 30-LINES NETWORK

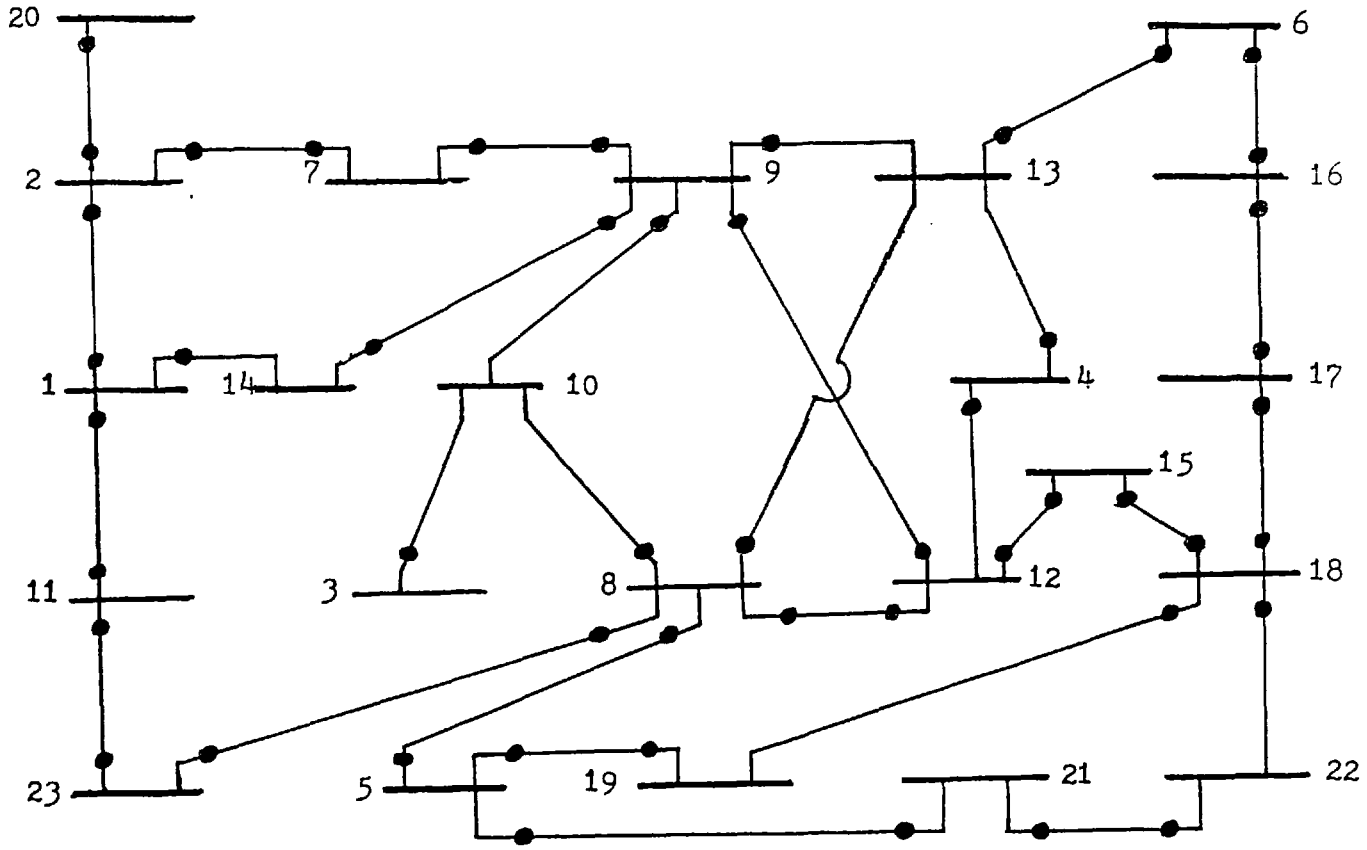

FIGURE 2.18: 50 - COMPLEX BRANCH POWER FLOW MEASUREMENTS ON 23-NODES, 30-LINES NETWORK

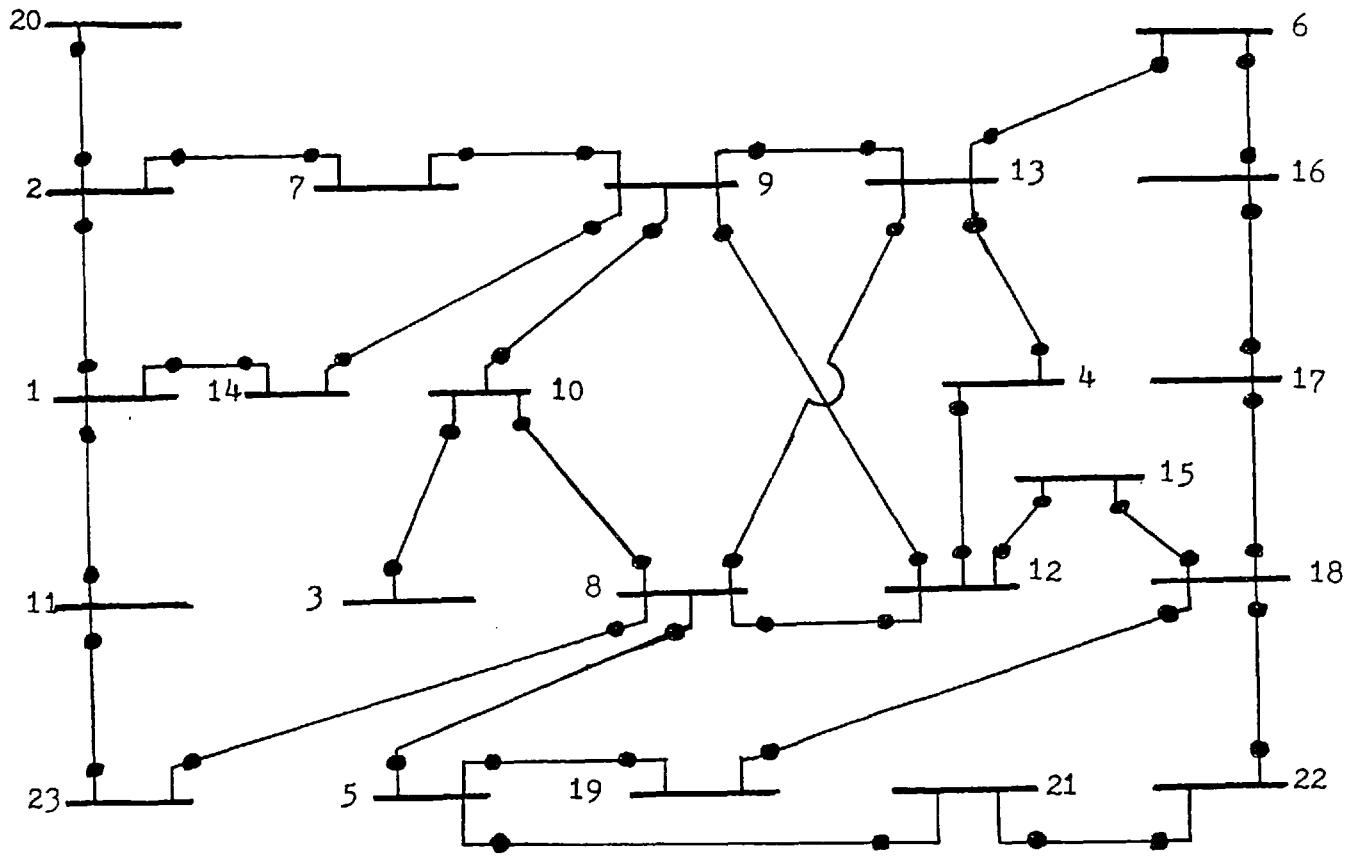

FIGURE 2.19: 60 - COMPLEX BRANCH POWER FLOW MEASUREMENTS ON 23-NODES, 30-LINES NETWORK

$\sigma_{p_{ik}} = 2\% P_{ik}$ and $\sigma_{Q_{ik}} = 2\% Q_{ik}$

Therefore, the variance of the effective complex measurement error, v_{ik} is determined as:

$$\text{var}(v_{ik}) = E(v_{ik} v_{ik}^{*}) = E(v_{p_{ik}}^2 + v_{Q_{ik}}^2)$$

$$= E(v_{p_{ik}}^2) + E(v_{Q_{ik}}^2)$$

$$= \sigma_{p_{ik}}^2 + \sigma_{Q_{ik}}^2$$

These random numbers were used in corrupting the true load flow complex branch power flows, as additive noise, to give the complex branch flow power measurements.

Before any estimation scheme is deemed adequate for an on-line monitoring scheme it ought to possess, amongst other qualities, the following desirable characteristics[29]:

- possess small computer core storage requirements
- possess very good and strong convergence properties
- yield reliable estimates in short execution times
- afford a quantitative index for evaluating the reliability of the estimated states
- yield state estimates that are not degenerate in terms of accuracy.

Finally it is essential that the technique be simple enough to be implementable on small process control computers for real-time operations.

In Tables 2.1 to 2.4 the estimated network voltage profiles for all the networks at their respective specified degrees of measurement redundancies are shown. These results show that despite the

linearising transformation that converted the non-linear problem into a linear one suitable for LWLS estimation techniques, the AEP method does not lead to degenerate state estimates. The convergence of the method was also monitored during the simulations, assuming a rectangular complex voltage convergence tolerance of 0.00005 pu. From a flat voltage start of 1.0 pu (nominal) for all the nodes of each test network, the AEP algorithm converged to the stipulated tolerance in 3 to 6 iteration steps, as shown in Table 2.5. The AEP method hence possesses strong convergence characteristics. The maximum value of 6 iterations is in agreement with recommended and quoted values in the literature for the method [30,34]. The computational speed of the technique was also partially assessed (excluding input output functions) in that the sparse matrix oriented computer codes developed for ordering the gain matrix, reducing it to the bi-factorisation form and solving the resulting system of linear equations for the state vector $\underline{\hat{x}}$ were all timed in CPU seconds of the ICCC CDC 6600 Computer. In Table 2.5 the three components of the total solution time, namely, t_{order}, t_{reduce}, t_{back}, are all presented. From these it is concluded that the principal contributor to t_{total} is t_{back}. This observation arises because until convergence is attained, the back-substitution procedure must be repeated several times. The total execution times, t_{total} for the networks are all extremely low. On this basis it is justifiable to assert that the technique possesses the property of short computation times that are a necessary feature for all real-time monitoring schemes desirable for power system operation. As it is inadequate, and indeed cumbersome, to compare each estimated busbar voltage against its true load-flow value to determine

the reliability of the estimate, the performance index, $J(\hat{\underline{x}})$, was computed at the end of each estimation process and compared to its corresponding statistical chi-square limit of $\chi^2_{df,\alpha}$. In all the tests, a significance level of $\alpha = 99.0\%$ was used in obtaining the threshold values of $\chi^2_{df,\alpha}$ given in Table 2.5. The value of $J(\hat{\underline{x}})$ is always less than $\chi^2_{df,99.0\%}$, a clear indication that $J(\hat{\underline{x}})$ is a sufficient statistical index for testing the acceptability of the estimated network busbar complex voltages. In most LWLS estimation techniques, a by-product, $\hat{\sigma}$ generally referred to as the covariance scaling factor is computable [34,49]. It is defined as: $\hat{\sigma} = \sqrt{\frac{J(\hat{\underline{x}})}{df(=m-n)}}$ The theoretical equivalent of $\hat{\sigma}$ is σ_{true} which is similarly defined by $\sigma_{true} = \sqrt{\frac{E\{J(\hat{\underline{x}})\}}{df}}$. Given that the expectation of $J(\hat{\underline{x}})$ is exactly equal to the measurement degrees of freedom, df, σ_{true} has a constant value of 1.0 for all measurement redundancies. $\hat{\sigma}$ values are presented in Table 2.6 and the trajectory against df shown in Fig. 2.20. The apparent deviations of $\hat{\sigma}$ from the ideal value σ_{true} are due mainly to physical differences between the test networks, such as degree of node connectivity, and more importantly because the $\hat{\sigma}$ values were obtained from one-off estimation instead of from averaged values obtained from Monte-Carlo simulation studies[38,46]. Charts in the form of Fig. 2.20 are extremely useful since they provide a pictorial control chart that may be kept in Control Centres to give a ready record of the history of the behaviour of the estimator.

A further indirect approach adopted for testing the validity of the estimation technique involved the determination of the complex network voltages from a set of noise-free or deterministic branch flow

power measurements taken at both terminals of each transmission line of the test systems. From the results (example shown in Table 2.7) it is concluded that the AEP technique is devoid of any serious round-off errors since the estimated voltages are equal to the assumed true load flow values to 6 decimal places.

Confidence limits were established for the calculated state estimates and are shown in Tables 2.8(a) and 2.8(b). In these tables, the meter configuration corresponding to the maximum measurement redundancy for each of the test networks was used. As anticipated from the theory, the confidence limits span each of the true network load-flow voltage profiles.

From Tables 2.8(a) and 2.8(b), the root-mean-square estimation errors are generally less than the standard deviations of the estimated voltages; thus verifying noise filtering. Improper filtering arises following an improper choice of the input measurement noise covariance matrix. A more detailed discussion of the choice of suitable weighting matrices can be found in S.A. Molina [53].

2.5 General comments

It is worth mentioning now that the basic AEP algorithm does not possess statistically optimal properties due to the fact that the linearising transformation applied to derive the linear form of the AEP technique is, strictly speaking, dependent on the unknown state $\underline{x}$. These assumptions notwithstanding, the AEP technique lends itself to efficient formulation and solution with sparse matrix techniques; it also yields reasonably reliable estimates of the complex voltages at all network nodes. It possesses strong convergence characteristics and

yields unbiased solutions of $\underline{x}$. Its formulation is closely related to conventional load-flow solutions making it computationally highly efficient and simple.

The derived performance index $J(\hat{\underline{x}})$ has been proved to be an invaluable variable for either rejecting or accepting derived state estimates.

Since one of the basis of comparing different approaches to state estimation entails computing time and storage requirements, the application of the non-linear or generalized weighted least-squares techniques (GWLS) (Appendix A) to the power system state estimation problem is the subject of study in the next chapter.

TABLE 2.1

ESTIMATED NETWORK VOLTAGE PROFILES 5-NODES, 7-LINES NETWORK

BUS	VREAL, e_i	VIMAG, f_i	VREAL, e_i	VIMAG, f_i
1	1.06000	0	1.06000	0
2	1.04596	-.05162	1.04587	-.05187
3	1.02006	-.08960	1.01996	-.08982
4	1.01896	-.09547	1.01886	-.09569
5	1.01207	-.10847	1.01197	-.10870
	$J(\hat{\underline{x}})$ = .188E+01		$J(\hat{\underline{x}})$ = .205E+01	
	No. of measurements = 7		No. of measurements = 9	

BUS	VREAL, e_i	VIMAG, f_i	VREAL, e_i	VIMAG, f_i
1	1.06000	0	1.06000	0
2	1.04589	-.05176	1.04591	-.05174
3	1.01988	-.09018	1.01982	-.09024
4	1.01878	-.09605	1.01874	-.09610
5	1.01186	-.10908	1.01186	-.10933
	$J(\hat{\underline{x}})$ = .424E+01		$J(\hat{\underline{x}})$ = .586E+01	
	No. of measurements = 11		No. of measurements = 14	

TABLE 2.2

ESTIMATED NETWORK VOLTAGE PROFILES 10-NODES, 13-LINES NETWORK

BUS	VREAL, e_i	VIMAG, f_i	VREAL, e_i	VIMAG, f_i
1	1.04000	0	1.04000	0
2	1.04830	.03451	1.04822	.03443
3	1.04244	-.11650	1.04300	-.11535
4	1.03391	-.11074	1.03454	-.10946
5	.99214	-.18398	.99364	-.18264
6	1.02853	-.15403	1.02909	-.15308
7	1.02038	-.13741	1.02101	-.13621
8	.94529	-.12724	.94614	-.12547
9	.97905	-.18440	.98052	-.18305
10	1.02948	-.06967	1.03006	-.06841
	$J(\hat{\underline{x}})$ = .313E+01		$J(\hat{\underline{x}})$ = .118E+02	
	No. of measurements = 13		No. of measurements = 18	

BUS	VREAL, e_i	VIMAG, f_i	VREAL, e_i	VIMAG, f_i
1	1.04000	0	1.04000	0
2	1.04823	.03386	1.04822	.03385
3	1.04356	-.11487	1.04325	-.11515
4	1.03478	-.10934	1.03460	-.10940
5	.99411	-.18227	.99370	-.18287
6	1.02944	-.15282	1.02907	-.15366
7	1.02122	-.13611	1.02093	-.13637
8	.94672	-.12500	.94633	-.12525
9	.98099	-.18268	.98058	-.18327
10	1.03029	-.06830	1.03034	-.06901
	$J(\hat{\underline{x}})$ = .178E+02		$J(\hat{\underline{x}})$ = .227E+02	
	No. of measurements = 21		No. of measurements = 26	

TABLE 2.3

ESTIMATED NETWORK VOLTAGE PROFILES 14-NODES, 20-LINES NETWORK

BUS	VREAL, e_i	VIMAG, f_i	VREAL, e_i	VIMAG, f_i
1	1.06000	0	1.06000	0
2	1.04050	-.09152	1.04070	-.09095
3	1.03542	-.26563	1.03643	-.26378
4	.98416	-.22381	.98457	-.22275
5	1.05921	-.25287	1.06001	-.25135
6	1.00167	-.18297	1.00238	-.18163
7	1.03244	-.24656	1.03324	-.24509
8	1.00807	-.15582	1.00868	-.15457
9	1.01954	-.27425	1.02056	-.27243
10	1.01376	-.27591	1.01479	-.27409
11	1.02080	-.27182	1.02181	-.26999
12	1.01710	-.27706	1.01813	-.27527
13	1.01226	-.27726	1.01323	-.27550
14	.99412	-.28829	.99512	-.28654
	$J(\hat{\underline{x}})$ = .738E+01		$J(\hat{\underline{x}})$ = .138E+02	
	No. of measurements = 20		No. of measurements = 27	

BUS	VREAL, e_i	VIMAG, f_i	VREAL, e_i	VIMAG, f_i
1	1.06000	0	1.06000	0
2	1.04093	-.09049	1.04101	-.09032
3	1.03703	-.26269	1.03718	-.26250
4	.98497	-.22210	.98498	-.22212
5	1.06062	-.25073	1.06066	-.25069
6	1.00275	-.18096	1.00271	-.18109
7	1.03353	-.24441	1.03356	-.24437
8	1.00905	-.15385	1.00877	-.15436
9	1.02088	-.27176	1.02094	-.27168
10	1.01512	-.27335	1.01519	-.27326
11	1.02213	-.26933	1.02222	-.26922
12	1.01871	-.27425	1.01886	-.27399
13	1.01380	-.27448	1.01396	-.27421
14	.99563	-.28567	.99558	-.28574
	$J(\hat{\underline{x}})$ = .236E+02		$J(\hat{\underline{x}})$ = .337E+02	
	No. of measurements = 33		No. of measurements = 40	

TABLE 2.4

ESTIMATED NETWORK VOLTAGE PROFILES 23-NODES, 30-LINES NETWORK

BUS	VREAL, e_i	VIMAG, f_i	VREAL, e_i	VIMAG, f_i
1	1.01860	0	1.01860	0
2	1.02135	-.02888	1.02133	-.02914
3	1.03118	.08924	1.03126	.08930
4	1.03621	.16853	1.03627	.16854
5	1.00616	.30016	1.00576	.30053
6	.99042	.34908	.99045	.34941
7	.99541	.00658	.99529	.00625
8	.98664	.16702	.98670	.16707
9	1.00326	.03948	1.00335	.03953
10	.98216	.04738	.98225	.04744
11	1.00963	.02220	1.00983	.02220
12	1.02571	.14597	1.02575	.14596
13	1.01864	.18457	1.01870	.18461
14	1.00108	.00556	1.00110	.00557
15	1.00687	.14138	1.00705	.14136
16	.98888	.25084	.98896	.25118
17	.98902	.21357	.98907	.21361
18	.99694	.19386	.99695	.19368
19	.99405	.18607	.99406	.18588
20	.98693	-.06737	.98690	-.06762
21	1.00097	.24042	1.00085	.24044
22	1.00228	.23833	1.00216	.23832
23	.98041	.08316	.98044	.08319
	$J(\hat{x})$ = .197E+02		$J(\hat{x})$ = .277E+02	
	No. of measurements = 30		No. of measurements = 40	

BUS	VREAL, e_i	VIMAG, f_i	VREAL, e_i	VIMAG, f_i
1	1.01860	0	1.01860	0
2	1.02136	-.02912	1.02133	-.02911
3	1.03142	.08936	1.03049	.08992
4	1.03636	.17007	1.03586	.17044
5	1.00553	.30240	1.00510	.30256
6	.99023	.35121	.98977	.35136
7	.99542	.00624	.99534	.00626
8	.98670	.16866	.98631	.16863
9	1.00351	.03955	1.00339	.03958
10	.98242	.04750	.98215	.04761
11	1.01013	.02276	1.01011	.02276
12	1.02593	.14743	1.02562	.14747
13	1.01873	.18614	1.01812	.18636
14	1.00110	.00559	1.00091	.00562
15	1.00723	.14282	1.00692	.14285
16	.98896	.25269	.98860	.25276
17	.98914	.21509	.98879	.21514
18	.99705	.19516	.99671	.19520
19	.99416	.18735	.99376	.18746
20	.98697	-.06782	.98695	-.06782
21	1.00092	.24172	1.00050	.24189
22	1.00223	.23960	1.00181	.23977
23	.98090	.08451	.98073	.08449
	$J(\hat{x})$ = .385E+02		$J(\hat{x})$ = .464E+02	
	No. of measurements = 50		No. of measurements = 60	

TABLE 2.5

SUMMARY OF SALIENT RESULTS OF AEP ESTIMATOR

Number of network nodes	Number of complex power flow measurements	Measurement redundancy or degrees of freedom	Redundancy ratio	Performance index	Chi-Square limit	Number of iterations for convergence	Time for optimal ordering (ms) *	Time for reduction (ms) *	Time for back substitution (ms) *	Total time for solution (ms) *
n	m	df=m-n+1	$\eta=\frac{df}{n-1}$	$J(\hat{x})$	$\chi^2_{df,99\%}$	iter	t_{order}	t_{reduce}	t_{back}	t_{total}
5	7	3	0.75	1.88	11.30	3	2.0	1.0	0.0	3.0
5	9	5	1.25	2.05	15.10	4	1.0	1.0	2.0	4.0
5	11	7	1.75	4.24	18.50	4	1.0	1.0	4.0	6.0
5	14	10	2.50	5.86	23.20	4	2.0	1.0	4.0	7.0
10	13	4	0.44	3.13	13.30	4	2.0	3.0	10.0	15.0
10	18	9	1.00	11.80	21.70	4	2.0	1.0	8.0	11.0
10	21	12	1.33	17.80	26.20	4	3.0	2.0	7.0	12.0
10	26	17	1.89	22.70	33.40	5	3.0	1.0	12.0	16.0
14	20	7	0.54	7.38	18.50	4	15.0	5.0	24.0	44.0
14	27	14	1.08	13.80	29.10	5	8.0	8.0	28.0	44.0
14	33	20	1.54	23.60	37.60	5	6.0	6.0	28.0	40.0
14	40	27	2.08	33.70	47.00	5	7.0	6.0	27.0	40.0
23	30	8	0.36	19.70	20.10	6	15.0	7.0	54.0	76.0
23	40	18	0.82	27.70m	34.80	5	14.0	9.0	41.0	64.0
23	50	28	1.27	38.50	48.30	5	13.0	8.0	43.0	64.0
23	60	38	1.73	46.40	63.70	5	13.0	9.0	45.0	67.0

* Computation times based on CDC 6600 Computer (ICCC) CPU times

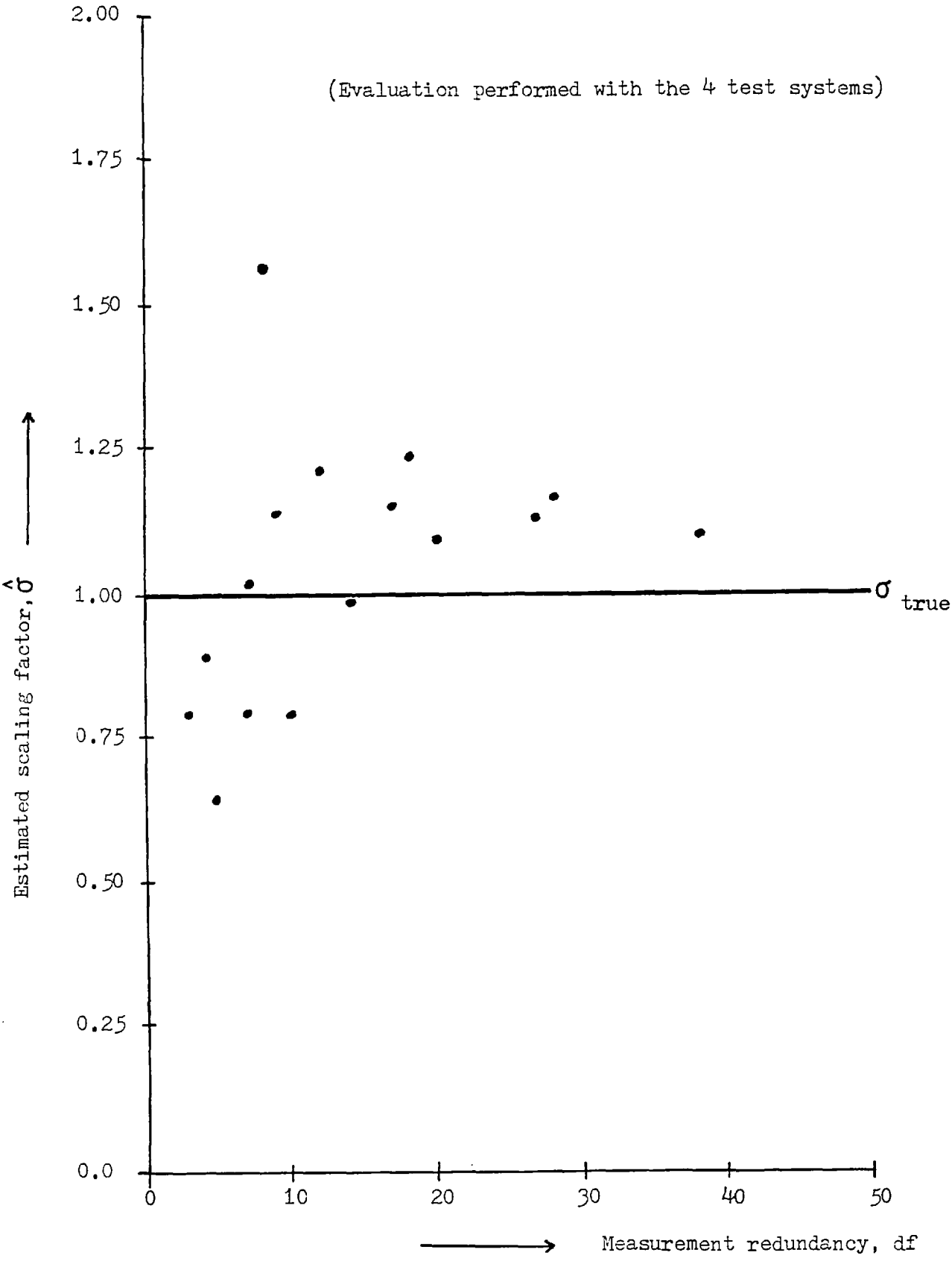

FIGURE 2.20: TRAJECTORY OF SCALING FACTOR, $\hat{\sigma}$ VERSUS DEGREES OF FREEDOM, df (=m-n)

TABLE 2.6

COMPUTED VALUES OF SCALING FACTOR, $\hat{\sigma}$

$\sigma_{true} = 1.0$

Redundancy and Expectation of $J(\underline{\hat{x}})$	Estimated Scaling Factor
df and $E\{J(\underline{\hat{x}})\}$	$\hat{\sigma} = \sqrt{\frac{J(\underline{\hat{x}})}{df}}$
3	0.79
4	0.88
5	0.64
7	0.78
7	1.02
8	1.57
9	1.14
10	0.77
12	1.22
14	0.99
17	1.15
18	1.24
20	1.09
27	1.12
28	1.17
38	1.10

TABLE 2.7

ESTIMATED VOLTAGES FOR NOISE-FREE INPUT MEASUREMENTS
23-NODES, 30-LINES SYSTEM

	Estimated Voltages		Load Flow Voltages	
BUS	VREAL, e_i	VIMAG, f_i	ETRUE, e_i	FTRUE, f_i
1	1.01860	0	1.01860	0
2	1.02141	-.02900	1.02140	-.02900
3	1.03128	.09020	1.03130	.09020
4	1.03595	.17070	1.03600	.17070
5	1.00526	.30321	1.00530	.30320
6	.98946	.35131	.98950	.35130
7	.99541	.00600	.99540	.00600
8	.98626	.16791	.98630	.16790
9	1.00371	.03990	1.00370	.03990
10	.98238	.04800	.98240	.04800
11	1.01000	.02280	1.01000	.02280
12	1.02556	.14740	1.02560	.14740
13	1.01825	.18600	1.01830	.18600
14	1.00100	.00550	1.00100	.00550
15	1.00705	.14280	1.00710	.14280
16	.98875	.25311	.98880	.25310
17	.98895	.21571	.98900	.21570
18	.99695	.19590	.99700	.19590
19	.99405	.18820	.99410	.18820
20	.98701	-.06760	.98700	-.06760
21	1.00085	.24201	1.00090	.24200
22	1.00215	.23991	1.00220	.23990
23	.98087	.08460	.98090	.08460

TABLE 2.8(a)

ESTIMATED VOLTAGES, ERRORS AND STATISTICS FOR 5-NODES, 7-LINES; 10-NODES, 13-LINES; 14-NODES, 20-LINES SYSTEMS

BUS	Estimated Voltages VREAL, e_i	VIMAG, f_i	RMS Error RMSER	Standard Deviation STDEV	Confidence Limits CONFL
2	1.04591	-.05174	.00053	.00067	±.00211
3	1.01982	-.09024	.00114	.00074	±.00233
4	1.01874	-.09610	.00110	.00074	±.00233
5	1.01186	-.10933	.00041	.00076	±.00241
2	1.04822	.03385	.00067	.00049	±.00143
3	1.04325	-.11515	.00137	.00101	±.00292
4	1.03460	-.10940	.00120	.00094	±.00273
5	.99370	-.18287	.00310	.00122	±.00352
6	1.02907	-.15366	.00268	.00109	±.00317
7	1.02093	-.13637	.00125	.00098	±.00284
8	.94633	-.12525	.00253	.00118	±.00341
9	.98058	-.18327	.00313	.00121	±.00350
10	1.03034	-.06901	.00156	.00110	±.00319
2	1.04101	-.09032	.00038	.00116	±.00320
3	1.03718	-.26250	.00041	.00145	±.00403
4	.98498	-.22212	.00022	.00140	±.00387
5	1.06066	-.25069	.00130	.00149	±.00413
6	1.00271	-.18109	.00158	.00130	±.00359
7	1.03356	-.24437	.00131	.00144	±.00398
8	1.00877	-.15436	.00146	.00128	±.00354
9	1.02094	-.27168	.00090	.00144	±.00399
10	1.01519	-.27326	.00081	.00144	±.00400
11	1.02222	-.26922	.00072	.00145	±.00401
12	1.01886	-.27398	.00049	.00146	±.00406
13	1.01396	-.27421	.00053	.00146	±.00406
14	.99558	-.28574	.00052	.00147	±.00407

TABLE 2.8(b)

ESTIMATED VOLTAGES, ERRORS AND STATISTICS FOR 23-NODES, 30-LINES SYSTEM

	Estimated Voltages		RMS Error	Standard Deviation	Confidence Limits
BUS	VREAL, e_i	VIMAG, f_i	RMSER	STDEV	CONFL
2	1.02133	-.02911	.00013	.00038	±.00102
3	1.03049	.08992	.00086	.00107	±.00288
4	1.03586	.17044	.00029	.00095	±.00255
5	1.00510	.30256	.00067	.00136	±.00367
6	.98977	.35136	.00027	.00165	±.00446
7	.99534	.00626	.00026	.00052	±.00140
8	.98631	.16863	.00073	.00091	±.00246
9	1.00339	.03958	.00044	.00046	±.00123
10	.98215	.04761	.00046	.00055	±.00148
11	1.01011	.02276	.00012	.00034	±.00092
12	1.02562	.14747	.00007	.00093	±.00251
13	1.01812	.18636	.00040	.00093	±.00251
14	1.00091	.00562	.00014	.00025	±.00068
15	1.00692	.14285	.00019	.00096	±.00260
16	.98860	.25276	.00040	.00129	±.00350
17	.98879	.21514	.00060	.00120	±.00325
18	.99671	.19520	.00076	.00117	±.00317
19	.99376	.18746	.00081	.00118	±.00318
20	.98695	-.06782	.00022	.00082	±.00222
21	1.00050	.24189	.00042	.00128	±.00346
22	1.00181	.23977	.00041	.00128	±.00346
23	.98073	.08449	.00020	.00087	±.00234

CHAPTER III

APPLICATION OF GENERALIZED WEIGHTED LEAST SQUARES (GWLS) TO STATIC POWER SYSTEMS STATE ESTIMATION

3.1 Introduction

Static power system state estimators are data processing algorithms designed to establish the power network voltage profile from a set of noisy but redundant telemetered system measurements. Historically, least squares methods were first adapted for the power system problem in the 1970s [8-10, 29]. Of the various approaches that have been presented the most general and optimal procedure is the Generalised Weighted Least Squares (GWLS) technique which utilizes all of the available system measurement information. However, because estimators are required for on-line operation needing fast solution times and low storage requirements, the basic GWLS approach is unsuitable for direct on-line implementation since it generally results in the formulation and manipulation of very large dimensional Jacobian and coefficient matrices and, in addition, requires excessively long computational times. Although considerable efforts have been expended by several investigators[14,16,17,19,57] with a view to obtain approximate methods competitive with fast-low-storage methods like the AEP technique (Chapter II), the majority of reported results are either rather specialised or dependent on the magnitudes of the network line reactance-to-resistance ratios, X/R.

In this chapter, the GWLS estimation problem is described in terms of active and reactive power related measurements. As a consequence, certain physically justifiable power system assumptions are made subsequent to which two enhanced estimation techniques, p-δ, Q-E and

Fast Decoupled Estimator (FDE) methods, are derived. Differences between the method of this thesis and others reported in the literature are discussed. It is also proved, through extensive simulation tests performed on four selected test networks at various measurement redundancies, that the P-δ, Q-E and FDE methods are orders of magnitude faster in computation than the full GWLS technique.

3.2 Review of GWLS static power system state estimation

Following the customary definition of the static power system state estimation problem [29] the n-dimensional state vector $\underline{x}$ and the m-dimensional noise-corrupted observation vector $\underline{z}_m$ are defined by:

$$\underline{x}^T = (\underline{\delta}, \underline{E}) \qquad (3.2.1)$$

$$\underline{Z}_m = \underline{z}_t + \underline{V} = \underline{h}(\underline{x}) + \underline{V} \quad . \qquad (3.2.2)$$

where

$\underline{\delta}$ and $\underline{E}$ are the network busbar voltage angles and magnitudes respectively, and $\underline{V}$ is the vector of observation errors.

Making the usual theoretical assumptions, $\underline{V}$ is supposed to belong to a Gaussian distribution of zero-mean and finite covariance matrix R. That is:

$$E(\underline{V}) = \underline{0} \qquad E(\underline{V}\,\underline{V}^T) = R$$

$$\underline{V} \sim N(\underline{0}, R)$$

where R is diagonal and of dimension $m \times m$.

In practical measurement schemes there are always more measurements $\underline{Z}_m$ than there are state variables to be estimated $\underline{x}$, i.e. $m > n$, to ensure some degree of measurement redundancy. To solve the over-determined system of non-linear equations (3.2.2) for $\underline{x}$ involves the

application of least-squares techniques. The optimal minimum mean squared unbiased estimate $\hat{\underline{x}}$ of $\underline{x}$ is generated by minimising the sum of weighted squared errors, $J(\underline{x})$ where:

$$J(\underline{x}) = \left[\underline{Z}_m - \underline{h}(\underline{x})\right]^T R^{-1} \left[\underline{Z}_m - \underline{h}(\underline{x})\right] \qquad (3.2.3)$$

A direct application of the Gauss-Newton Method[53] to the minimisation of $J(\underline{x})$ yields the system of equations:

$$H^T(\hat{\underline{x}})R^{-1}\left\{\underline{z}_m - \underline{h}(\hat{\underline{x}})\right\} = 0 \qquad (3.2.4a)$$

$$H^T(\hat{\underline{x}})R^{-1}H(\hat{\underline{x}})\ (\underline{x}-\hat{\underline{x}}) = H^T(\hat{\underline{x}})R^{-1}\left\{\underline{Z}_m - \underline{h}(\hat{\underline{x}})\right\} \qquad (3.2.4b)$$

where

$$H(\hat{\underline{x}}) = \left.\frac{\partial \underline{h}(\underline{x})}{\partial \underline{x}}\right|_{\underline{x} = \hat{\underline{x}}},$$ the (mxn)-dimensional measurement Jacobian matrix.

In addition to consisting of n-nonlinear state dependent equations, equation (3.2.4b) is also inexact as a direct consequence of the linearisation and truncation of $\underline{h}(\underline{x})$ about $\hat{\underline{x}}$ during its derivation. The state estimate $\hat{\underline{x}}$ is therefore given by the converged value of $\hat{\underline{x}}_{k+1}$ derived from the iterative scheme:

$$(H_k^T R^{-1} H_k)(\hat{\underline{x}}_{k+1} - \hat{\underline{x}}_k) = (H_k^T R^{-1})\left\{\underline{z}_m - \underline{h}(\hat{\underline{x}}_k)\right\} \qquad (3.2.5)$$

where:

$$H_k \triangleq H(\hat{\underline{x}}_k)$$

Convergence is attained once $|\hat{\underline{x}}_{k+1} - \hat{\underline{x}}_k| \leq \Delta$, a prespecified convergence tolerance index.

In an electric power system, however, the measurement vector has two distinct physical components namely $\underline{Z}_p$, a vector of active power related observations ($\underline{P}_i$, $\underline{P}_{ik}$), and $\underline{Z}_Q$, a vector of reactive power related measurements ($\underline{Q}_i$, $\underline{Q}_{ik}$, $\underline{E}_i$). When defined in terms of active and reactive power related measurements, the system measurement equation and the Jacobian matrix assume the following forms:

$$\underline{Z}_m = \begin{bmatrix} \underline{z}_p \\ \underline{Z}_Q \end{bmatrix} = \begin{bmatrix} \underline{h}_p(\underline{\delta},\underline{E}) \\ \underline{h}_Q(\underline{\delta},\underline{E}) \end{bmatrix} + \begin{bmatrix} \underline{v}_p \\ \underline{v}_Q \end{bmatrix} \qquad (3.2.6)$$

$$H = \frac{\partial \underline{h}(\underline{x})}{\partial \underline{x}} = \begin{bmatrix} \frac{\partial \underline{h}_p}{\partial \underline{\delta}} & \frac{\partial \underline{h}_p}{\partial \underline{E}} \\ \frac{\partial \underline{h}_Q}{\partial \underline{\delta}} & \frac{\partial \underline{h}_Q}{\partial \underline{E}} \end{bmatrix} \triangleq \begin{bmatrix} H_{p\delta} & H_{pE} \\ H_{Q\delta} & H_{QE} \end{bmatrix} \quad \text{and}$$

$$R = \begin{bmatrix} R_p & 0 \\ 0 & R_Q \end{bmatrix}$$

Employing these newly defined notational expressions, the following estimation equation is obtained:

$$\begin{bmatrix} H_{p\delta}^T R_p^{-1} H_{p\delta} + H_{Q\delta}^T R_Q^{-1} H_{Q\delta} & H_{p\delta}^T R_p^{-1} H_{pE} + H_{Q\delta}^T R_Q^{-1} H_{QE} \\ H_{pE}^T R_p^{-1} H_{p\delta} + H_{QE}^T R_Q^{-1} H_{Q\delta} & H_{PE}^T R_p^{-1} H_{PE} + H_{QE}^T R_Q^{-1} H_{QE} \end{bmatrix} \times \begin{bmatrix} \hat{\underline{\delta}}_{k+1} - \hat{\underline{\delta}}_k \\ \hat{\underline{E}}_{k+1} - \hat{\underline{E}}_k \end{bmatrix}$$

$$= \begin{bmatrix} H_{p\delta}^T R_p^{-1} & H_{Q\delta}^T R_Q^{-1} \\ H_{PE}^T R_p^{-1} & H_{QE}^T R_Q^{-1} \end{bmatrix} \times \begin{bmatrix} \underline{Z}_p - \underline{h}_p(\hat{\underline{\delta}}_k, \hat{\underline{E}}_k) \\ \underline{Z}_Q - \underline{h}_Q(\hat{\underline{\delta}}_k, \hat{\underline{E}}_k) \end{bmatrix} \qquad (3.2.7)$$

or more generally as:

$$\begin{bmatrix} G_{\delta\delta} & G_{\delta E} \\ G_{\varepsilon\delta} & G_{EE} \end{bmatrix} \begin{bmatrix} \Delta\underline{\delta}_k \\ \Delta\underline{E}_k \end{bmatrix} = \begin{bmatrix} C_{\delta P} & C_{\delta Q} \\ C_{EP} & C_{EQ} \end{bmatrix} \begin{bmatrix} \Delta\underline{Z}_p \\ \Delta\underline{Z}_Q \end{bmatrix} \equiv \begin{bmatrix} \Delta\underline{b}_p \\ \Delta\underline{b}_Q \end{bmatrix}$$

(3.2.8)

where all the identified block matrices are evaluated at
$\underline{x} = (\hat{\underline{\delta}}_k \; \hat{\underline{E}}_k)$ and $\Delta\underline{\delta}_k = \hat{\underline{\delta}}_{k+1} - \hat{\underline{\delta}}_k$, $\Delta\underline{E}_k = \hat{\underline{E}}_{k+1} - \hat{\underline{E}}_k$.

Now for even a medium-sized power system with a low degree of measurement redundancy, the matrices H and hence G are characterised by high dimensionality. The amount of matrix manipulation operations entailed in the direct application of the GWLS technique (equation 3.2.7) is therefore formidable and leads to exceptionally long computational times. These properties of the GWLS method are extremely undesirable especially for applications where fast solution times and low computer storage requirements are necessary for successful implementation in a real-time environment on small process control computers. The long solution times may be partially reduced by re-using some of the computed elements of $\underline{h}(\hat{\underline{x}})$ when calculating elements of $H(\hat{\underline{x}})$ having the same defining expressions. Additionally, the incorporation of sparse matrix programming concepts in the development of the GWLS computer algorithm will offset some of the high storage requirements. Because the speed gains and the core reductions obtainable from the above mentioned considerations are still insufficient on large systems, more effective means of achieving these objectives are proposed, investigated and tested in this chapter.

Basically, the enhancement of the GWLS technique to reduce significantly both the solution time and the core requirement can be based either on simple intuitive approximations made on the estimation equation (3.2.7) or on the exploitation of the actual physical laws that govern the behaviour and characteristics of the power system. The

former approach is termed Algorithm based enhancement methods whilst the latter is referred to as Model based enhancement techniques[19].

To obtain a lucid picture of the physical justifications for the approximations made to attain gains in solution speed and reductions in core storage, the relevant expressions for $\underline{h}(\underline{x})$ and $H(\underline{x})$ in active ($\underline{P}$) / reactive ($\underline{Q}$) measurement component forms $\underline{h}_p(\underline{x})$ and $\underline{h}_Q(\underline{x})$ are given, namely:

$$\underline{h}_p(\underline{\delta},\underline{E}) \triangleq \begin{bmatrix} \underline{P}_i \\ \underline{P}_{ik} \end{bmatrix} , \qquad \underline{h}_Q(\underline{\delta},\underline{E}) \triangleq \begin{bmatrix} \underline{Q}_i \\ \underline{Q}_{ik} \\ \underline{E}_i \end{bmatrix}$$

where:

$$P_i = \sum_{k=1}^{N} E_i E_k (G_{ik} \cos\delta_{ik} + B_{ik} \sin\delta_{ik})$$

$$P_{ik} = -G_{ik} E_i^2 + E_i E_k (G_{ik} \cos\delta_{ik} + B_{ik} \sin\delta_{ik}) \qquad i \neq k$$

$$Q_i = \sum_{k=1}^{N} E_i E_k (G_{ik} \sin\delta_{ik} - B_{ik} \cos\delta_{ik})$$

$$Q_{ik} = (B_{ik} - YS_{ik}) E_i^2 + E_i E_k (G_{ik} \sin\delta_{ik} - B_{ik} \cos\delta_{ik}) \qquad i \neq k$$

and

$$H_{p\delta}^T = \begin{bmatrix} \dfrac{\partial \underline{P}_i}{\partial \underline{\delta}_j} & \dfrac{\partial \underline{P}_{ik}}{\partial \underline{\delta}_j} \end{bmatrix} \qquad H_{PE}^T = \begin{bmatrix} \underline{E}_j \dfrac{\partial \underline{P}_i}{\partial \underline{E}_j} & \underline{E}_j \dfrac{\partial \underline{P}_{ik}}{\partial \underline{E}_j} \end{bmatrix}$$

$$H_{Q\delta}^T = \begin{bmatrix} \dfrac{\partial \underline{Q}_i}{\partial \underline{\delta}_j} & \dfrac{\partial \underline{Q}_{ik}}{\partial \underline{\delta}_j} & \dfrac{\partial \underline{E}_i}{\partial \underline{\delta}_j} \end{bmatrix} \qquad H_{QE}^T = \begin{bmatrix} \underline{E}_j \dfrac{\partial \underline{Q}_i}{\partial \underline{E}_j} & \underline{E}_j \dfrac{\partial \underline{Q}_{ik}}{\partial \underline{E}_j} & \underline{E}_j \dfrac{\partial \underline{E}_i}{\partial \underline{E}_j} \end{bmatrix}$$

where:

$$\frac{\partial P_i}{\partial \delta_j} = \begin{cases} E_i E_k (G_{ik} \sin\delta_{ik} - B_{ik} \cos\delta_{ik}) & j = k \\ -B_{ii} E_i^2 - Q_i & j = i \end{cases}$$

$$\frac{\partial P_{ik}}{\partial \delta_j} = \begin{cases} E_i E_i (G_{ik} \sin\delta_{ik} - B_{ik} \cos\delta_{ik}) & j = k \\ -E_i E_k (G_{ik} \sin\delta_{ik} - B_{ik} \cos\delta_{ik}) & j = i \end{cases}$$

$$E_j \frac{\partial P_i}{\partial E_j} = \begin{cases} E_i E_k (G_{ik} \cos\delta_{ik} + B_{ik} \sin\delta_{ik}) & j = k \\ G_{ii} E_i^2 + P_i & j = i \end{cases}$$

$$E_j \frac{\partial P_{ik}}{\partial E_j} = \begin{cases} E_i E_k (G_{ik} \cos\delta_{ik} + B_{ik} \sin\delta_{ik}) & j = k \\ -2G_{ik} E_i^2 + E_i E_k (G_{ik} \cos\delta_{ik} + B_{ik} \sin\delta_{ik} & j = i \end{cases}$$

$$\frac{\partial Q_i}{\partial \delta_j} = \begin{cases} -E_i E_k (G_{ik} \cos\delta_{ik} + B_{ik} \sin\delta_{ik}) & j = k \\ -G_{ii} E_i^2 + P_i & j = i \end{cases}$$

$$\frac{\partial Q_{ik}}{\partial \delta_j} = \begin{cases} -E_i E_k (G_{ik} \cos\delta_{ik} + B_{ik} \sin\delta_{ik}) & j = k \\ E_i E_k (G_{ik} \cos\delta_{ik} + B_{ik} \sin\delta_{ik}) & j = i \end{cases}$$

$$\frac{\partial E_i}{\partial \delta_j} = \begin{cases} 0 & j = k \\ 0 & j = i \end{cases}$$

$$E_j \frac{\partial Q_i}{\partial E_j} = \begin{cases} E_i E_k (G_{ik} \sin\delta_{ik} - B_{ik} \cos\delta_{ik}) & j = k \\ -B_{ii} E_i^2 + Q_i & j = i \end{cases}$$

$$E_j \frac{\partial Q_{ik}}{\partial E_j} = \begin{cases} E_i E_k (G_{ik} \sin\delta_{ik} - B_{ik} \cos\delta_{ik}) & j = k \\ 2(B_{ik} - YS_{ik}) E_i^2 + E_i E_k (G_{ik} \sin\delta_{ik} - B_{ik} \cos\delta_{ik}) & j = i \end{cases}$$

$$E_j \frac{\partial E_i}{\partial E_j} = \begin{cases} 0 & j = k \\ E_i & j = i \end{cases}$$

for i, j, k = 1, 2,...,N

where N is the total number of network busbars

$G_{ik}+jB_{ik}$ is the i-kth element of the bus admittance matrix

YS_{ik} is the charging admittance of line ik at node i

$\delta_{ik}=\delta_i-\delta_k$ is the voltage angle difference

Observe that in deriving the elements for $H(\underline{x})$, all derivatives with respect to E have been post-multiplied by the appropriate E_j term to yield a new state estimate mismatch vector $\Delta \underline{x} = (\Delta \underline{\delta} \Delta \underline{E}/\underline{E})^T$. This modification has led to some submatrices of $H(\underline{x})$ becoming identical - hence they need to be computed once only for every given iteration. Incidentally it has also given a conventional Newton-Raphson Load flow [54,55] flavour to the GWLS estimation problem. Garcia and Abreu[19] achieved slightly different results by artificially dividing all the measured variables (prior to differentiation), except the E variables, by E. Yet another arbitrary technique with the same goal was employed by Couch[16] where in contrast only the reactive power related measurements were divided by the appropriate E_j term. Because the GWLS estimation process is now structurally similar to the Newton-Raphson Load Flow problem, it is possible to assume all or some of the physically justifiable assumptions[54,55] made in deriving the conventional fast decoupled load flow technique to enhance the computational characteristics of the GWLS power system static state estimation problem.

3.3 Algorithm - and Model - based approximations to GWLS state estimation

3.3.1 Algorithm-based methods

With these techniques of computational enhancement, the actual system of linear estimation equations (3.2.7) is modified with the view of yielding a superior solution procedure. Generally these methods depend on the results of a linearised stability analysis[29] of equation (3.2.7) which indicate that, provided G is any full-rank, positive-definite matrix, the estimation scheme is stable and converges to a value of $\hat{\underline{x}}$ that satisfies equation (3.2.4). One such gain matrix, called a CONSTANT GAIN MATRIX ESTIMATOR was suggested by Schweppe and Handschin[29] and used in various modified forms by Hórisberger et al.[14] and Couch et al[18]. In their approach a constant gain matrix $G(\underline{x}_o) = H_o^T R^{-1} H_o$ is utilised where the off-diagonal block matrices of G, that is, $G_{\delta E}$; $G_{E\delta}$ are both ignored and the remaining sub-matrices $G_{\delta\delta}$, G_{EE} held constant at their nominal or flat start voltage values of $G_{\delta\delta}$ (1.0,0.0) and $G_{EE}(1.0,0.0)$. No approximations are assumed in evaluating and updating the right-hand-side independent vector terms $\Delta \underline{b}_p$ and $\Delta \underline{b}_Q$. The resulting system of equations are:

$$\begin{bmatrix} G_{\delta\delta}(1.0,0.0) & \cdots\ 0 \\ 0 & G_{EE}(1.0,0.0) \end{bmatrix} \begin{bmatrix} \Delta\underline{\delta}_k \\ \Delta E_{k/}\underline{E}_k \end{bmatrix} = \begin{bmatrix} \Delta \underline{b}_p \\ \Delta \underline{b}_Q \end{bmatrix} \qquad (3.3.1)$$

It can be appreciated from equation (3.3.1) that the computational effort of repeatedly updating G together with its triangular factors is substantially reduced because G is constant. Further, because of the decoupled nature of G, savings in storage requirements are also

possible if solutions for $\Delta\underline{\delta}_k$ and $\Delta\underline{E}_k/E_k$ are derived separately from:

$G_{\delta\delta}\ (1.0,0.0)\quad \Delta\underline{\delta}_k = \Delta\underline{b}_p$

$G_{EE}\ (1.0,0.0)\quad \Delta\underline{E}_k/\underline{E}_k = \Delta\underline{b}_Q$

3.3.2 Model-based methods

Model-based techniques rely on approximations to the GWLS estimation scheme that are derived from the physical laws of operational behaviour of real electric power systems. Two distinct estimation techniques may be obtained through such physical assumptions, viz: P-δ, Q-E DECOUPLED ESTIMATOR and FAST DECOUPLED ESTIMATOR, FDE.

(a) P-δ, Q-E decoupled estimator

For the majority of most real existing power systems, active power variables tend to be more predominantly affected by variations in bus voltage angles whereas reactive power variables are more sensitive to changes in node voltage magnitudes. Cross-coupling effects are either very insignificant or virtually non-existent [55,56]. This loose coupling, between real power and voltage magnitude on the one hand, and reactive power and voltage angle on the other, is exploited in the P-δ, Q-E Estimator by nulling the coupling submatrices H_{PE}, $H_{Q\delta}$ of $H(\underline{x})$ on both sides of equation (3.2.7) to yield the following completely decoupled and separated system of equations.

$$\begin{array}{|c|c|}\hline H_{p\delta}{}^{T}R_p^{-1}H_{p\delta} & 0 \\ \hline 0 & H_{QE}{}^{T}R_Q^{-1}H_{QE} \\ \hline \end{array} \quad \begin{array}{|c|}\hline \Delta\underline{\delta}_k \\ \hline \Delta\underline{E}_k/\underline{E}_k \\ \hline \end{array} = \begin{array}{|c|}\hline H_{p\delta}{}^{T}R_p^{-1}\,\Delta\underline{Z}_p \\ \hline H_{QE}^{T}R_Q^{-1}\,\Delta\underline{Z}_Q \\ \hline \end{array} \qquad (3.3.2)$$

To solve for $\Delta\underline{\delta}_k$ and $\Delta\underline{E}_k/\underline{E}_k$, all the elements of $H_{p\delta}$ and H_{QE} must be

repeatedly updated at each stage of the iterative solution procedure. This estimator leads to two distinct estimation loops - one for computing voltage angles from real power measurements and the other for evaluating voltage magnitudes (and transformer tap ratios if any) from reactive power measurements. From these two loops the state estimates may be derived in an accelerated fashion by iterating back-and-forth between the two loops, where only the most recent estimate of $\hat{\underline{\delta}}$ is used in the next evaluation of $\hat{\underline{E}}$ as in the fast decoupled load flow, namely:

$$H_{p\delta}^{T}(\hat{\underline{\delta}}_k,\hat{\underline{E}}_k)\, R_p^{-1} H_{p\delta}(\hat{\underline{\delta}}_k,\hat{\underline{E}}_k)\,\Delta\underline{\delta}_k = H_{p\delta}^{T}(\hat{\underline{\delta}}_k,\hat{\underline{E}}_k) R_p^{-1}\Delta \underline{Z}_p(\hat{\underline{\delta}}_k,\hat{\underline{E}}_k)$$

$$H_{QE}^{T}(\hat{\underline{\delta}}_{k+1},\hat{\underline{E}}_k) R_Q^{-1} H_{QE}(\hat{\underline{\delta}}_{k+1},\hat{\underline{E}}_k)\,\Delta\underline{E}_k/\hat{\underline{E}}_k = H_{QE}^{T}(\hat{\underline{\delta}}_{k+1},\hat{\underline{E}}_k) R_Q^{-1}\Delta \underline{Z}_Q(\hat{\underline{\delta}}_{k+1},\hat{\underline{E}}_k)$$

In this form the P-δ, Q-E Estimator obviously possesses a faster solution time and a lower core storage requirement than the fully-fledged GWLS estimation technique. Variants of this estimation technique have been applied by Uemura et al[17] and Aschmoneit et al[57,58] to networks with very high line X/R ratios, typically $\geq$ 10.0. It is shown from simulation results that the method of this thesis does not depend on this rather restrictive assumption.

(b) Fast Decoupled Estimator, FDE

The P-δ, Q-E Estimator serves as the ideal starting point for the derivation of the FDE. It is fairly straightforward to show that with H_{PE}, $H_{Q\delta}$ both nulled as in the P-δ, Q-E Estimator, the remaining submatrices $H_{p\delta}$, H_{QE} of $H(\underline{x})$ assume special values that correspond to the susceptances B_{ik} of the network bus admittance matrix provided the following practical network assumptions hold[54,55]:

$$Q_i \ll B_{ii}E_i^2 \quad ; \quad G_{ik}\sin\delta_{ik} \ll B_{ik} \quad ; \quad \cos\delta_{ik} \approx 1.0$$

$$E_i,\ E_k \approx 1.0 \text{ pu}$$

By invoking these assumptions, the following approximations may be obtained for the measurement Jacobian matrices:

$$\frac{\partial P_i}{\partial \delta_j} = E_j \frac{\partial Q_i}{\partial E_j} = \begin{pmatrix} -B_{ik} & j = k \\ -B_{ii} & j = i \end{pmatrix}$$

$$\frac{\partial P_{ik}}{\partial \delta_j} = E_j \frac{\partial Q_{ik}}{\partial E_j} = -B_{ik} \qquad j = k$$

$$\frac{\partial P_{ik}}{\partial \delta_j} = B_{ik} \qquad j = i$$

$$E_j \frac{\partial Q_{ik}}{\partial E_j} = B_{ik} - 2YS_{ik} \qquad j = i$$

The retained elements of the measurement Jacobian matrices are therefore constant and extremely sparse. Though the quadratic convergence of the full GWLS technique is lost, the FDE requires only one factorisation for solution and involves relatively fewer operations per iteration. Since no approximation is made to either $\Delta \underline{Z}_P$ or $\Delta \underline{Z}_Q$, it is not expected that the final solution will be seriously degenerate. The final form of the FDE algorithm is obtained by:

i. Omitting from $\partial P_i / \partial \delta_j$ and $\partial P_{ik} / \partial \delta_j$ all those network representations that predominantly affect reactive power quantities - line shunt admittances, off-nominal in-phase transformer taps,

ii. Omitting from $E_j \frac{\partial Q_i}{\partial E_j}$ and $E_j \frac{\partial Q_{ik}}{\partial E_j}$ the angle shifting effects of phase shifters, and lastly,

iii. Omitting line resistances in calculating $\partial P_i / \partial \delta_j$ and $\partial P_{ik} / \partial \delta_j$.

3.4 Interpretation of estimates

As in the LWLS technique of Chapter II, once a converged solution has been obtained for $\hat{\underline{x}}$, reliability checks are performed on the input measurements and the estimates by performing statistical hypothesis tests on the post-estimation performance index $J(\hat{\underline{x}})$ produced by each of the GWLS estimation methods.

In Table A.1 of Appendix A it is shown that $J(\hat{\underline{x}})$ possesses the statistics:

$$E\{J(\hat{\underline{x}})\} = df(= m-n)$$

$$J(\hat{\underline{x}}) \sim \chi^2_{df}$$

Since in the absence of any bad data $J(\hat{\underline{x}})$ also obeys the probability law

$$Pr\left[J(\hat{\underline{x}}) \leq \chi^2_{df,\alpha}\right] = \alpha$$

the states and input data are deemed reliable once the above law is satisfied. Subsequently confidence limits may be created for $\hat{\underline{x}}$, namely:

$$CL_{1,2}(\hat{x}_i) = \hat{x}_i \pm t_{df,\frac{1+\alpha}{2}} \sqrt{\Sigma^H_{x_{ii}}}$$

where

$\Sigma^H_x \triangleq \left[H^T(\hat{\underline{x}})R^{-1}H(\hat{\underline{x}})\right]^{-1}$ the covariance matrix of the estimates.

Such limits may similarly be derived for all the other calculated system measurements, $\hat{\underline{z}} = \underline{h}(\hat{\underline{x}})$.

3.5 Off-line computer simulations for GWLS P-δ , Q-E; and FDE state estimators

The four standard test systems of Appendix A Tables A.3.1 to A.3.8 were used to numerically assess the feasibility of the GWLS techniques derived in this chapter. Varying degrees of redundancies were obtained by considering various combinations of meter locations and types. The metering patterns adopted are shown in Figs. 3.1 to 3.4,

where the nodes have all been re-numbered so that the N-th node in each network is now the assumed reference . The simulated measurements were generated from the true load flow values corrupted with zero-mean Gaussian random numbers of standard deviations equal to 2% of the true load flow values.

Cholesky's Decomposition technique[53] is often the recommended method for solving the linearised equation of (3.2.7). However the bifactorisation method[44] is of comparable efficiency and was used in the simulations to provide a meaningful comparison of the solution times for the LWLS and GWLS methods.

A convergence tolerance index of $\Delta = 10^{-4}$ for both voltage magnitudes and angles was assumed, whilst the $J(\hat{\underline{x}})$ detection tests were performed at a significance level of $\alpha = 99$.

Fig. 3.5 shows a joint flow chart for the off-line simulations of all the GWLS algorithms. The results of all the schemes are shown separately in Tables 3.1 to 3.12 and a summary of the more important results (algorithm-wise) is given in Table 3.13.

3.6 Discussion of results and comments

The Constant-Gain-Matrix method generally either failed to converge or on the occasions when it did, it required an exceptionally large number of iterations and yet failed to produce acceptable estimates. For these reasons all subsequent efforts were focussed on the model algorithms, P-δ, Q-E and FDE methods.

The results of the estimated network voltage profiles presented in Tables 3.1 to 3.12 indicate that the estimates produced by the P-δ,

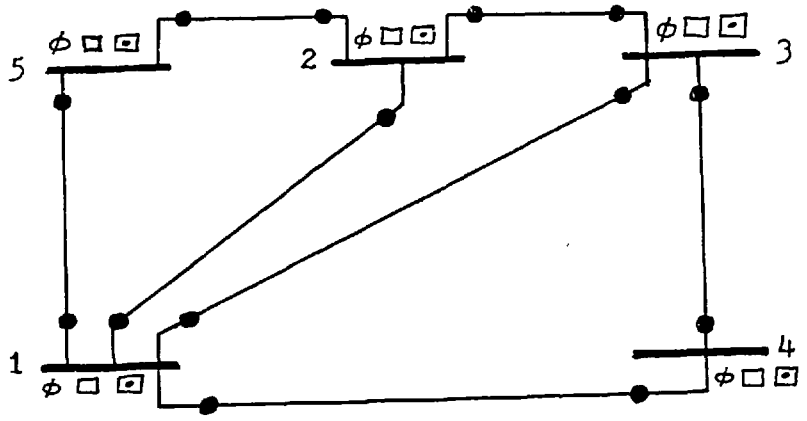

FIGURE 3.1: METERING PATTERN FOR SYSTEM OF 5-NODES, 7-LINES NETWORK

⊡,□Active, reactive power injection meter
• Active, reactive power flow meter
ϕ Voltage magnitude meter

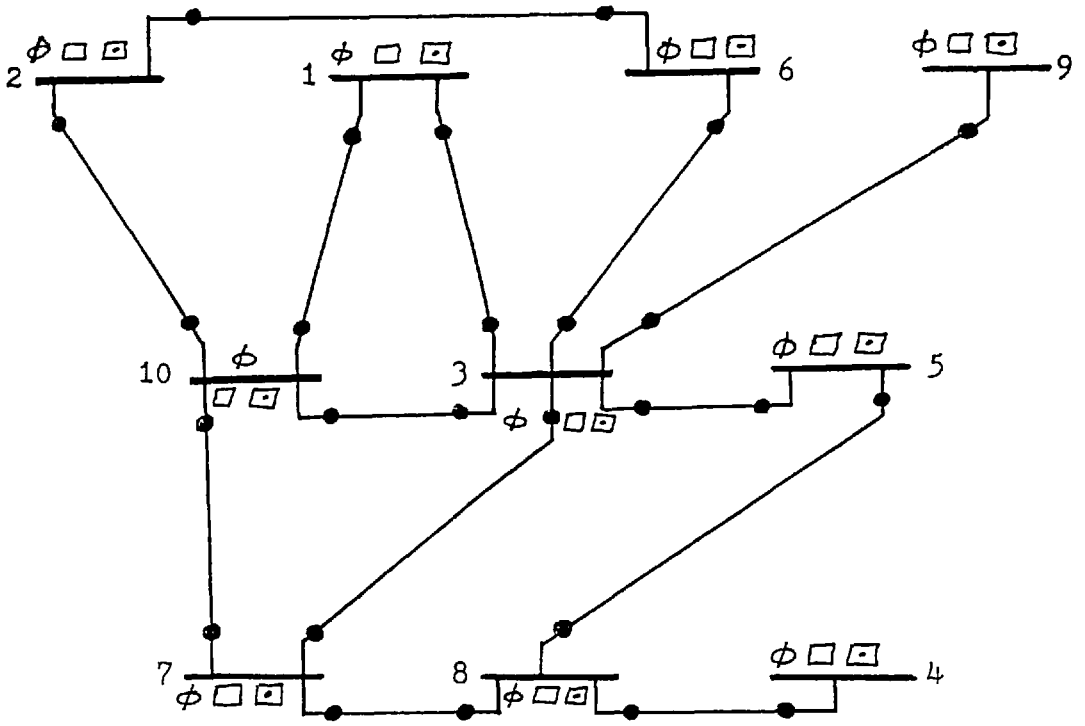

FIGURE 3.2: METERING PATTERN FOR SYSTEM OF 10-NODES, 13-LINES NETWORK

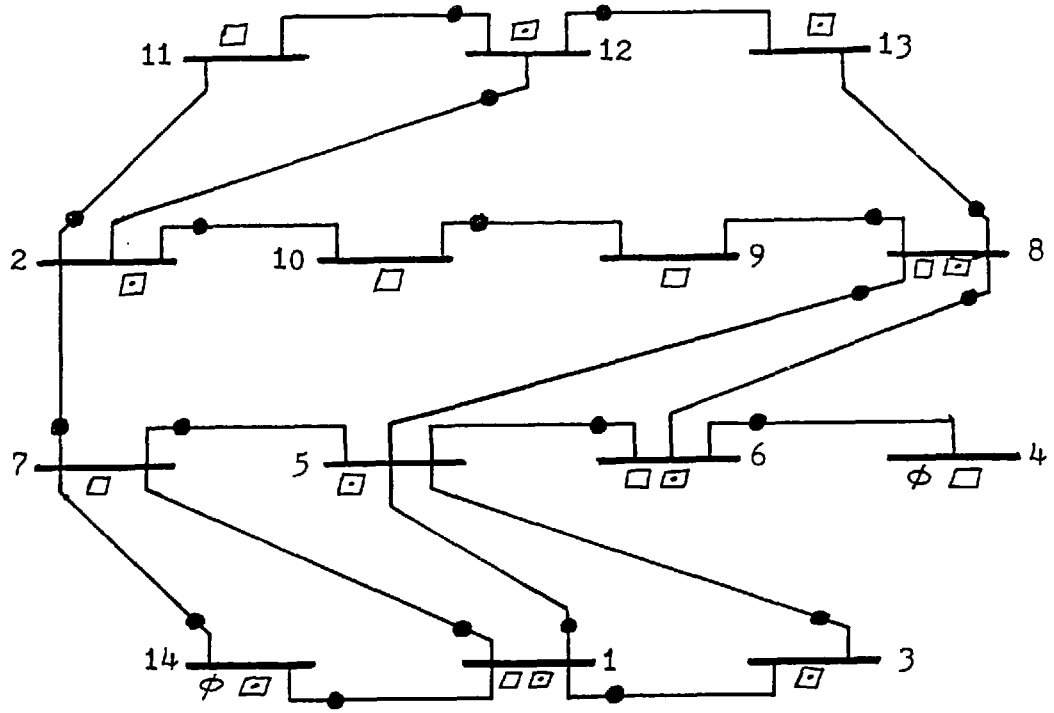

FIGURE 3.3: METERING PATTERN FOR SYSTEM OF 14-NODES, 20-LINES NETWORK

⊡, □ Active, reactive power injection meter
• Active, reactive power flow meter
ϕ Voltage magnitude meter

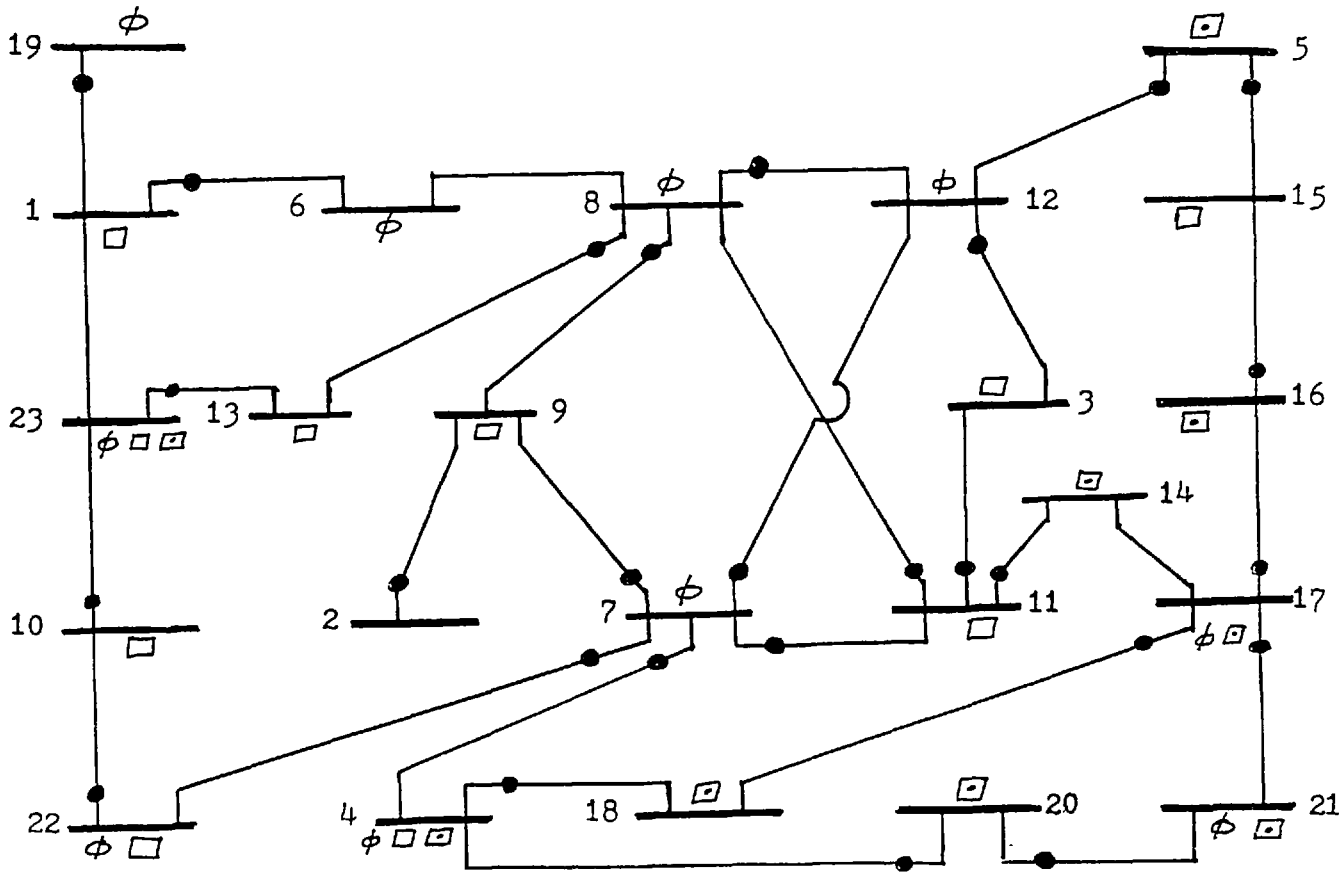

FIGURE 3.4: METERING PATTERN FOR SYSTEM OF 23-NODES, 30-LINES NETWORK

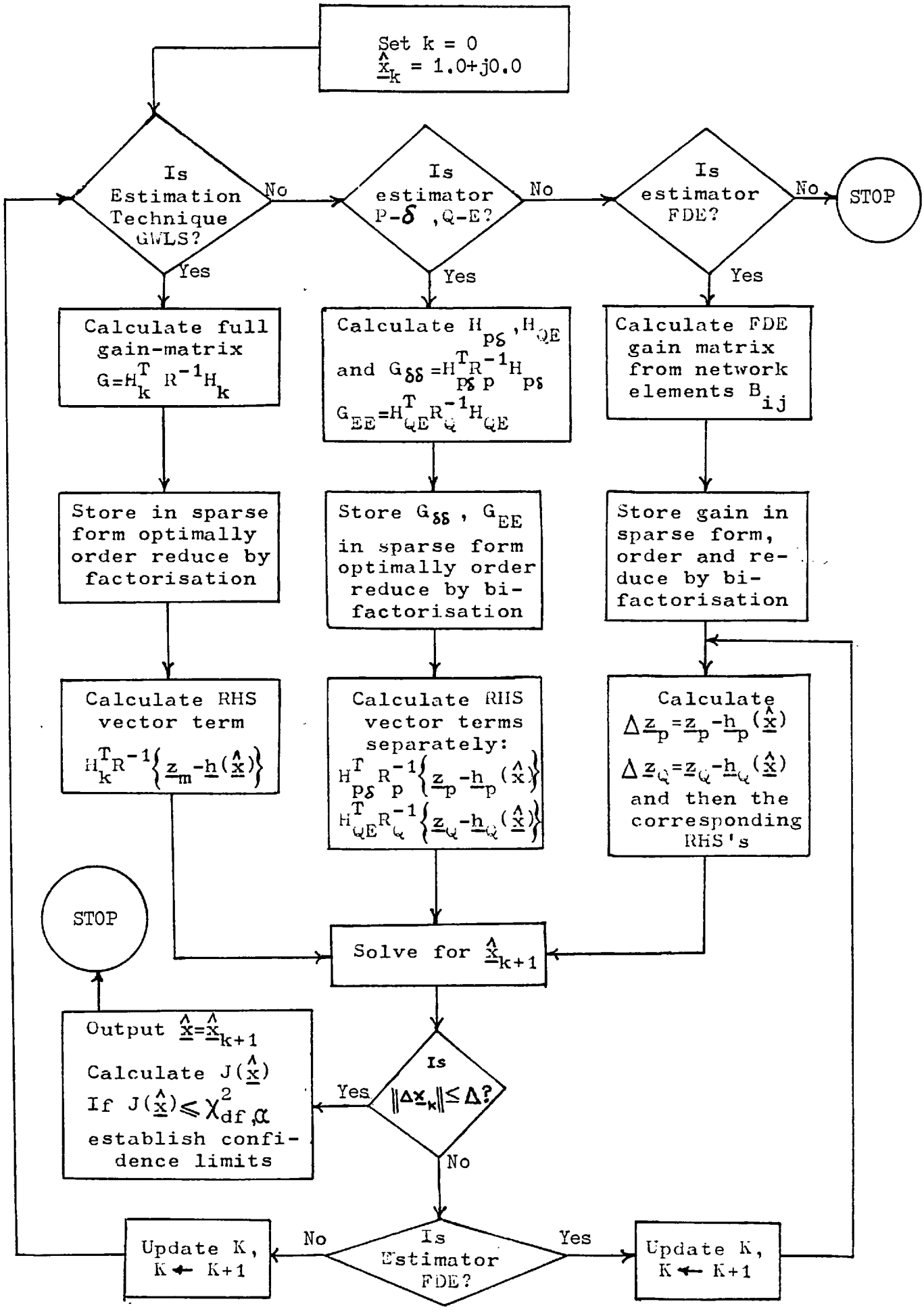

FIGURE 3.5: COMBINED FLOW CHART FOR GWLS ESTIMATION METHODS

Q-E estimator and FDE methods are all acceptable and of comparable accuracy to those of the full GWLS method. On the average the converged estimates required 4 iterations for GWLS, 9 iterations for P-δ, Q-E and 10 iterations for FDE method as shown in Table 3.13. The effective computation times, t_{total} verify the superiority in speed of the P-δ, Q-E and FDE estimators over the full GWLS method. The fastest execution time obtained was provided by the FDE method which gave a high speed gain of 10 to 1 for the 23-NODES, 30-LINES network at 45.0 degrees of freedom. It must be conceded, though, that to achieve this tremendous speed gain, the Newton-like quadratic convergence nature of the full GWLS method has been sacrificed for a geometric convergence characteristic[59] requiring an increased number of iterations.

Only very small variations in $J(\hat{\underline{x}})$ have occurred as a result of using the enhanced techniques as shown in Table 3.13. The values of the post-estimation performance indices $J(\hat{\underline{x}})$ are all less than their corresponding limiting chi-square values $\chi^2_{df,99.0\%}$ confirming the reliability of the estimated voltages and input measurements. Confidence limits, which span the true-but-unknown network voltage profiles, were also constructed as in Tables 3.1 to 3.12. In all cases, the algorithms provided the necessary filtering effects required of estimators as may be appreciated from the generally smaller magnitudes of rms estimation errors compared with their standard deviations.

No explicit statements regarding the storage requirements of the estimation techniques have been made so far. This is because the

algorithms were principally designed for simulation purposes and therefore involved the use of arbitrarily large dimensional arrays which could be used for all the test networks and larger systems if desired. A more effective assessment of storage requirements would be pertinent in an on-line environment where a direct input-solve-output arrangement would exist.

The contributions offered in this chapter are:

i. The formulation of the GWLS estimation problem in a load flow manner and the subsequent derivation of the P-δ , Q-E estimator and FDE method from the normal physical network characteristics.

ii. A comparison of the computational properties of the GWLS algorithm and its enhanced methods of P-δ, Q-E estimator and FDE method. The results show that active/reactive decoupling introduces into the generalized weighted least squares method the same computational advantages as in the load flow solution.

TABLE 3.1

ESTIMATED VOLTAGE PROFILE AND STATISTICS FOR 5-NODES, 7-LINES NETWORK OBTAINED WITH THE GWLS ESTIMATOR

Bus Number	Voltage Magnitude	Voltage Angle	True Magnitude	True Angle
1	1.04832	-.04914	1.04744	-.04898
2	1.02501	-.08746	1.02418	-.08722
3	1.02442	-.09327	1.02357	-.09302
4	1.01859	-.10760	1.01794	-.10734
5	1.06098	0	1.06000	0

Bus Number	Voltage Magnitude	Voltage Angle	RMS Error	Standard Deviation	Confidence Limits
1	1.04832	-.04914	.00090	.00087	±.00213
2	1.02501	-.08746	.00086	.00095	±.00232
3	1.02442	-.09327	.00089	.00095	±.00233
4	1.01859	-.10760	.00070	.00098	±.00240

TABLE 3.2

ESTIMATED VOLTAGE PROFILE AND STATISTICS FOR 10-NODES 13-LINES NETWORK OBTAINED WITH THE GWLS ESTIMATOR

Bus Number	Voltage Magnitude	Voltage Angle	True Magnitude	True Angle
1	1.04948	.03294	1.04897	.03290
2	1.04927	-.11099	1.04897	-.11110
3	1.04029	-.10678	1.03999	-.10645
4	1.01024	-.18539	1.00994	-.18503
5	1.04025	-.15102	1.04000	-.15076
6	1.02999	-.13391	1.02962	-.13394
7	.95406	-.13367	.95428	-.13422
8	.99733	-.18834	.99704	-.18786
9	1.03227	-.06946	1.03231	-.06835
10	1.04053	0	1.04000	0

Bus Number	Voltage Magnitude	Voltage Angle	RMS Error	Standard Deviation	Confidence Limits
1	1.04948	.03294	.00052	.00073	±.00172
2	1.04927	-.11099	.00032	.00084	±.00199
3	1.04029	-.10678	.00045	.00087	±.00206
4	1.01024	-.18539	.00047	.00108	±.00256
5	1.04025	-.15102	.00036	.00091	±.00215
6	1.02999	-.13391	.00037	.00090	±.00214
7	.95406	-.13367	.00059	.00109	±.00258
8	.99733	-.18834	.00056	.00108	±.00257
9	1.03227	-.06946	.00111	.00098	±.00233

TABLE 3.3

ESTIMATED VOLTAGE PROFILE AND STATISTICS FOR 14-NODES, 20-LINES NETWORK OBTAINED WITH THE GWLS ESTIMATOR

Bus Number	Voltage Magnitude	Voltage Angle	True Magnitude	True Angle
1	1.04534	-.08697	1.04494	-.08691
2	1.06932	-.25029	1.06968	-.24822
3	1.01023	-.22209	1.00987	-.22194
4	1.08983	-.23498	1.08971	-.23327
5	1.01882	-.18052	1.01848	-.18016
6	1.06157	-.23506	1.06167	-.23335
7	1.02051	-.15322	1.02015	-.15322
8	1.05608	-.26260	1.05613	-.26087
9	1.05088	-.26545	1.05102	-.26365
10	1.05669	-.25988	1.05682	-.25815
11	1.05451	-.26524	1.05491	-.26314
12	1.04977	-.26660	1.05014	-.26456
13	1.03529	-.28184	1.03551	-.27993
14	1.06052	0	1.06000	0

Bus Number	Voltage Magnitude	Voltage Angle	RMS Error	Standard Deviation	Confidence Limits
1	1.04534	-.08697	.00041	.00139	±.00337
2	1.06932	-.25029	.00210	.00168	±.00408
3	1.01023	-.22209	.00039	.00158	±.00385
4	1.08983	-.23498	.00171	.00167	±.00406
5	1.01882	-.18052	.00050	.00152	±.00371
6	1.06157	-.23506	.00172	.00170	±.00413
7	1.02051	-.15322	.00036	.00150	±.00365
8	1.05608	-.26260	.00173	.00169m	±.00411
9	1.05088	-.26545	.00180	.00171	±.00416
10	1.05669	-.25988	.00174	.00170	±.00413
11	1.05451	-.26524	.00213	.00173	±.00421
12	1.04977	-.26660	.00207	.00174	±.00424
13	1.03529	-.28184	.00192	.00181	±.00440

TABLE 3.4

ESTIMATED VOLTAGE PROFILE AND STATISTICS FOR 23-NODES, 30-LINES NETWORK OBTAINED WITH THE GWLS ESTIMATOR

Bus Number	Voltage Magnitude	Voltage Angle	True Magnitude	True Angle
1	1.02204	-.02892	1.02181	-.02838
2	1.03630	.08689	1.03524	.08724
3	1.05008	.16210	1.04997	.16330
4	1.05042	.29208	1.05003	.29293
5	1.05039	.34032	1.05001	.34115
6	.99566	.00581	.99542	.00603
7	1.00061	.16697	1.00049	.16862
8	1.00470	.03945	1.00449	.03973
9	.98453	.04819	.98357	.04882
10	1.01059	.02276	1.01026	.02257
11	1.03634	.14182	1.03614	.14274
12	1.03557	.17912	1.03515	.18067
13	1.00128	.00541	1.00102	.00549
14	1.01765	.13991	1.01717	.14085
15	1.02107	.24986	1.02068	.25059
16	1.01266	.21377	1.01225	.21474
17	1.01646	.19340	1.01606	.19402
18	1.01217	.18658	1.01176	.18710
19	.98930	-.06939	.98931	-.06838
20	1.03033	.23651	1.02974	.23723
21	1.03109	.23425	1.03051	.23495
22	.98504	.08546	.98454	.08603
23	1.01885	0	1.01860	0

Bus Number	Voltage Magnitude	Voltage Angle	RMS Error	Standard Deviation	Confidence Limits
1	1.02204	-.02892	.00059	.00083	±.00199
2	1.03630	.08689	.00112	.00137	±.00330
3	1.05008	.16210	.00121	.00132	±.00320
4	1.05042	.29208	.00094	.00133	±.00320
5	1.05039	.34032	.00091	.00148	±.00358
6	.99566	.00581	.00033	.00090	±.00217
7	1.00061	.16697	.00166	.00132	±.00319
8	1.00470	.03945	.00035	.00087	±.00211
9	.98453	.04819	.00115	.00094	±.00226
10	1.01059	.02276	.00039	.00075	±.00181
11	1.03634	.14182	.00094	.00133	±.00320
12	1.03557	.17912	.00161	.00131	±.00317
13	1.00128	.00541	.00027	.00072	±.00173
14	1.01765	.13991	.00106	.00134	±.00323
15	1.02107	.24986	.00083	.00153	±.00368
16	1.01266	.21377	.00106	.00139	±.00336
17	1.01646	.19340	.00074	.00134	±.00324
18	1.01217	.18658	.00066	.00136	±.00327
19	.98930	-.06939	.00101	.00132	±.00320
20	1.03033	.23651	.00093	.00134	±.00323
21	1.03109	.23425	.00091	.00134	±.00322
22	.98504	.08546	.00075	.00117	±.00283

TABLE 3.5

ESTIMATED VOLTAGE PROFILE AND STATISTICS FOR 5-NODES, 7-LINES NETWORK OBTAINED WITH THE P-δ , Q-E ESTIMATOR

Bus Number	Voltage Magnitude	Voltage Angle	True Magnitude	True Angle
1	1.04840	-.04895	1.04744	-.04898
2	1.02515	-.08706	1.02418	-.08722
3	1.02456	-.09287	1.02357	-.09302
4	1.01872	-.10726	1.01794	-.10734
5	1.06100	0	1.06000	0

Bus Number	Voltage Magnitude	Voltage Angle	RMS Error	Standard Deviation	Confidence Limits
1	1.04840	-.04895	.00096	.00093	$\pm$.00228
2	1.02515	-.08706	.00098	.00105	$\pm$.00257
3	1.02456	-.09287	.00100	.00105	$\pm$.00258
4	1.01872	-.10726	.00078	.00107	$\pm$.00263

TABLE 3.6

ESTIMATED VOLTAGE PROFILE AND STATISTICS FOR 10-NODES, 13-LINES NETWORK OBTAINED WITH THE P-δ , Q-E ESTIMATOR

Bus Number	Voltage Magnitude	Voltage Angle	True Magnitude	True Angle
1	1.04944	.03297	1.04897	.03290
2	1.04922	-.11130	1.04897	-.11110
3	1.04019	-.10727	1.03999	-.10645
4	1.01014	-.18584	1.00994	-.18503
5	1.04016	-.15148	1.04000	-.15076
6	1.02992	-.13427	1.02962	-.13394
7	.95394	-.13411	.95428	-.13422
8	.99724	-.18880	.99704	-.18786
9	1.03219	-.06992	1.03231	-.06835
10	1.04047	0	1.04000	0

Bus Number	Voltage Magnitude	Voltage Angle	RMS Error	Standard Deviation	Confidence Limits
1	1.04944	.03297	.00047	.00079	$\pm$.00186
2	1.04922	-.11130	.00032	.00089	$\pm$.00211
3	1.04019	-.10727	.00085	.00095	$\pm$.00225
4	1.01014	-.18584	.00084	.00113	$\pm$.00268
5	1.04016	-.15148	.00074	.00097	$\pm$.00230
6	1.02992	-.13427	.00045	.00096	$\pm$.00228
7	.95394	-.13411	.00036	.00115	$\pm$.00273
8	.99724	-.18880	.00096	.00113	$\pm$.00268
9	1.03219	-.06992	.00158	.00108	$\pm$.00255

TABLE 3.7

ESTIMATED VOLTAGE PROFILE AND STATISTICS FOR 14-NODES, 20-LINES NETWORK OBTAINED WITH THE P-δ , Q-E ESTIMATOR

Bus Number	Voltage Magnitude	Voltage Angle	True Magnitude	True Angle
1	1.04637	-.08683	1.04494	-.08691
2	1.07032	-.24974	1.06968	-.24822
3	1.01127	-.22170	1.00987	-.22194
4	1.09077	-.23449	1.08971	-.23327
5	1.01985	-.18024	1.01848	-.18016
6	1.06257	-.23457	1.06167	-.23335
7	1.02155	-.15298	1.02015	-.15322
8	1.05709	-.26205	1.05613	-.26087
9	1.05189	-.26490	1.05102	-.26365
10	1.05771	-.25934	1.05682	-.25815
11	1.05555	-.26468	1.05491	-.26314
12	1.05081	-.26604	1.05014	-.26456
13	1.03635	-.28125	1.03551	-.27993
14	1.06154	0	1.06000	0

Bus Number	Voltage Magnitude	Voltage Angle	RMS Error	Standard Deviation	Confidence Limits
1	1.04637	-.08683	.00143	.00139	$\pm$.00337
2	1.07032	-.24974	.00165	.00156	$\pm$.00379
3	1.01127	-.22170	.00142	.00140	$\pm$.00341
4	1.09077	-.23449	.00162	.00156	$\pm$.00378
5	1.01985	-.18024	.00137	.00142	$\pm$.00345
6	1.06257	-.23457	.00152	.00158	$\pm$.00384
7	1.02155	-.15298	.00142	.00143	$\pm$.00348
8	1.05709	-.26205	.00152	.00154	$\pm$.00373
9	1.05189	-.26490	.00152	.00155	$\pm$.00378
10	1.05771	-.25934	.00148	.00155	$\pm$.00378
11	1.05555	-.26468	.00167	.00159	$\pm$.00385
12	1.05081	-.26604	.00162	.00159	$\pm$.00387
13	1.03635	-.28125	.00156	.00164	$\pm$.00398

TABLE 3.8

ESTIMATED VOLTAGE PROFILE AND STATISTICS FOR 23-NODES, 30-LINES NETWORK OBTAINED WITH THE P-δ , Q-E ESTIMATOR

Bus Number	Voltage Magnitude	Voltage Angle	True Magnitude	True Angle
1	1.02179	-.02883	1.02181	-.02838
2	1.03604	.08704	1.03524	.08724
3	1.04994	.16293	1.04997	.16330
4	1.05030	.29297	1.05003	.29293
5	1.05026	.34122	1.05001	.34115
6	.99544	.00586	.99542	.00603
7	1.00046	.16777	1.00049	.16862
8	1.00446	.03953	1.00449	.03973
9	.98427	.04828	.98357	.04882
10	1.01031	.02274	1.01026	.02257
11	1.03620	.14268	1.03614	.14274
12	1.03545	.17994	1.03515	.18067
13	1.00101	.00540	1.00102	.00549
14	1.01752	.14076	1.01717	.14085
15	1.02094	.25070	1.02068	.25059
16	1.01254	.21464	1.01225	.21474
17	1.01633	.19427	1.01606	.19402
18	1.01204	.18746	1.01176	.18710
19	.98896	-.06957	.98931	-.06838
20	1.03020	.23740	1.02974	.23723
21	1.03097	.23513	1.03051	.23495
22	.98476	.08581	.98454	.08603
23	1.01860	0	1.01860	0

Bus Number	Voltage Magnitude	Voltage Angle	RMS Error	Standard Deviation	Confidence Limits
1	1.02179	-.02883	.00045	.00080	$\pm$.00192
2	1.03604	.08704	.00082	.00148	$\pm$.00356
3	1.04994	.16293	.00037	.00141	$\pm$.00341
4	1.05030	.29297	.00027	.00141	$\pm$.00341
5	1.05026	.34122	.00026	.00155	$\pm$.00374
6	.99544	.00586	.00017	.00089	$\pm$.00216
7	1.00046	.16777	.00085	.00139	$\pm$.00336
8	1.00446	.03953	.00020	.00089	$\pm$.00214
9	.98427	.04828	.00088	.00093	$\pm$.00225
10	1.01031	.02274	.00018	.00073	$\pm$.00176
11	1.03620	.14268	.00009	.00141	$\pm$.00340
12	1.03545	.17994	.00079	.00140	$\pm$.00339
13	1.00101	.00540	.00009	.00067	$\pm$.00161
14	1.01752	.14076	.00036	.00142	$\pm$.00343
15	1.02094	.25070	.00028	.00161	$\pm$.00389
16	1.01254	.21464	.00030	.00148	$\pm$.00357
17	1.01633	.19427	.00037	.00143	$\pm$.00346
18	1.01204	.18746	.00046	.00145	$\pm$.00349
19	.98896	-.06957	.00124	.00138	$\pm$.00333
20	1.03020	.23740	.00049	.00143	$\pm$.00345
21	1.03097	.23513	.00049	.00143	$\pm$.00345
22	.98476	.08581	.00032	.00121	$\pm$.00291

TABLE 3.9

ESTIMATED VOLTAGE PROFILE AND STATISTICS FOR 5-NODES, 7-LINES NETWORK OBTAINED WITH THE FDE ESTIMATOR

Bus Number	Voltage Magnitude	Voltage Angle	True Magnitude	True Angle
1	1.04829	-.04898	1.04744	-.04898
2	1.02503	-.08712	1.02418	-.08722
3	1.02444	-.09293	1.02357	-.09302
4	1.01859	-.10733	1.01794	-.10734
5	1.06092	0	1.06000	0

Bus Number	Voltage Magnitude	Voltage Angle	RMS Error	Standard Deviation	Confidence Limits
1	1.04829	-.04898	.00085	.00094	$\pm$.00231
2	1.02503	-.08712	.00085	.00106	$\pm$.00259
3	1.02444	-.09293	.00087	.00107	$\pm$.00261
4	1.01859	-.10733	.00065	.00109	$\pm$.00266

TABLE 3.10

ESTIMATED VOLTAGE PROFILE AND STATISTICS FOR 10-NODES, 13-LINES NETWORK OBTAINED WITH THE FDE ESTIMATOR

Bus Number	Voltage Magnitude	Voltage Angle	True Magnitude	True Angle
1	1.04954	.03296	1.04897	.03290
2	1.04929	-.11130	1.04897	-.11110
3	1.04028	-.10726	1.03999	-.10645
4	1.01020	-.18580	1.00994	-.18503
5	1.04025	-.15146	1.04000	-.15076
6	1.03000	-.13425	1.02962	-.13394
7	.95402	-.13409	.95428	-.13422
8	.99730	-.18875	.99704	-.18786
9	1.03228	-.06992	1.03231	-.06835
10	1.04057	0	1.04000	0

Bus Number	Voltage Magnitude	Voltage Angle	RMS Error	Standard Deviation	Confidence Limits
1	1.04954	.03296	.00058	.00081	±.00193
2	1.04929	-.11130	.00038	.00094	±.00222
3	1.04028	-.10726	.00086	.00099	±.00235
4	1.01020	.18580	.00081	.00116	±.00275
5	1.04025	-.15146	.00075	.00102	±.00241
6	1.03000	-.13425	.00050	.00101	±.00238
7	.95402	-.13409	.00029	.00112	±.00265
8	.99730	-.18875	.00093	.00115	±.00272
9	1.03228	-.06992	.00157	.00112	±.00265

TABLE 3.11

ESTIMATED VOLTAGE PROFILE AND STATISTICS FOR 14-NODES, 20-LINES NETWORK OBTAINED WITH THE FDE ESTIMATOR

Bus Number	Voltage Magnitude	Voltage Angle	True Magnitude	True Angle
1	1.04570	-.08694	1.04494	-.08691
2	1.06964	-.25005	1.06968	-.24822
3	1.01059	-.22198	1.00987	-.22194
4	1.09014	-.23478	1.08971	-.23327
5	1.01917	-.18046	1.01848	-.18016
6	1.06191	-.23487	1.06167	-.23335
7	1.02087	-.15316	1.02015	-.15322
8	1.05642	-.26238	1.05613	-.26087
9	1.05122	-.26523	1.05102	-.26365
10	1.05703	-.25966	1.05682	-.25815
11	1.05488	-.26500	1.05491	-.26314
12	1.05014	-.26636	1.05014	-.26456
13	1.03568	-.28157	1.03551	-.27993
14	1.06087	0	1.06000	0

Bus Number	Voltage Magnitude	Voltage Angle	RMS Error	Standard Deviation	Confidence Limits
1	1.04570	-.08694	.00076	.00137	±.00333
2	1.06964	-.25005	.00183	.00167	±.00405
3	1.01059	-.22198	.00072	.00139	±.00337
4	1.09014	-.23478	.00157	.00171	±.00415
5	1.01917	-.18046	.00076	.00141	±.00342
6	1.06191	-.23487	.00153	.00169	±.00410
7	1.02087	-.15316	.00072	.00141	±.00342
8	1.05642	-.26238	.00153	.00162	±.00394
9	1.05122	-.26523	.00159	.00163	±.00397
10	1.05703	-.25966	.00153	.00164	±.00399
11	1.05488	-.26500	.00186	.00168	±.00409
12	1.05014	-.26636	.00180	.00168	±.00408
13	1.03568	-.28157	.00165	.00171	±.00417

TABLE 3.12

ESTIMATED VOLTAGE PROFILE AND STATISTICS FOR 23-NODES, 30-LINES NETWORK OBTAINED WITH THE FDE ESTIMATOR

Bus Number	Voltage Magnitude	Voltage Angle	True Magnitude	True Angle
1	1.02195	-.02881	1.02181	-.02838
2	1.03623	.08696	1.03524	.08724
3	1.05010	.16289	1.04997	.16330
4	1.05046	.29288	1.05003	.29293
5	1.05042	.34111	1.05001	.34115
6	.99558	.00588	.99542	.00603
7	1.00064	.16773	1.00049	.16862
8	1.00462	.03953	1.00449	.03973
9	.98440	.04828	.98357	.04882
10	1.01050	.02274	1.01026	.02257
11	1.03636	.14263	1.03614	.14274
12	1.03561	.17990	1.03515	.18067
13	1.00118	.00542	1.00102	.00549
14	1.01768	.14072	1.01717	.14085
15	1.02110	.25061	1.02068	.25059
16	1.01270	.21457	1.01225	.21474
17	1.01650	.19421	1.01606	.19402
18	1.01220	.18740	1.01176	.18710
19	.98912	-.06951	.98931	-.06838
20	1.03037	.23732	1.02974	.23723
21	1.03113	.23506	1.03051	.23495
22	.98492	.08579	.98454	.08603
23	1.01876	0	1.01860	0

Bus Number	Voltage Magnitude	Voltage Angle	RMS Error	Standard Deviation	Confidence Limits
1	1.02195	-.02881	.00045	.00085	±.00206
2	1.03623	.08696	.00103	.00155	±.00373
3	1.05010	.16289	.00043	.00145	±.00350
4	1.05046	.29288	.00043	.00144	±.00347
5	1.05042	.34111	.00042	.00159	±.00384
6	.99558	.00588	.00022	.00091	±.00220
7	1.00064	.16773	.00090	.00141	±.00341
8	1.00462	.03953	.00024	.00090	±.00217
9	.98440	.04828	.00099	.00094	±.00227
10	1.01050	.02274	.00030	.00076	±.00184
11	1.03636	.14263	.00024	.00144	±.00348
12	1.03561	.17990	.00090	.00143	±.00345
13	1.00118	.00542	.00017	.00069	±.00167
14	1.01768	.14072	.00053	.00144	±.00348
15	1.02110	.25061	.00042	.00164	±.00395
16	1.01270	.21457	.00048	.00149	±.00360
17	1.01650	.19421	.00048	.00145	±.00349
18	1.01220	.18740	.00054	.00146	±.00351
19	.98912	-.06951	.00115	.00143	±.00345
20	1.03037	.23732	.00063	.00145	±.00349
21	1.03113	.23506	.00063	.00145	±.00349
22	.98492	.08579	.00045	.00120	±.00289

TABLE 3.13

SUMMARY OF RESULTS FOR THE GWLS ESTIMATORS

Number of network nodes	Estimation technique	Number of measurements	Measurement redundancy or degrees of freedom	Redundancy ratio	Performance index	Chi-Square limit	Number of iterations for convergence	Time for optimal ordering (ms) *	Time for reduction (ms) *	Time for back substitution (ms) *	Total time for solution (ms) *
N	—	m	df=m-n	$\eta = \frac{df}{n}$	$J(\hat{\underline{x}})$	$\chi^2_{df,99\%}$	iter	t_{order}	t_{reduce}	t_{back}	t_{total}
5	GWLS	43	34	3.78	49.38	56.00	3	35.0	28.0	7.0	70.0
5	P-δ,Q-E	43	34	3.78	50.50	56.00	8	31.0	23.0	9.0	63.0
5	FDE	43	34	3.78	50.50	56.00	10	4.0	3.0	15.0	22.0
10	GWLS	82	63	3.32	63.30	92.00	3	163.0	123.0	19.0	305.0
10	P-δ,Q-E	82	63	3.32	64.10	92.00	6	102.0	70.0	22.0	194.0
10	FDE	82	63	3.32	64.02	92.00	7	18.0	13.0	26.0	57.0
14	GWLS	58	31	1.15	40.57	52.20	4	422.0	316.0	44.0	782.0
14	P-δ,Q-E	58	31	1.15	50.50	52.20	9	220.0	150.0	47.0	417.0
14	FDE	58	31	1.15	51.30	52.20	11	24.0	17.0	55.0	96.0
23	GWLS	90	45	1.00	51.31	71.60	4	549.0	379.0	61.0	989.0
23	P-δ,Q-E	90	45	1.00	59.60	71.60	9	375.0	195.0	69.0	639.0
23	FDE	90	45	1.00	60.03	71.60	10	43.0	21.0	79.0	143.0

n = 2N-1

*Computation times based on CDC 6600 Computer (ICCC) CPU times

CHAPTER IV

THE DETECTION AND IDENTIFICATION OF WRONG INPUT INFORMATION IN STATIC POWER SYSTEM STATE ESTIMATION

4.1 Introduction

Occasionally during a typical normal operating day, grossly erroneous input information may be fed to an on-line static power system state estimator. Erroneous input information may arise from a variety of causes, chief amongst which are:

i. Bad measurement data

ii. Network parameter errors

iii. Network structural errors

Bad measurement data is an inconsistent measurement with an error process not adequately described in terms of its initially assumed Gaussian error statistics. It happens when meter-communication failures occur or when meters are improperly calibrated giving rise to a distorted Gaussian error process of broad distribution around the tails of the normal distribution function. Under these conditions, the telemetered analogue measurements received by the on-line computer are either full-scale or zero readings.

Parameter errors are due mainly to miscalculated line parameters. This type of error is extremely rare for once a power system has been commissioned and operational for some considerable period of time, its line constants are known to a fairly high degree of accuracy.

Structural errors are caused by the lack of knowledge of the current updated network configuration because of possibly unreported breaker/

isolator status changes and line-switching operations. In estimation problems, configuration errors may be modelled as parameter errors if desired.

Since the LWLS and GWLS estimation methods of Chapters II and III respectively have been demonstrated to be viable only in the presence of normal small Gaussian random measurement noise, it is important also to evaluate their reliabilities, capabilities and flexibilities when handling wrong input information. Obviously when grossly erroneous input information is present, the performance of the estimators will be seriously degraded producing distorted, inaccurate and hence unacceptable complex busbar voltage state estimates. For these reasons it is necessary for any on-line power system estimation scheme to be capable of detecting the presence of wrong information (DETECTION), identifying the cause(s) and source(s) of this wrong information (IDENTIFICATION) and most important of all correcting or completely eliminating this anomalous situation. Because the two sources (ii) and (iii) of wrong information are not very common[7,29,49] the detection and identification schemes to be described will consider mainly the problem of bad input measurement data.

4.2 Statistical methods of detection and identification

When bad measurement data exist, the observation equation becomes biased by a constant vector $\underline{b}$ such that:

$$\underline{z}_m^{bad} = \begin{bmatrix} A\underline{x}_t + \underline{V} + \underline{b} & \text{LWLS} \\ \underline{h}(\underline{x}_t) + \underline{V} + \underline{b} & \text{GWLS} \end{bmatrix} \qquad (4.1)$$

where if the i-th measurement is bad, $\underline{b} = \alpha \underline{e}_i$ and $\underline{e}_i^T = (o,o,\ldots,o,1,o,\ldots o)$ and α = size of the bad data. Perhaps the simplest means of removing

bad data is through simple limit checks on the incoming telemetered raw measurements as prescribed in the CERL method [60]. Inevitably, however, some bad data will probably escape screening through these pre-filtering checks necessitating the prescription of more reliable and sophisticated means of removing them.

Detecting the presence of bad data, $\underline{b}$, and identifying its source is viewed as an hypothesis testing procedure of two probable outcomes H_o and H_1 where:

H_o : no bad data present

H_1 : H_o not true, i.e. bad data is present

For small random Gaussian measurement noise assumptions, the estimated performance index is shown to be (Appendix A)

$$J(\hat{\underline{x}}) = \begin{cases} \hat{\underline{r}}_A^T R^{-1} \hat{\underline{r}}_A = \underline{V}^T R^{-1} W_A \underline{V} & \text{LWLS} \\ \hat{\underline{r}}_A^T R^{-1} \hat{\underline{r}}_H = \underline{V}^T R^{-1} W_H \underline{V} & \text{GWLS} \end{cases} \tag{4.2}$$

where the sensitivity matrix W is:

$$\begin{aligned} W_A &= I - A(A^T R^{-1} A)^{-1} A^T R^{-1} && \text{LWLS} \\ W_H &= I - H(H^T R^{-1} H)^{-1} H^T R^{-1} && \text{GWLS} \end{aligned} \tag{4.3}$$

and $\hat{\underline{r}}$, the estimated measurement residual, is given as:

$$\begin{aligned} \hat{\underline{r}}_A &= \underline{z}_m - A\hat{\underline{x}} = W_A \underline{V} && \text{LWLS} \\ \hat{\underline{r}}_H &= \underline{z}_m - \underline{h}(\hat{\underline{x}}) = W_H \underline{V} && \text{GWLS} \end{aligned} \tag{4.4}$$

Further, because $J(\hat{\underline{x}})$ is chi-square distributed with df(=m-n) degrees of freedom and has expected value of df i.e

$E\{J(\hat{\underline{x}})\} = df$ and $J(\hat{\underline{x}}) \sim \chi^2_{df}$ the variance of $J(\hat{\underline{x}})$ is:

$Var\{J(\hat{\underline{x}})\} = 2df$

Therefore for a large measurement redundancy ($df \geq 30$) the standardised random variables ξ_1, ξ_2 are both unit normal, giving

$$\left.\begin{aligned} \xi_1 &= \frac{J(\hat{\underline{x}}) - df}{\sqrt{2df}} && \sim N(0, 1) \\ \xi_2 &= \sqrt{2J(\hat{\underline{x}})} - \sqrt{2df} && \sim N(0, 1) \end{aligned}\right\} \qquad (4.5)$$

In the presence of bad data, $\underline{v}$ is now effectively $\underline{v}+\alpha\underline{e}_i$ and the performance index becomes [47]:

$$J(\underline{x}) = \underline{v}^T R^{-1} W \underline{v} + 2\alpha e_i^T R^{-1} W \underline{v} + \alpha^2 \underline{e}_i^T R^{-1} W \underline{e}_i \qquad (4.6)$$

where the first term is as usual χ^2 distributed

the second term is normally distributed

the third term is a constant.

From equation (4.6) it is clear that in the presence of bad data, the contribution to $J(\hat{\underline{x}})$ from α is quadratic and predominates over that produced by the χ^2 distributed term. Hence $J(\hat{\underline{x}})$ provides a suitable test statistic for the detection theory.

The established approach to the detection problem consists of specifying a threshold parameter γ against which $J(\hat{\underline{x}})$ and/or ξ_1, ξ_2 are compared and the hypothesis tested as follows:

If $J(\hat{\underline{x}})$ or ξ_1 or ξ_2 $\left\{\begin{array}{ll} \leq \gamma & \text{Accept } H_o\text{, i.e no bad data exists} \\ > \gamma & \text{reject } H_o\text{, i.e bad data is present} \end{array}\right.$

The value of γ is statistically specified as the abscissa at which the chi-square probability distribution function is at a given probability of confidence (usually 99%). In the case of ξ_1, ξ_2, the normal distribution abscissa is used. For derived state estimates to be acceptable at a given γ, the probability of concluding that bad data exists when there is actually no bad data must be very low and

conversely the probability of detecting bad data when bad data exists must be very high. It is on these premises that the threshold value of γ is chosen as $\gamma = \chi^2_{df,\ 99.0\%}$. If the H_o hypothesis is accepted the state estimates $\hat{\underline{x}}$ are deemed reliable. However should H_o be rejected because $J(\hat{\underline{x}})$ is unusually larger than $\chi^2_{df,99.0\%}$, an identification must be performed to locate and correct the source of error.

The identification tests are based on the estimated measurement residuals $\hat{\underline{r}}$ of equation (4.4). Two modified residuals may be defined, namely weighted residuals, $\hat{\underline{r}}_w$, and normalized residuals, $\hat{\underline{r}}_N$ and are expressed as:

$$\hat{\underline{r}}_w = \begin{cases} \hat{\underline{r}}_A / \sqrt{R} & \text{LWLS} \\ \hat{\underline{r}}_H / \sqrt{R} & \text{GWLS} \end{cases}$$

$$\hat{\underline{r}}_N = \begin{cases} \hat{\underline{r}}_A / \sqrt{\Sigma_r^A} & \text{LWLS} \\ \hat{\underline{r}}_H / \sqrt{\Sigma_r^H} & \text{GWLS} \end{cases} \qquad (4.7)$$

where $\sum_r$ is the covariance matrix of the estimated measurement residuals given in Appendix A as:

$$\sum_r = \begin{cases} \sum_r^A = R - A(A^T R^{-1} A)^{-1} A^T & \text{LWLS} \\ \sum_r^H = R - H(H^T R^{-1} H)^{-1} H^T & \text{GWLS} \end{cases} \qquad (4.8)$$

Under Gaussian measurement noise assumptions both $\hat{\underline{r}}_w$ and $\hat{\underline{r}}_N$ are therefore unit normal random variables. Thus given a γ corresponding to the normal distribution threshold value at 99% probability of confidence, all those measurements whose $\hat{\underline{r}}_w$ and/or $\hat{\underline{r}}_N$ components exceed γ are assumed to be most probably in error. In practical situations only the measurement with the largest $\hat{\underline{r}}_w$ and/or $\hat{\underline{r}}_N$ component is assumed to be in error because others might exceed γ

as a result of bad data spreading effect(s). In most cases the identified bad data is deleted from the input measurement set and re-estimation performed until the H_o hypothesis is accepted. It is important to note that the $\hat{\underline{r}}_W$ test is the simplest compared to the $\hat{\underline{r}}_N$ test which requires extra computations when calculating $\sum_r$. It is also pertinent to point out that the $\hat{\underline{r}}_N$ test is the more sensitive test as a result of the inequality $(\sum_r)_{ii} \leq R_{ii}$.

Recently it has been shown that because of the gain matrix retriangulations involved during re-estimation cycles,[19] a better way to treat identified bad data is to replace them by pseudo-measurements generated from the estimation process itself. The pseudo-measurement generation proceeds as follows:

From equations (4.1) and (4.4)

$$\hat{\underline{r}} = \underline{z}_m^{bad} - \hat{\underline{z}}^{bad} = W(\underline{v}+\underline{b}) = \sum_r R^{-1}(\underline{v} + \underline{b})$$

Hence

$$(\underline{v} + \underline{b}) \approx \sum_r^{-1} R(\underline{z}_m^{bad} - \hat{\underline{z}}^{bad}) \qquad (4.9)$$

However the exact value of $(\underline{v}+\underline{b})$ is given by:

$$(\underline{v} + \underline{b}) = \underline{z}_m^{bad} - \underline{z}_{true} \qquad (4.10)$$

Equating the right-hand-sides of equations (4.9) and (4.10) yields

$$\underline{z}_{true} \approx \underline{z}_m^{bad} - \sum_r^{-1} R(\underline{z}_m^{bad} - \hat{\underline{z}}^{bad}) \qquad (4.11)$$

where $\hat{\underline{z}}^{bad}$ = calculated measurement obtained with the distorted estimate of $\underline{x}$.

Equation (4.11) shows that from the known bad measurement $\underline{z}_m^{bad}$, its corresponding poor estimate $\hat{\underline{z}}^{bad}$ and the error covariance matrices $\sum_r$

and R, an approximate value of the true measurement may be derived. In such cases any identified bad measurement is replaced by its pseudo-measurement thus curtailing the expense required in updating the system matrices when identified bad measurements are deleted from the input information.

4.3 Discussion of simulations and results

The detection and identification tests were performed on all the chosen standard test systems using the LWLS AEP estimation technique as well as the various forms of the GWLS method. Bad data was generated by biasing some of the system measurements. These biased data were established randomly with a pseudo random number generator in the following way:

If r_n is the random number used to simulate the n-th measurement, then this n-th measurement is biased if $|r_n| \geq \beta$, where β is $n\sigma$, and $n\sigma$ = the bad data size, and

σ = the measurement standard deviation.

The magnitude of β determines the number of bad data points simulated, the smaller the value of β the greater the number of bad measurements.

The subsequent discussion centres mainly on the results obtained with the IEEE 14-NODES, 20-LINES network. Results obtained with 1 and 2 bad data points are given (Tables 4.1 to 4.2). Two types of detection and identification tests may be prescribed.

TYPE 1 Detection Tests with $J(\hat{\underline{x}}) < \chi^2_{df,99.0\%}$ and normal distribution identification tests with $\hat{\underline{r}}_w$, $\hat{\underline{r}}_N < \gamma$

TYPE 2 Detection Tests with ξ_1 $(\xi_2) < \gamma$ and normal distribution identification tests with $\hat{\underline{r}}_w$, $\hat{\underline{r}}_N < \gamma$

TABLE 4.1

$J(\hat{\underline{x}})$ Vs $\hat{\underline{r}}_W$, $\hat{\underline{r}}_N$ DETECTION AND IDENTIFICATION TESTS

Total number of measurements containing bad data	Selection stage	Measurements containing gross error	Objective function $J(\hat{\underline{x}})$	Total number of measurements whose $\hat{\underline{r}}_W > N(0,1)$	Total number of measurements whose $\hat{\underline{r}}_N > N(0,1)$	Measurement with largest $\hat{\underline{r}}_W$ value	Measurement with largest $\hat{\underline{r}}_N$ value
1	1st	7	31850	3	4	3	3
2	1st	3,9	32200	2	5	3	3
	2nd	9	4050	1	1	9	9

TABLE 4.2

ξ_1 Vs $\hat{\underline{r}}_W$, $\hat{\underline{r}}_N$ DETECTION AND IDENTIFICATION TESTS

Total number of measurements containing bad data	Selection stage	Measurements containing gross error	Normalised objective function	Total number of measurements whose $\hat{\underline{r}}_W > N(0,1)$	Total number of measurements whose $\hat{\underline{r}}_N > N(0,1)$	Measurement with largest $\hat{\underline{r}}_W$ value	Measurement with largest $\hat{\underline{r}}_N$ value
1	1st	3	3058	14	14	3	3
2	1st	3,9	3094	15	11	3	3
	2nd	9	384	7	7	9	9

These tests were performed at 99.0% probability of confidence, at which $\chi^2_{df,99\%} = 90.9$ and $\gamma = 2.81$.

In the presence of bad data (whether single or multiple), $J(\hat{\underline{x}})$ and ξ_1 (ξ_2) always detected this anomaly as manifested by their unusually large values shown in Tables 4.1 to 4.2. Subsequent identification of the source of bad data led to a selection of a much larger number of possible bad data points, because a greater number of weighted and normalized residuals $\hat{\underline{r}}_w$ and $\hat{\underline{r}}_N$ exceeded the stipulated normal distribution threshold value of $\gamma = 2.81$. However, for single bad data points, the largest residual always corresponded to the bad measurement. It was also observed that in certain cases some bad data were not initially selected as their residuals fell within the threshold values. They were identified in the next selection, after the previously selected bad data points had been deleted from the input measurement set or replaced by their pseudo-measurements.

To assess whether bad data effects spread appreciably, the residual sensitivity matrix W was always evaluated at the end of each estimation run. From this, the off-diagonal terms were found to be generally orders of magnitude smaller than the diagonal terms implying minimal bad data spreading effects.

The main concern of this chapter has been the assessment of the performance of all the static state estimators in the presence of bad data. The results obtained indicate that all the estimators are capable of detecting and identifying the sources of grossly erroneous input measurement information.

4.4 General comments

The results of Chapter III have shown that the FDE estimator is much faster than the full GWLS method. The computational speed is also comparable to that of the AEP method (compare Tables 2.5 and 3.13) and its core requirements are low when compounded with sparse matrix techniques. The results of this chapter have also confirmed that the residuals of FDE is as well capable of detecting and identifying bad data. These reasons, together with the fact that it accepts all kinds and types of input measurements make it probably the best technique to adopt for on-line static power system state estimation.

CHAPTER V

DECENTRALIZED DYNAMIC POWER SYSTEM STATE ESTIMATION

5.1 Introduction

All present-day power systems are identifiable as single contiguous entities where operating conditions at one location affect conditions at others; system operation therefore depends both on local conditions and controls as much as on the system-wide monitoring and control functions at a central location. Today, interruptions in power supply to consumers is almost totally intolerable necessitating that a power system operator be presented, with pertinent and relevant operating information that is required for crucial decision taking and vital remedial and corrective actions during emergency operation following system disturbances. The importance of having readily available complete and reliable knowledge of the power system operating state, essential for the secure and economic operation of the power system cannot be over-emphasized.

Most power system disturbances that originate from load fluctuations lead to changes in tie-line real power transfers and area frequency. In consequence some form of Load frequency control, LFC is merited[19].

The commonest LFC is based on an error signal derived from a linear combination of the net area-interchange and frequency error[20]. Application of modern control theory, using the Linear-Quadratic and Gaussian (LQG) design methods[61], has led to the realisation of suitable optimal and/or sub-optimal load frequency control techniques; however one of the pre-requisites for the success of these advanced design procedures entails a knowledge of all states of the power system

for feedback[62]. Feasible optimal and/or sub-optimal power system control is achievable provided all the states of the power system are identifiable.

As a power system is often recognisable as several sub-divisions interconnected by tie-lines, direct application of optimal control theory is often difficult for the following reasons:

i. the complete system description in its full non-linear representation leads to an unusually complicated set of differential equations of high dimensions

ii. power system areas often have partially independent controls of their own; hence it is impossible to collect continuously all system parameters and states of the overall power system at a given locality

iii. information exchange amongst the various power system areas is either non-existent or limited in amount . Consequently control signals are generated by processing information that are either wholly or, at best, partially local.

It is concluded that, for highly interconnected power systems composed of a number of areas, system security monitoring which involves the determination of the actual power system operating state and the optimal LFC of such a system involves system-wide instrumentation on a large scale, involving high investment cost for measurement and telemetry devices.

In an attempt to circumvent the problem of dimensionality and feedback of other area states and measurements, controllers may be designed on

a local basis[63]. Whilst global control involves the feedback of all area states and/or measurements, decentralized or local controls derive their feedback signals entirely from local area states. All these controllers are determined deterministically. It is assumed that all the system state variables (either local or global) are accessible for direct measurement and also that the instrumentation and transmission of the metered signals is perfect. Obviously, the fidelity and reliability of the controls obtained under these assumptions will be seriously impaired should the instrumentation be non-perfect or worse, should it be impossible to directly access and measure the state variables that are required for feedback control purposes.

To release these restrictive assumptions, recourse is taken to the reconstruction of the states from accessible but noise-corrupted system measurements which are not necessarily measurements of the state variables themselves but functions thereof by use of a Kalman filter technique based on the system dynamical equations[23,64,65].

Because of dimensionality problems encountered when designing single state estimators for power systems consisting of a large number of areas, this chapter considers the design of both global and decentralised power system state estimators.

5.2 LFC power system modelling

Block diagram representations of interconnected power systems of either steam or hydro generating plants are illustrated in Figs. 5.1 and 5.2 respectively. A steam unit is modelled by a turbine, a speed-governor and a generator; a hydro unit, on the other hand, has an additional control block on account of the gate water inertia. All control blocks

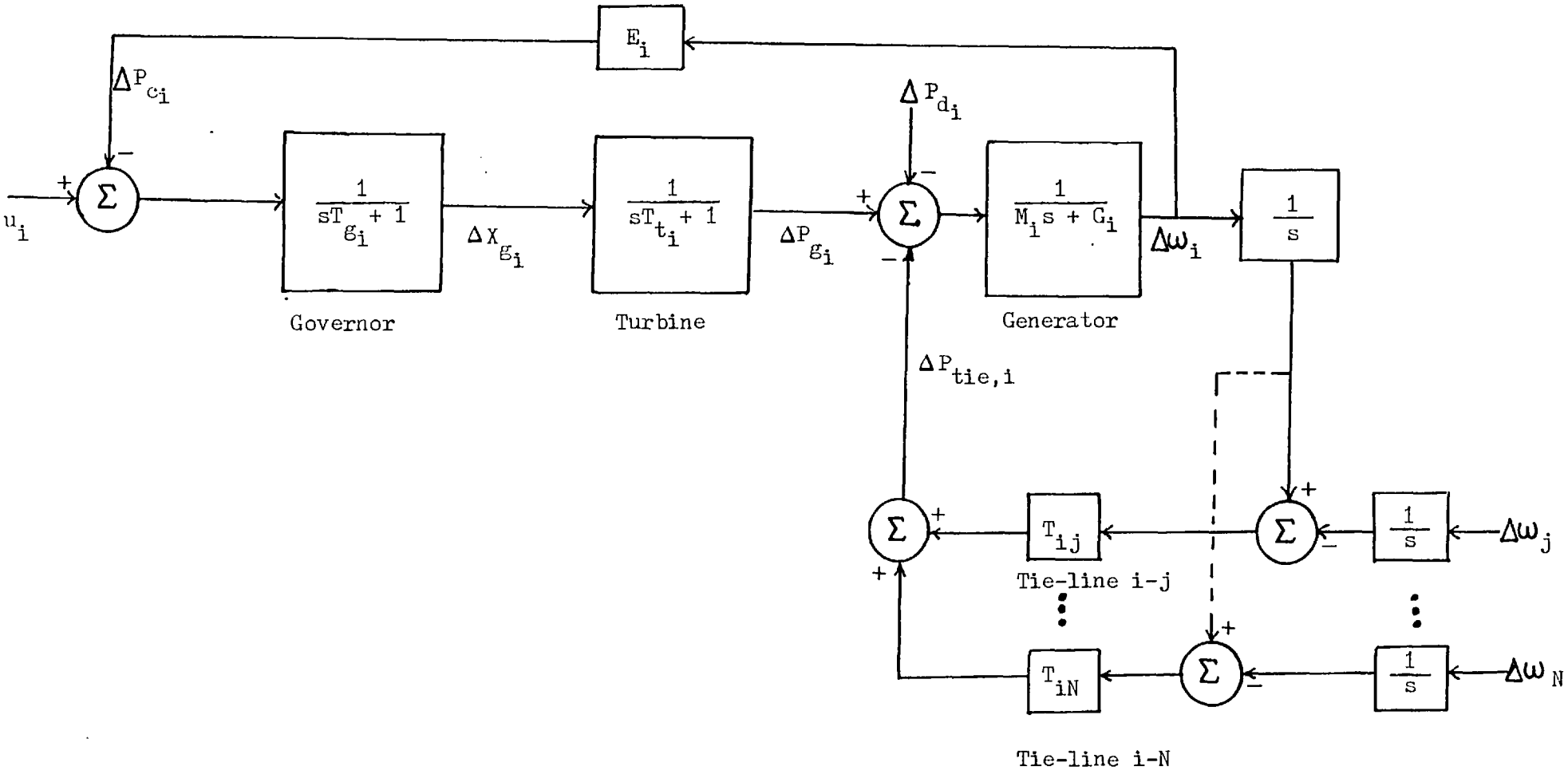

FIGURE 5.1: LFC STEAM PLANT BLOCK DIAGRAM

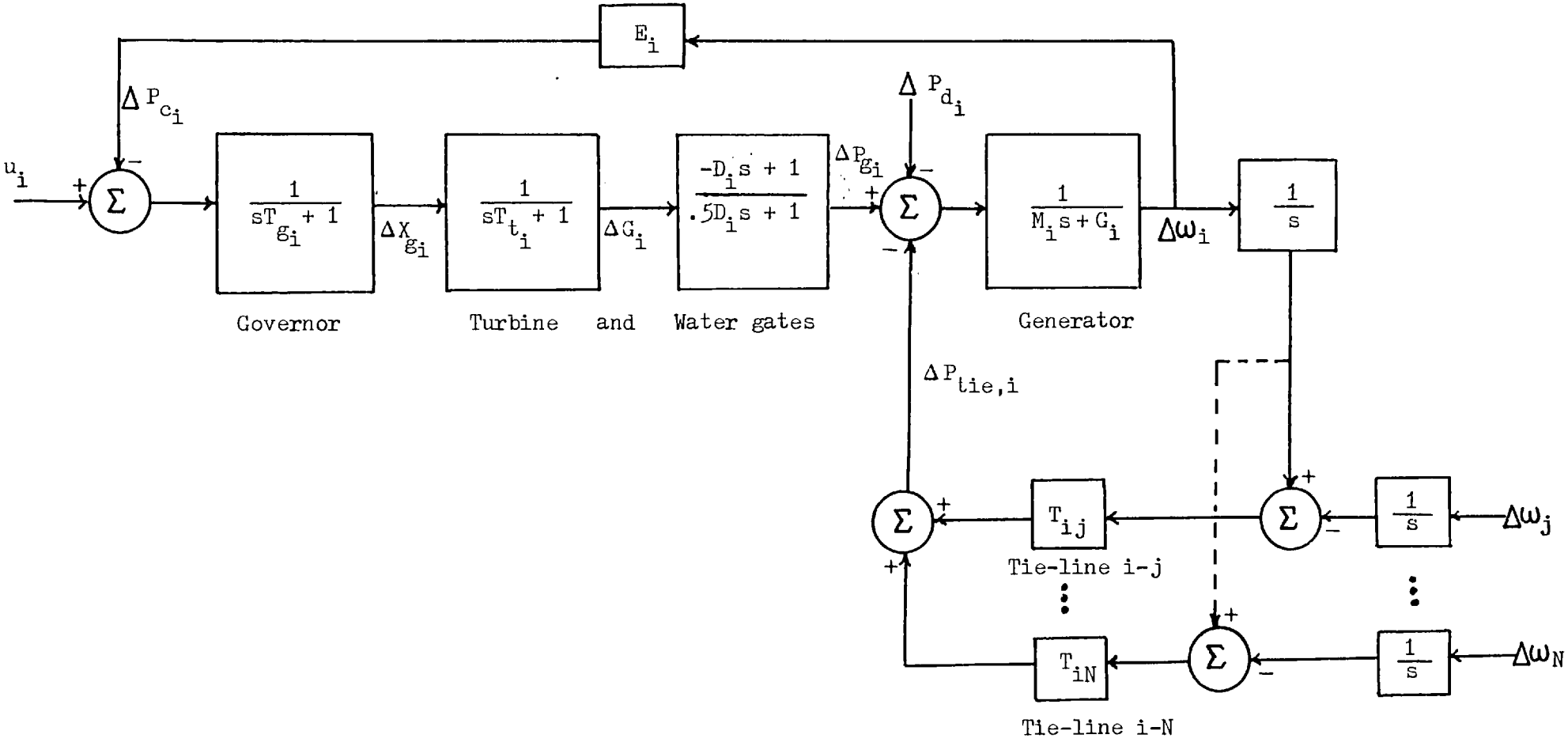

FIGURE 5.2: LFC HYDRO PLANT BLOCK DIAGRAM

are made up of first order delay transfer functions except the inter-area real power transfer phenomenon which is modelled by a simple constant gain block. The difference in the dynamics of the hydro and steam plants arises because when the water gates of the hydro plant open, the turbine torque tends to decrease momentarily and then increases thereafter. The extra block in the hydro plant model represents this behaviour of hydro sets.

5.2.1 State variables, $\underline{x}_i$, and control vectors, $\underline{u}_i$

The state variables, $\underline{x}_i$, for the i-th power plant are defined as follows:

$$\underline{x}_i^T = (\Delta P_{tie,i}\ \Delta\omega_i\ \Delta P_{g_i}\ \Delta X_{g_i}) \qquad (5.2.1)$$

for a steam plant, and

$$\underline{x}_i^T = (\Delta P_{tie,i}\ \Delta\omega_i\ \Delta P_{g_i}\ \Delta G_i\ \Delta X_{g_i}) \qquad (5.2.2)$$

for a hydro set.

The control vector, $\underline{u}_i$, for the i-th area is defined as (for both steam and hydro sets):

$$\underline{u}_i = (\Delta P_{c_i}) \qquad (5.2.3)$$

where, in p.u. power,

$\Delta P_{tie,i}$: is the tie-line power deviation

ΔP_{g_i} : is the deviation in mechanical power = deviation in generated power (assuming that the time constant of the generator is negligible compared to the governor and turbine time constants)

ΔG_i : is the deviation in gate position (for hydro unit)

ΔX_{g_i} is the deviation in governor position

ΔP_{c_i} : is the deviation in speed changer position

$\Delta \omega_i$: is the angular frequency deviation in rad./sec.

5.2.2 Power system dynamics in state variable form

The dynamics of each power system area may be described by the following set of linear differential equations:

For a steam plant model:

$$\Delta \dot{P}_{tie,i} = \sum_{\substack{j=1 \\ i \neq j}}^{N} T_{ij} (\Delta \omega_i - \Delta \omega_j)$$

$$\Delta \dot{\omega}_i = -\frac{1}{M_i} \Delta P_{tie,i} - \frac{G_i}{M_i} \Delta \omega_i + \frac{1}{M_i} \Delta P_{g_i} - \frac{1}{M_i} \Delta P_{d_i}$$

$$\Delta \dot{P}_{g_i} = -\frac{1}{T_{t_i}} \Delta P_{g_i} + \frac{1}{T_{t_i}} \Delta X_{g_i} \qquad (5.2.4)$$

$$\Delta \dot{X}_{g_i} = -\frac{E_i}{T_{g_i}} \Delta \omega_i - \frac{1}{T_{g_i}} \Delta X_{g_i} + \frac{1}{T_{g_i}} u_i$$

whilst for a hydro area, the describing equations are:

$$\Delta \dot{P}_{tie,i} = \sum_{\substack{j=1 \\ i \neq j}}^{N} T_{ij} (\Delta \omega_i - \Delta \omega_j)$$

$$\Delta \dot{\omega}_i = -\frac{1}{M_i} \Delta P_{tie,i} - \frac{G_i}{M_i} \Delta \omega_i + \frac{1}{M_i} \Delta P_{g_i} - \frac{1}{M_i} \Delta P_{d_i}$$

$$\Delta \dot{P}_{g_i} = -\frac{2}{D_i} \Delta P_{g_i} + \left(\frac{2}{T_{t_i}} + \frac{2}{D_i} \right) \Delta G_i - \frac{2}{T_{t_i}} \Delta X_{g_i} \qquad (5.2.5)$$

$$\Delta \dot{G}_i = -\frac{1}{T_{t_i}} \Delta G_i + \frac{1}{T_{t_i}} \Delta X_{g_i}$$

$$\Delta \dot{X}_{g_i} = -\frac{E_i}{T_{g_i}} \Delta \omega_i - \frac{1}{T_{g_i}} \Delta X_{g_i} + \frac{1}{T_{g_i}} u_i$$

The parameters used in the describing equations are defined as follows:

M_i = inertia constant in pu-power-secs^2/rad.

G_i = load damping coefficient in pu-power sec/rad.

T_{t_i} = turbine time constant in seconds

T_{g_i} = governor time constant in seconds

D_i = water starting time in seconds

E_i = the reciprocal of the area speed regulation

$T_{ij} = T_{ij}^{o} \sin (\delta_i^{o} - \delta_j^{o})$

$T_{ij}^{o} = E_i E_j \left\| Y_{ij} \right\|$

T_{ij}^{o} is assumed constant, and

$$v_i = E_i e^{j \delta_i} \qquad (5.2.6)$$

is the complex voltage at the i-th area interconnection. $\left\| Y_{ij} \right\|$ is the magnitude of the tie-line admittance between the i-th and j-th areas with line resistance neglected. The superscript (o) denotes nominal values.

The dynamics of each plant as described by equations (5.2.5) and (5.2.6) may be generally expressed in the form:

$$\dot{\underline{x}}_i(t) = A_i \underline{x}_i(t) + B_i \underline{u}_i(t) + \Gamma_i \Delta P_{d_i}(t) + \sum_{\substack{j=1 \\ i \neq j}}^{N} H_{ij} \underline{x}_j(t) \qquad (5.2.7)$$

where:

$\underline{x}_i(t)$ is a vector of state variables of dimension n_i

$\underline{u}_i(t)$ is a vector of control variables of dimension m_i

$\Delta P_{d_i}(t)$ is the deterministic power demand deviation of the i-th area in pu-power

$\underline{x}_j(t)$ denotes the state vector of the j-th area that is interconnected with the i-th area.

The matrices A_i, B_i, Γ_i and H_{ij} which are time invariant and of appropriate dimensions are defined as follows:

$$A_i = \begin{array}{|c|c|c|c|} \hline & T_{ij} & & \\ \hline -\frac{1}{M_i} & -\frac{G_i}{M_i} & \frac{1}{M_i} & \\ \hline & & -\frac{1}{T_{t_i}} & \frac{1}{T_{t_i}} \\ \hline & -\frac{E_i}{T_{g_i}} & & -\frac{1}{T_{g_i}} \\ \hline \end{array}$$

$$B_i^T = \begin{array}{|c|c|c|c|} \hline & & & \frac{1}{T_{g_i}} \\ \hline \end{array}$$

$$\Gamma_i^T = \begin{array}{|c|c|c|c|} \hline & -\frac{1}{M_i} & & \\ \hline \end{array}$$

for a steam plant

and for a hydro plant

$$A_i = \begin{array}{|c|c|c|c|c|} \hline & T_{ij} & & & \\ \hline -\frac{1}{M_i} & -\frac{G_i}{M_i} & \frac{1}{M_i} & & \\ \hline & & -\frac{2}{D_i} & \frac{2}{D_i}+\frac{2}{T_{t_i}} & -\frac{2}{T_{t_i}} \\ \hline & & & -\frac{1}{T_{t_i}} & \frac{1}{T_{t_i}} \\ \hline & -\frac{E_i}{T_{g_i}} & & & -\frac{1}{T_{g_i}} \\ \hline \end{array}$$

$$B_i^T = \begin{array}{|c|c|c|c|c|} \hline & & & & \frac{1}{T_{g_i}} \\ \hline \end{array}$$

$$\Gamma_i^T = \begin{array}{|c|c|c|c|c|} \hline & \frac{1}{M_i} & & & \\ \hline \end{array}$$

For N interconnected power plants of either steam and/or hydro plants the dynamical equation governing the operation of the overall system can be expressed in terms of a general composite system-wide state vector $\underline{X}(t)$:

$$\dot{\underline{X}}(t) = (A + H)\,\underline{X}(t) + B\underline{U}(t) \qquad (5.2.8)$$

where A, H and B are time-invariant system block diagonal matrices derived from the decomposed subsystem matrices A_i, B_i, H_{ij} Γ_i. The composite overall system state vector, $\underline{X}(t)$, and the composite overall control vector, $\underline{U}(t)$, are derived from the individual subsystem state vectors, $\underline{x}_i(t)$, and individual control vector terms, $\underline{u}_i(t)$, and area power demand deviation terms, ΔP_{d_i}, such that:

$$\underline{X}^T(t) = (\underline{x}_1^T, \underline{x}_2^T, \ldots, \underline{x}_N^T) \qquad (5.2.9)$$

$$\underline{U}^T(t) = (\underline{u}_1^T, \underline{u}_2^T, \ldots, \underline{u}_N^T, \Delta P_{d_1}, \Delta P_{d_2}, \ldots, \Delta P_{d_N}) \qquad (5.2.10)$$

It is clear that as the number of areas in the interconnected power system increases, the overall composite system state vector and the associated system matrices assume very high dimensions.

5.2.3 Power system measurements

Presently used load frequency control schemes (tie-line bias control) all require knowledge of the tie-line power and area frequency deviations [66-68]. Given a perfect data acquisition system in a given area, i, the two measurements, namely tie-line power and area frequency deviations, may be described by the deterministic linear equation:

$$\underline{z}_i = C_i \underline{x}_i(t) \qquad (5.2.11)$$

where C_i is referred to as the measurement matrix and is defined by:

Steam plant

$C_i =$

1.0			
	1.0		

Hydro plant

1.0				
	1.0			

When described in terms of the enlarged state vector, $\underline{X}(t)$, the measurement vector is:

$$\underline{Z} = C\underline{X}(t) \qquad (5.2.12)$$

where C is an enlarged block diagonal matrix of appropriate dimensions.

5.2.4 Stochastic modelling of the dynamics and measurements of the power system

Up to now, it has been tacitly assumed that the system dynamic models of equations (5.2.4) and (5.2.5) are accurate and that the data or measurement acquisition system of equations (5.2.11) and (5.2.12) is perfect. Realistically, there is always uncertainty in the dynamic system model and measurement systems invariably introduce observation noise or bias. It is common engineering practice to utilize a probabilistic approach to the modelling and implications of physical uncertainty[61]. In the design of dynamical systems the continuous existence in time of plant disturbances and sensor or measurement errors is modelled by representing the uncertain time functions by random processes.

In stochastic modelling, the plant is described by the vector differential equations:

$$\dot{\underline{x}}_i(t) = A_i\underline{x}_i(t) + B_i\underline{u}_i(t) + \sum H_{ij}\underline{x}_j(t) + G_i\underline{\omega}_i(t) \qquad (5.2.13)$$

or in block form

$$\dot{\underline{X}}(t) = (A+H)\,\underline{X}(t) + B\underline{U}(t) + G\underline{\omega}\ (t) \qquad (5.2.14)$$

The addition of $\underline{\omega}_i(t)$ a stochastic disturbance vector term to the otherwise deterministic model implies that

i. the system is driven by unknown disturbance input, $\underline{\omega}_i(t)$

ii. the deterministic equations may be in error due to over-simplification of the system model

iii. some of the parameters in the defining dynamical system equations may not be exact (nominal values are frequently employed).

G_i is referred to as the stochastic disturbance input distribution matrix.

To model sensor errors, measurement uncertainties and meter inaccuracies, it is assumed that the sensor measures the output variable $C_i\underline{x}_i(t)$ and yields the measurement signal $\underline{z}_i(t)$ which equals $C_i\underline{x}_i(t)$ plus a noise term $\underline{v}_i(t)$.

That is:

$$\underline{z}_i(t) = C_i\underline{x}_i(t) + \underline{v}_i(t) \qquad (5.2.15)$$

or in block form:

$$\underline{Z}(t) = C\underline{X}(t) + \underline{v}(t) \qquad (5.2.16)$$

Equations (5.2.13) and (5.2.15) refer to the individual power system areas whereas equations (5.2.14) and (5.2.16) refer to the composite overall system.

5.3 General statement of state estimation problem

For a precise description of the state estimation problem, consider the large-scale dynamical system as an interconnection of N subsystems $S_1, S_2, \ldots, S_N$ described by:

$$\dot{\underline{x}}_i(t) = A_i \underline{x}_i(t) + B_i \underline{u}_i(t) + \sum H_{ij} \underline{x}_j(t) + G_i \underline{\omega}_i(t) \qquad (5.3.1)$$

$$\underline{z}_i(t) = C_i \underline{x}_i(t) + \underline{v}_i(t) \qquad (5.3.2)$$

where:

$\underline{x}_i(t)$ is the n_i dimensional state vector of subsystem S_i

$\underline{u}_i(t)$ is the m_i dimensional input control vector of subsystem S_i

$\underline{z}_i(t)$ is the p_i dimensional observation vector or output of subsystem S_i

$\underline{\omega}_i(t)$ is the n_i dimensional state excitation noise

$\underline{v}_i(t)$ is the p_i dimensional measurement noise

The uncertainties considered are quantitatively characterised in statistical terms as follows:

1. The initial state vector, $\underline{x}_i(t_o)$, is assumed to be Gaussian distributed with known mean and covariance matrix, i.e.

$$E\{\underline{x}_i(t_o)\} = \underline{x}_i^o \text{ (assumed known)}$$

$$\text{cov}\{\underline{x}_i(t_o), \underline{x}_i(t_o)\} = E\{(\underline{x}_i(t_o) - \underline{x}_i^o)(\underline{x}_i(t_o) - \underline{x}_i^o)^T\}$$

$$= P_i^o \text{ (assumed known)}$$

P_o is at least positive semi-definite i.e. $P_i^o \geq 0$

2. The system noise, $\underline{\omega}_i(t)$ is assumed to be white, Gaussian with zero mean and known covariance matrix for all $t \geq t_o$, i.e.

$$E\{\underline{\omega}_i(t)\} = \underline{0}$$

$$\text{cov}\{\underline{\omega}_i(t), \underline{\omega}_i(t+\tau)\} = Q_i(t)\,\delta(\tau), \text{ where } \delta \text{ is the dirac-delta function}$$

$Q_i(t) \geq 0$ i.e. positive semi-definite

3. The measurement noise $\underline{v}_i(t)$ is also assumed to be white, Gaussian with zero mean and known covariance matrix for all $t \geq t_o$, i.e.

$$E\{\underline{v}_i(t)\} = \underline{0}$$

$\text{cov}\{\underline{v}_i(t),\ \underline{v}_i(t+\tau)\} = R_i(t)\,\delta(\tau)$

$R_i(t) > 0$ i.e. positive definite.

It is also assumed that $\underline{x}_i(t_o)$, $\underline{\omega}(t)$,$\underline{v}(t)$ are all mutually independent, i.e.

$\text{cov}\{\underline{x}_i(t_o),\ \underline{\omega}(t)\} = 0$

$\text{cov}\{\underline{x}_i(t_o),\ \underline{v}_i(t)\} = 0$

$\text{cov}\{\underline{\omega}_i(t),\ \underline{v}_i(t+\tau)\} = 0$

for all $t \geq t_o$.

The covariance matrices $Q_i(t)$, $R_i(t)$ and P_i^o are all assumed to be symmetric.

The system-wide or global state estimation problem may now be stated as follows: 'Derive good and acceptable estimates, $\hat{\underline{x}}_i(t)$, of the system state variables, $\underline{x}_i(t)$, from the system-wide measurements

$\{\underline{z}_i(\tau),\ \tau = t_o,\ t_o+\Delta t,\ t_o+2\Delta t,\ldots,t;\ \ i = 1,2,\ldots N\}$

which are imprecise and subject to errors given that the overall system and its subsystems are themselves subject to random input disturbances'.

5.3.1 Composite system state estimation

An optimal, linear least-squares, filtered estimate, $\hat{\underline{X}}(t)$, of the state of the composite system and the covariance matrix, $P(t)$, of the estimation error, $\underline{\delta}_x = \underline{X}(t) - \hat{\underline{X}}(t)$, can be derived from equations (5.3.1) and (5.3.2) by applying the well known linear Kalman filtering theory[23,64,65] to give:

$$\dot{\hat{\underline{X}}}(t) = (A+H)\hat{\underline{X}}(t) + B\underline{U}(t) + K(t)\{\underline{Z}(t) - C\hat{\underline{X}}(t)\} \qquad (5.3.3)$$

$$\dot{P}(t) = P(t)\,[A+H]^T + [A+H]\,P(t) - P(t)C^T R^{-1}(t)CP(t) + GQ(t)G^T \qquad (5.3.4)$$

where $K(t)$ is the time-varying nxm dimensional Kalman filter gain matrix and $n = \sum_{i=1}^{N} n_i$ $\qquad m = \sum_{i=1}^{N} m_i$

Equation (5.3.4) is a system of first order ordinary matrix differential equations of second degree. It is worth mentioning that it is assumed that the block diagonal system matrices $\{(A+H), C\}$ form an observable pair; otherwise observability must be initially established.

If the matrices A, B, C, Q(t), R(t) and G are all time-invariant (as indeed is the case for the LFC model), the filtering process may reach a steady-state in the sense that, the error covariance matrix, P(t), becomes a constant matrix, i.e. $\dot{P}(t) = 0$. In principle, this steady state matrix is obtainable by solving the $\frac{n}{2}(n+1)$ simultaneous quadratic matrix equations (5.3.4) by setting $\dot{P}(t)$ to zero.
Then:

$$P(A+H)^T+(A+H)P-PC^TR^{-1}CP+GQG^T = 0 \qquad (5.3.5)$$

Equation (5.3.5) conveys the notion that at steady-state, the rate at which information goes out of the system (represented by the GQG^T term) is just balanced by the rate at which information enters the system (represented by $PC^TR^{-1}CP$) and by any damping the system may have (as expressed by the terms in (A+H)). The Kalman filter described is therefore essentially an adaptive, gain-tuning technique in which the prediction of the system state at any time instant is weighted between the extrapolated past value and the present observed value.

The solution of equation (5.3.5) in closed form is impracticable for a system of order $n > 2$. An effective method of solution will be described in the section 5.3.2. The quadratic matrix equation (5.3.5) is generally referred to in the literature as the matrix Riccati equation.

5.3.2 Solution of the matrix Riccati equation

The solution of linear least-squares quadratic Gaussian estimation and control problems revolves around the solution of a first-order non-linear matrix quadratic equation, the Riccati equation [64,69,70]. For the general constant coefficient matrices case, an analytical asymptotic or stationary, i.e. constant matrix, solution is possible. The method described here generates the asymptotic solution by converting the n dimensional Riccati equation to a 2n dimensional homogeneous, linear differential equation and using an eigen-value, eigen-vector analysis of the resulting Riccati system matrices.

★ Determination of the steady-state Kalman filter gain, K

To obtain the steady-state solution of the time-invariant Riccati equation the following system Hamiltonian matrix, Z_H, may be defined[69].

$$Z_H = \begin{array}{|c|c|} \hline -(A+H)^T & C^T R^{-1} C \\ \hline GQG^T & (A+H) \\ \hline \end{array} \qquad (5.3.6)$$

Z_H is a 2n x 2n matrix whose 2n eigen-values (e-values) and 2n eigen-vectors (e-vectors) may be determined using any standard numerical technique, e.g. the QR algorithm [71,72]. The e-values of Z_H may initially be assumed distinct from which the following properties are then true:

a. If λ is an e-value of Z_H, then so is $-\lambda$

b. If Z_H is diagonalizable in the form:

$$Z_H = \begin{bmatrix} W_{11} & W_{12} \\ W_{21} & W_{22} \end{bmatrix} \begin{bmatrix} \Lambda & \\ & -\Lambda \end{bmatrix} \begin{bmatrix} W_{11} & W_{12} \\ W_{21} & W_{22} \end{bmatrix}^{-1} \qquad (5.3.7)$$

where the diagonal matrix, Λ has as its diagonal elements the e-values of Z_H with negative real parts, the steady-state solution of the Riccati equation is:

$$P = W_{22}\, W_{12}^{-1} \qquad (5.3.8)$$

where W_{ij}, i,j = 1,2 are obtained by partitioning W assuming its inverse, W^{-1}, exists. The columns of the partitioned matrices

$\begin{bmatrix} W_{11} \\ W_{21} \end{bmatrix}$ consist of the elements of the eigen-vectors of Z_H corresponding to eigen-values with negative real parts, whilst those of

$\begin{bmatrix} W_{12} \\ W_{22} \end{bmatrix}$ consist of the elements of the eigen-vectors of Z_H corresponding to eigen-values with positive real parts. The algorithm for the determination of the estimation error covariance matrix, P, is summarised below:

a. Form the 2n x 2n system Hamiltonian matrix, Z_H, and by using any standard numerical technique determine those e-vectors that correspond to e-values with positive real parts.

b. From these n e-vectors form the 2n x n block matrix

$\begin{bmatrix} W_{12} \\ W_{22} \end{bmatrix}$ where W_{12} and W_{22} are n x n submatrices determined as follows:

i. If $\underline{e}$ is a real characteristic vector, then $\underline{e}$ is one of the

columns of $\begin{bmatrix} W_{12} \\ W_{22} \end{bmatrix}$

ii. If $\underline{e}$ and $\underline{e}^*$ form a complex-conjugate pair, then Real ($\underline{e}$) is one

column of $\begin{bmatrix} W_{12} \\ W_{22} \end{bmatrix}$ and Imaginary ($\underline{e}$) another column

c. P at steady-state is then determined from:

$$P = W_{22}\, W_{12}^{-1}$$

The reliability and effectiveness of the method described depends to a large extent on the efficiency of the subprograms for computing the characteristic values and vectors of the system Hamiltonian matrix, Z_H, as well as the efficiency of the matrix inversion routine adopted for determining the matrix inverse, W_{12}^{-1}. Having determined P, the steady-state Kalman filter gain, K, is then derived from

$$K = PC^T R^{-1} \qquad (5.3.9)$$

Fig. 5.3 is a flow-chart of the algorithmic approach to the determination of P and K at steady state.

5.4 Decentralized solution to the state estimation problem

Design of suitable estimators for obtaining estimates of system states is very important for system theoretic studies involving state feedback techniques. For large-scale systems, however, a straight forward and direct application of these estimator design principles is not attractive due to computational difficulties associated with highly dimensional system coefficient matrices and sometimes due to the infeasibility of implementing a single estimator of large dimension,

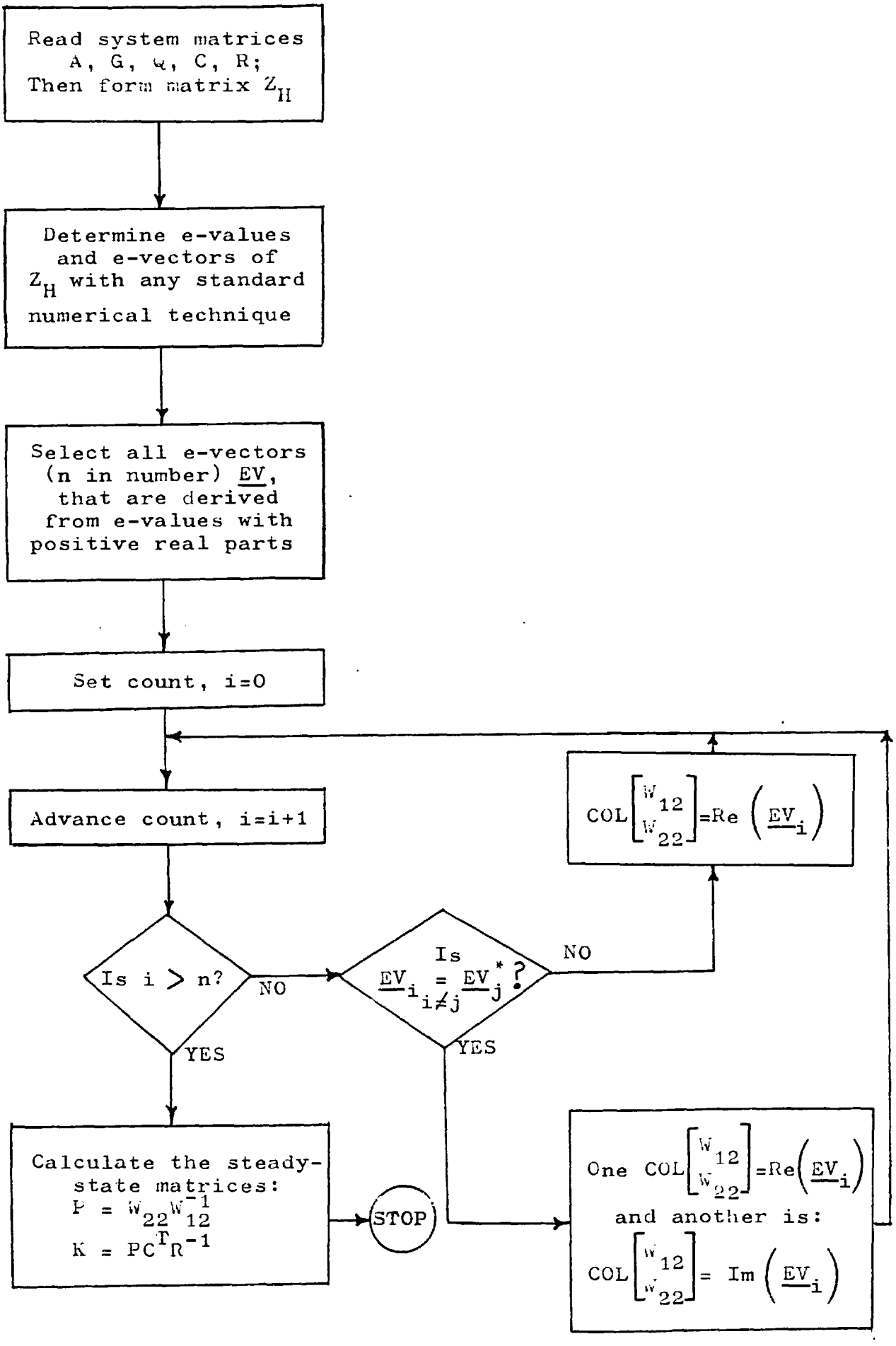

FIGURE 5.3: DETERMINATION OF STEADY-STATE P AND K MATRICES

especially on small process control computers for real-time operation.

Since most large-scale dynamical systems are usually easily identifiable as interconnections of several low-order subsystems, it is desirable to exploit the natural decomposed structure of the available overall composite system model. The decentralized state estimation schemes considered here are used to determine whether estimators based on local subsystem dynamics alone can serve as adequate estimators of the overall system state.

5.4.1 Completely decentralized estimators, $H_{ij} \equiv 0$

For systems with completely decoupled subsystems,

$$H_{ij} \equiv 0 \quad \begin{matrix} i,j = 1,2,\ldots,N \\ i \neq j \end{matrix} \tag{5.4.1}$$

independent decentralized estimators may be designed for the individual i-th subsystems by[73,74]:

$$\dot{\hat{\underline{x}}}_i(t) = A_i \hat{\underline{x}}_i(t) + B_i \underline{u}_i(t) + K_i \left\{ \underline{z}_i(t) - C_i \hat{\underline{x}}_i(t) \right\} \qquad i = 1,2,\ldots,N \tag{5.4.2}$$

where the $n_i \times p_i$ Kalman filter gain matrix K_i is given by:

$$K_i = P_i C_i^T R_i^{-1} \tag{5.4.3}$$

and P_i satisfies the matrix Riccati equation:

$$P_i A_i^T + A_i P_i - P_i C_i^T R_i^{-1} C_i P_i + G_i Q_i G_i^T = 0 \tag{5.4.4}$$

What is of interest now is to determine the conditions under which the above decentralized estimation scheme or equivalently, any modifications thereof, lead to state estimates that are optimal in the least-squares sense and have the same degree of convergence and accuracy as the overall system state estimates $\hat{\underline{X}}(t)$, derived from the equivalent composite system model:

$$\dot{\underline{X}}(t) = (A+H)\underline{X}(t) + B\underline{U}(t) + G\underline{\omega}(t) \qquad (5.4.5)$$

$$\underline{Z}(t) = C\underline{X}(t) + \underline{V}(t) \qquad (5.4.6)$$

Clearly the decentralised estimator of equations (5.4.2), (5.4.3), and (5.4.4) developed under the assumption that $H_{ij} \equiv 0$ will be far from satisfactory when used for the composite system. This is because of the lack or neglect of knowledge of the interconnection functions, H_{ij}, and of the outputs of the other subsystems, $\{\underline{z}_j(t), \quad j = 1,2,\ldots,N\}$

5.4.2 Modified estimation schemes utilizing other subsystem measurements, $\underline{z}_j(t)$

When the measurements of other subsystems are available together with a knowledge of the interconnection pattern, H_{ij}, at the i-th area, a simple modification of the estimation scheme of equations (5.4.2), (5.4.3) and (5.4.4) are obtainable as:

$$\dot{\hat{\underline{x}}}_i(t) = A_i\hat{\underline{x}}_i(t) + B_i\underline{u}_i(t) + K_i\left\{\underline{z}_i(t) - C_i\hat{\underline{x}}_i(t)\right\} + \sum_{\substack{j=1 \\ i\neq j}}^{N} \tilde{K}_{ij}\,\underline{z}_j(t) \qquad (5.4.7)$$

where the measurement gain matrix, $\tilde{K}_{ij}$, is defined by:

$$\tilde{K}_{ij} = \left[HC^T\,(CR^{-1}C^T)^{-1}\right]_{ij} \qquad (5.4.8)$$

The subscripts ij denote the ij-th block matrix. It can be shown that this modified scheme yields system state estimates of comparable accuracy and a similar degree of convergence for each subsystem as for the overall system [73,74].

A comparison of equations (5.4.2) and (5.4.7) reveals that the only change in the estimation equations is the use of the measurements of the other subsystems as additional measurement signals

together with the measurement gains $\tilde{K}_{ij}$ that are determined from the bulk system matrices H, C and R.

The method's attractiveness may be viewed in the context of the reduced core storage requirements as only the local subsystem matrices, which are necessarily of relatively smaller dimensions, are involved in computing the filter gains K_i and more importantly, the fact that the derivation of these gains is performed only at the subsystem level. The available system decomposed structure is therefore effectively exploited.

5.4.3 Modified estimation schemes utilizing other subsystem state estimates, $\hat{\underline{x}}_j(t)$

When the state estimates of the other subsystems, $\hat{\underline{x}}_j(t)$, are available at a particular area, i, and the interconnection matrix H_{ij} is known, then an intuitively simple modified decentralized estimation scheme may be derived as follows:

$$\dot{\hat{\underline{x}}}_i(t) = A_i\hat{\underline{x}}_i(t) + B_i\underline{u}_i(t) + K_i\left\{\underline{z}_i(t) - C_i\hat{\underline{x}}_i(t)\right\} + \sum_{\substack{j=1 \\ i\neq j}}^{N} H_{ij}\,\hat{\underline{x}}_j(t) \qquad (5.4.9)$$

$$i = 1,2, \ldots,N$$

where K_i is defined as previously mentioned. This scheme also yields the same degree of accuracy and convergence as the overall system state estimation scheme.

In the same manner as the estimator in section (5.4.2), the estimator of this section derives additional signals from the other subsystems, except that here these extra signals are the already available state estimates of the other subsystems.

In summary, three distinct methods for decentralized estimation schemes for linear systems with linear interconnection phenomena have been highlighted, namely:

i. Completely decentralized estimation schemes where all interconnection patterns are assumed negligible, $H_{ij} \equiv 0$

ii. Modified decentralized estimation schemes where, together with the knowledge of the interconnection effects, the observed outputs of other subsystems are assumed available. And finally,

iii. A further modified estimator that relies on both the knowledge of the interconnection pattern and the availability of the pre-computed or pre-determined state estimates of areas outside the locality under consideration.

5.5 Computer simulation tests of dynamic state estimators

The classical two-area perturbation power system model was employed to assess the performance, effectiveness and reliability of the decentralized state estimators compared to the global estimators. The first area, AREA-1, was assumed to be a steam plant, whereas the second area, AREA-2, was assumed to be a hydro unit. The control term, u, was derived on the basis of the conventional LFC tie-line bias control technique, which is expressible in transfer function form by [75] :

$$u = \frac{a}{s} \frac{1}{bs + 1} (c\Delta\omega + \Delta P_{tie})$$

where a, b, c are constant coefficients.

Table 5.1 lists the values of the constant system parameters used in the computer simulations. These values are based on those quoted in references 19,62,63,66,75.

The variables ΔP_{tie} and $\Delta\omega$ are normally readily available and as such constituted the system observation variables. For all the estimator tests described, the initial state estimates were arbitrarily set to $\hat{\underline{x}}(t_o) = 0.005$ pu whilst the initial actual system states were chosen as $\underline{x}(t_o) = 0.0$ pu. All the results presented subsequently were obtained for area deterministic power demands of $\Delta P_{d_1} = -0.005$ pu and $\Delta P_{d_2} = +0.005$ pu.

Two distinct operating modes of the state estimators were investigated, namely:

a. the effect of the noise intensity matrices Q and R on estimation performance

TABLE 5.1

VALUES OF SYSTEM CONSTANTS

System Constant	Steam Unit (AREA-1)	Hydro Unit (AREA-2)
M_i	0.040	0.030
G_i	0.010	0.008
T_{ti}	0.500	0.500
T_{gi}	0.050	1.200
E_i	0.030	0.013
D_i	-	0.500
T^o_{ij}	0.050	0.050
a_i	0.090	0.400
b_i	0.300	0.300
c_i	0.020	0.020

b. the effect of tie-line strength (dependent on coefficient T^{o}_{ij}) on estimation performance.

The various simulations performed in effecting these operating modes together with the results obtained from them are tabulated in Tables 5.2 and 5.3. To enable a meaningful discussion and analysis of the results, the following steps were adopted in the simulations:

i. Generation of the system-wide state variables $\underline{x}_i(t)$ assuming absence of system state excitation noise $\underline{\omega}_i(t)$.

ii. Derivation of the assumed system measurement signals, i.e. ΔP_{tie_i} and $\Delta\omega_i$ according to the relation

$$\underline{z}_i(t) = C_i \underline{x}_i(t) + \underline{V}_i(t)$$

where $\underline{V}_i(t)$ is the time varying observation noise. The measurement noise was assumed to be a white-noise Gaussian random variable with the distribution $\sim N\left(0, 10\% C_i \underline{x}_i\right) + N\left(0, 0.0005\right)$. The extra normal random variable $N\left(0, 10\% C_i \underline{x}_i\right)$ introduces uncertainty about the observation noise covariance matrix, R, since $\underline{x}_i$ is a time varying state variable. $\underline{V}_i(t)$ was obtained from a normally distributed pseudo-random number generator with a library subroutine.

iii. Calculation of the global Kalman filter gain matrix by using the eigen-value, eigen-vector technique. This method was adopted because it avoids the need to specify yet another noise moment, the initial estimation error covariance matrix P_o, which is required if other techniques for solving the differential matrix Ricatti equation are used. Note that the principal diagonal block matrices of the global Kalman filter gain matrix are identical to the area Kalman filter gains.

TABLE 5.2

TESTS PERFORMED ON ESTIMATORS WITH MEASUREMENT MODEL $\underline{z} = C\underline{x} + \underline{V}$

Test Number		Type of Estimator	Covariance Matrices	Tie-Line Constant T_{12}^{o}
1	a	Global	$Q=R=(I)$	0.05
	b	Decoupled $H_{ij}=0$	"	"
	c	Local with $\hat{\underline{x}}_j$	"	"
	d	Local with $\underline{z}_j$	"	"
2	a	Global	$Q=10^{-4}(I)$ $R=10^{-3}(I)$	"
	b	Decoupled $H_{ij}=0$	"	"
	c	Local with $\hat{\underline{x}}_j$	"	"
	d	Local with $\underline{z}_j$	"	"
3	a	Global	"	0.20
	b	Decoupled $H_{ij}=0$	"	"
	c	Local with $\hat{\underline{x}}_j$	"	"
	d	Local with $\underline{z}_j$	"	"

TABLE 5.3

LIST OF FIGURES OBTAINED WITH ESTIMATORS

Figure	Test No.	Plant
5.4	1	Measurements
5.5 a	1b	Steam
b	1b	Hydro
5.6 a	1c	Steam
b	1c	Hydro
5.7	3	Measurements
5.8 a	3b	Steam
b	3b	Hydro
5.9 a	3c	Steam
b	3c	Hydro

iv. Generation of state estimates using the described methods and plots of both the assumed true system states and these state estimates on the same set of axes.

5.5.1 Discussion of results

The noisy measurement signals used in Test 1 and Test 2 are shown in Fig. 5.4. As the results of the two tests showed very little discernible difference between the global estimators, decentralised estimators with $\underline{\hat{x}}_j$ signals and decentralised estimators with $\underline{z}_j$ signals in terms of superiority of performance, only the responses of the completely decoupled estimators and those with $\underline{\hat{x}}_j$ signals are presented. However all three estimators exhibit the presence of spurious, noisy signals superimposed on the estimates. In contrast, the completely decentralised estimator yields results that are hardly acceptable. With the exception of the estimated speed deviations, all the estimated state variables show a marked deviation from their desired responses. This is explained by the fact that the simulations yield area speed deviation measurement noises of comparatively low magnitudes, and therefore have very little effect on the estimates even when the presence of the tie-line has been entirely ignored. It would therefore appear that for LFC purposes a very high confidence can be attached to area speed-deviation and/or area frequency deviation measurements.

In assessing the impact of the values of the noise intensity matrices Q and R on the performance of the estimators, the matrices were chosen in the following way: $Q = \alpha(I)$ and $R = \beta(I)$ where α, β are variable parameters and (I) the equivalent unit matrix of compatible dimension to Q or R as the case may be.

It was observed in a series of simulations that as in all filtering processes involving unknown noise moments an incompatible and/or inappropriate choice of α, β led to either filter divergence or filter instability in all the estimators. The following observations were made in respect of the choice of the matrices Q, R:

i. the rate of convergence of the estimates to the desired responses is controlled by the value of α; low values yielded a slow convergence rate and high values led to fast convergence. At high α values, though there is always the possibility of the estimator becoming unstable.

ii. the degree to which measurement noise is filtered is dependent on the choice of R viz-a-viz, β. When not properly chosen to reflect the expected standard deviation of the measurement noise, the observation noise persisted as is evident from Figs 5.5 to 5.6. This noise was not exhibited in Test 2 where the proper noise covariance matrices were used.

The optimum settings for the parameters α , β after a series of trial-and-error procedures were $\alpha = 0.0001$ and $\beta = 0.001$. These correspond to individual excitation noise variance of $\sigma_x^2 = 10^{-4}$ and individual observation noise variance of $\sigma_z^2 = 10^{-3}$.

The tie-line constant, T_{12}^o , was drastically increased in magnitude by 300% of its assumed nominal value of 0.05 to 0.20 in Test 3. The effect of this dramatic change was manifested not only in the increased oscillation of the system state variables but it also led to seriously degraded state estimates in the case of the completely decentralised estimation scheme. In this case even the area speed deviation estimates,

which were hitherto estimated by the decentralised scheme with little observable deviations, showed a marked degradation, as in Fig. 5.8. However, in spite of this extreme change in the tie-line constant, the decentralised but modified estimation schemes with $\hat{\underline{x}}_j$ and $\underline{z}_j$ both performed creditably to provide stable and acceptable state estimates that were comparable to those yielded by the global estimator.

5.5.2 Conclusions

The estimation results have confirmed that:

a. Local estimation, where power plant interaction is completely ignored yields physically feasible state estimates of the power plant states although the estimates produced are accuracy-wise degenerate.

b. Improved state estimates may be obtained using local estimators provided these local estimators are augmented with other power system area signals in the form of other area state estimates $\hat{\underline{x}}_j$ or other area measurement signals $\underline{z}_j$. This appears to be the only effective way to suitably account for power plant interaction.

c. Although not explicitly discussed in the results, the solution of the global matrix Ricatti equation requires four times as much computation time and computer core storage as the decentralised estimators. It is this result which proves the superiority of the local estimators because all computations can then be performed at the subsystem level only.

d. Any estimation scheme must make a compromise between speed of estimation and immunity to measurement noise. This balance has been shown to depend on the magnitudes of the system excitation noise intensity matrix Q and the observation noise covariance matrix R.

The disadvantage of the decentralized estimators described in this chapter is the increased burden of transmitting other area signals to the particular locality in question. Because the interconnection matrix H_{ij} for a normal power system is usually very sparse the amount of supplementary data required is consequently small. As is reported in Cory et al.[76] it would be extremely desirable if estimation schemes could be designed that use only subsystem dynamics alone.

Finally, the availability of on-site dedicated digital computers in modern power stations provides an opportunity to implement sophisticated monitoring schemes that will ultimately lead to improved control schemes. To be feasible for implementation in real-time, the first stage involves the design of suitable decentralised estimators as described in this chapter.

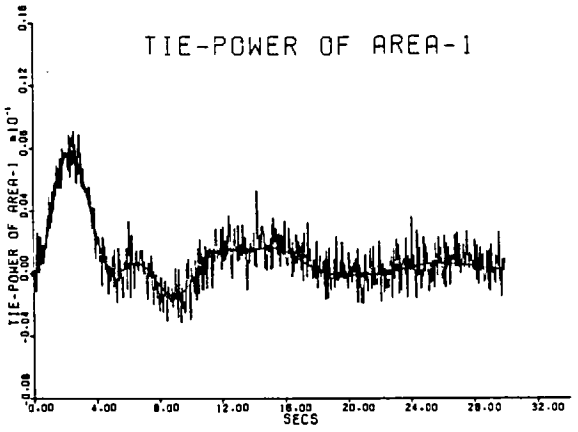

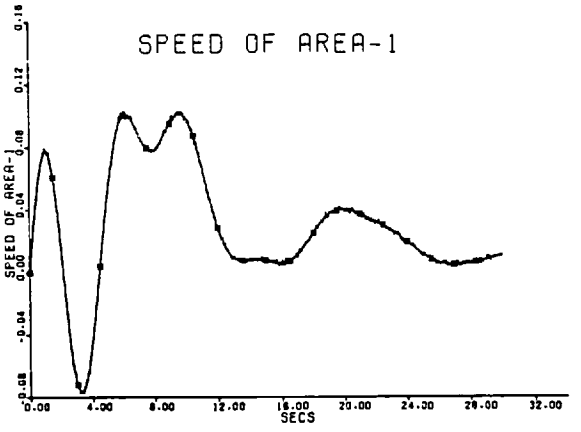

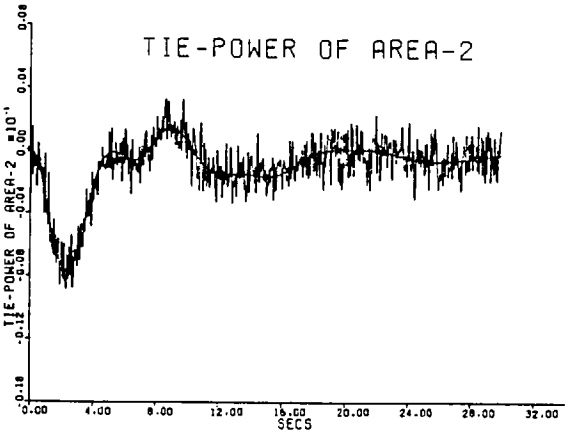

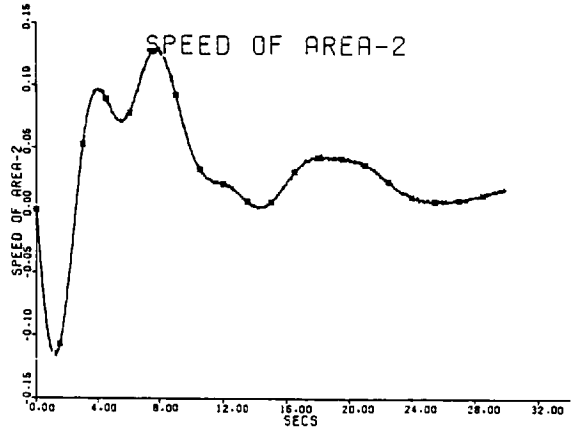

FIGURE 5.4: NOISY MEASUREMENTS OF TIE-LINE POWER AND AREA SPEED DEVIATION FOR TESTS 1 AND 2

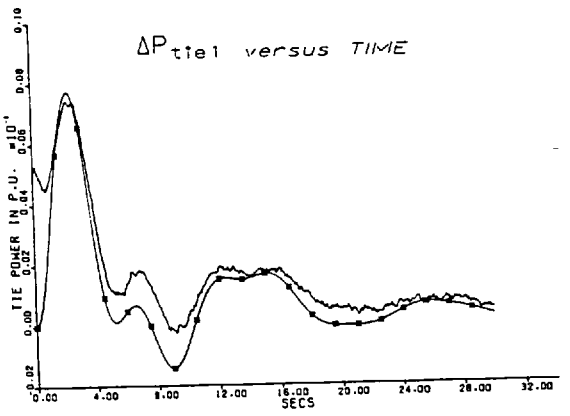

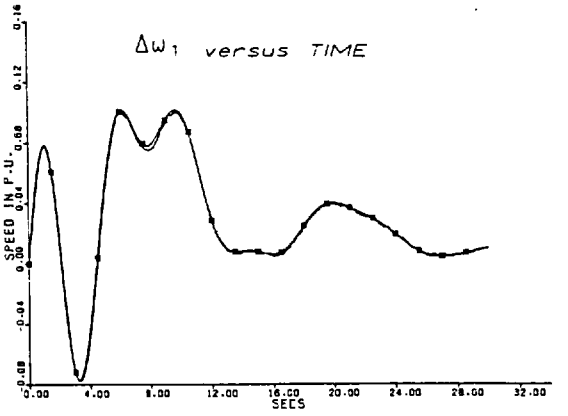

true system response

system state estimates

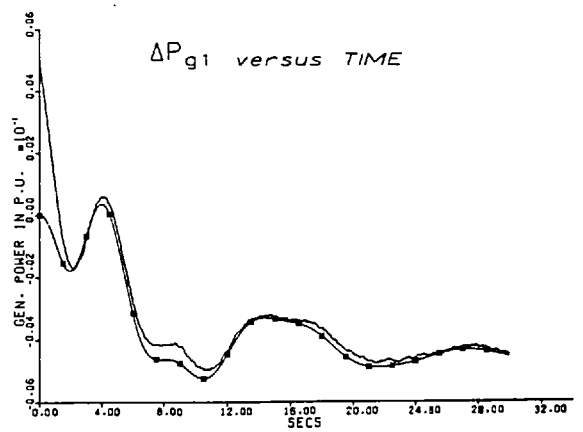

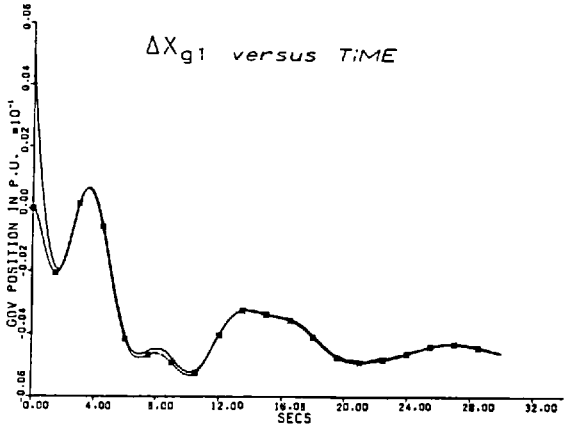

FIGURE 5.5: COMPLETELY DECOUPLED ESTIMATOR AT NOMINAL TIE-LINE STRENGTH:
a. STEAM PLANT STATE ESTIMATES

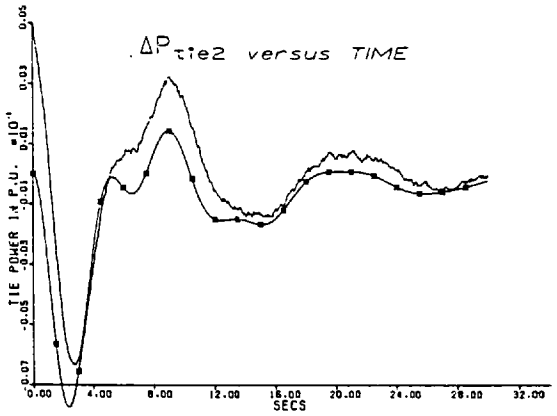

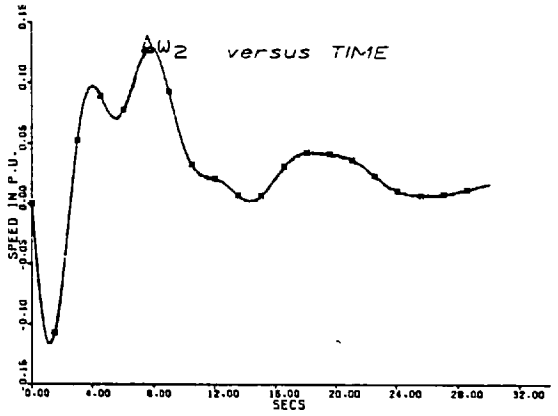

true system response

system state estimates

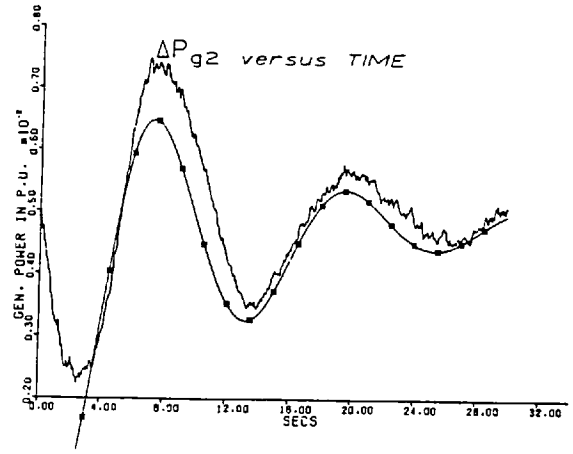

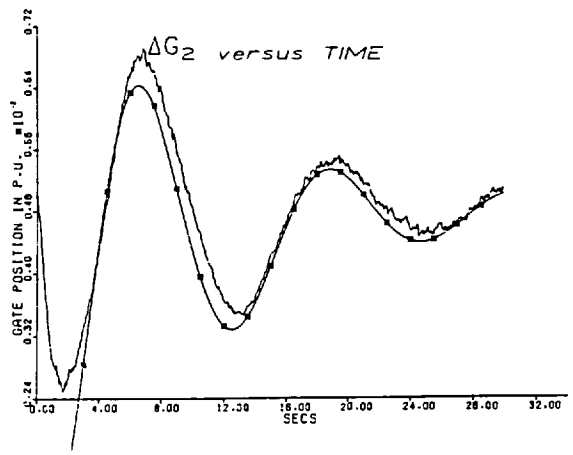

FIGURE 5.5: b. HYDRO PLANT STATE ESTIMATES

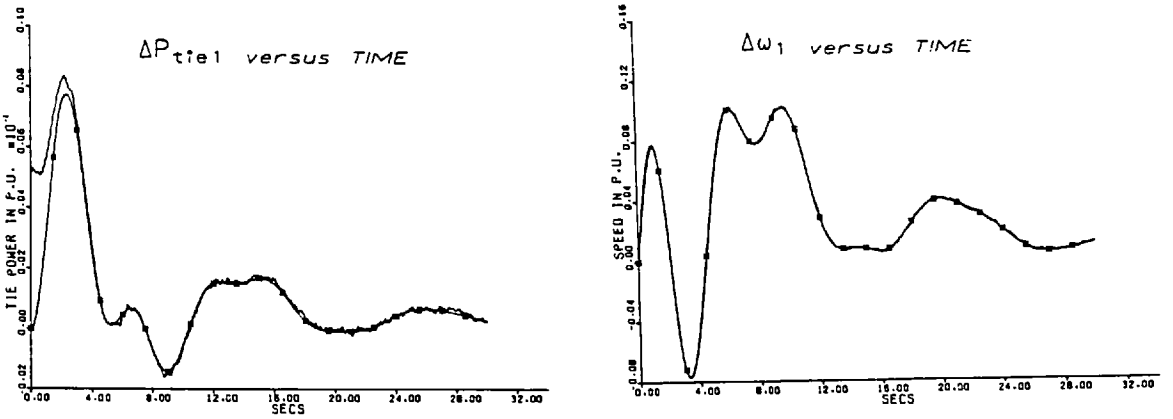

—*—*— true system response

——— system state estimates

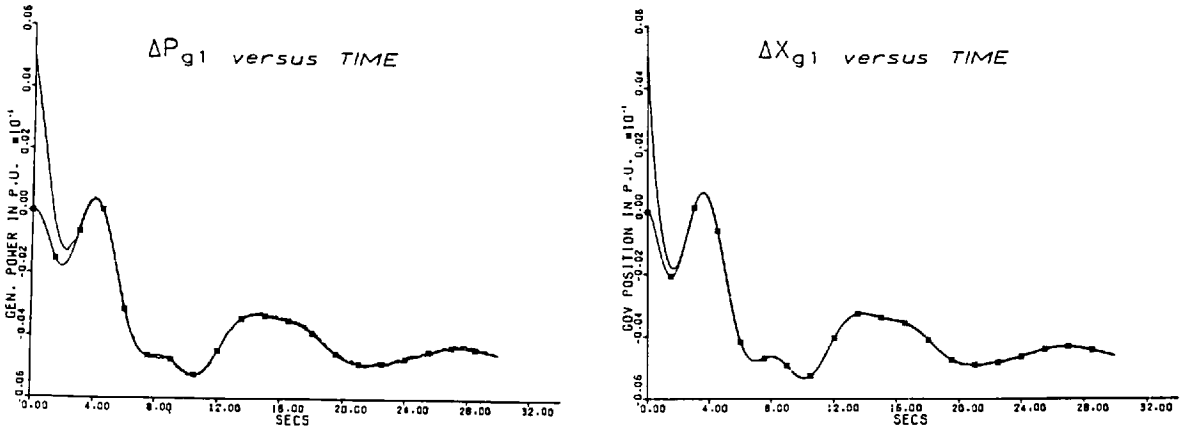

FIGURE 5.6: DECENTRALISED ESTIMATOR WITH $\hat{\underline{x}}_j$ SIGNALS AT NOMINAL TIE-LINE STRENGTH:
a. STEAM PLANT STATE ESTIMATES

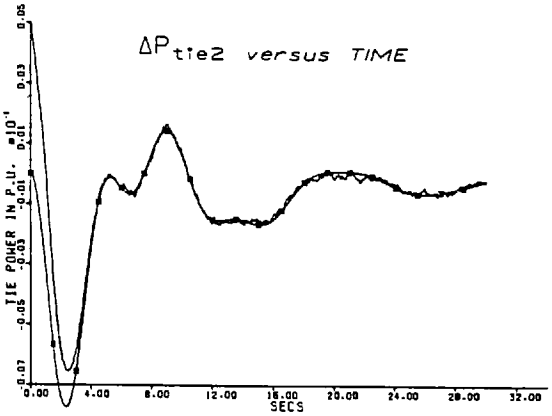

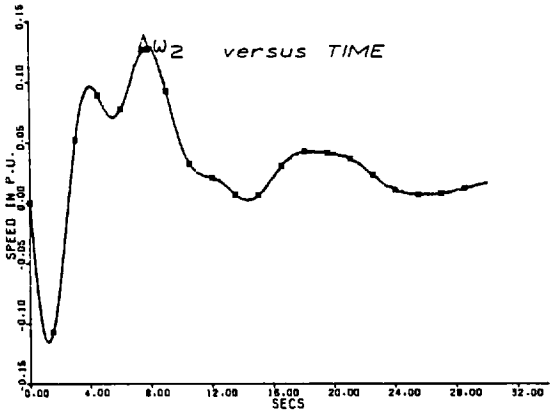

—*—*— true system response

——— system state estimates

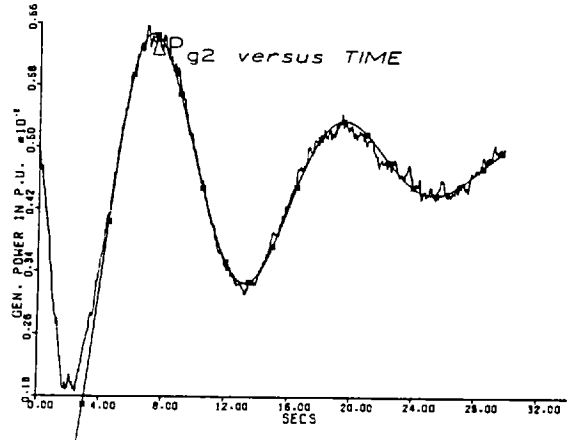

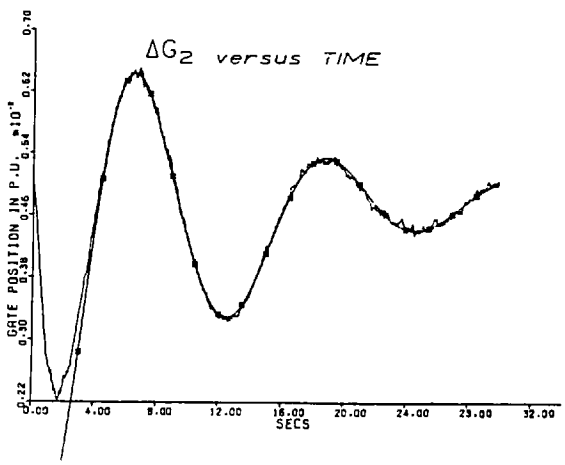

FIGURE 5.6: b. HYDRO PLANT STATE ESTIMATES

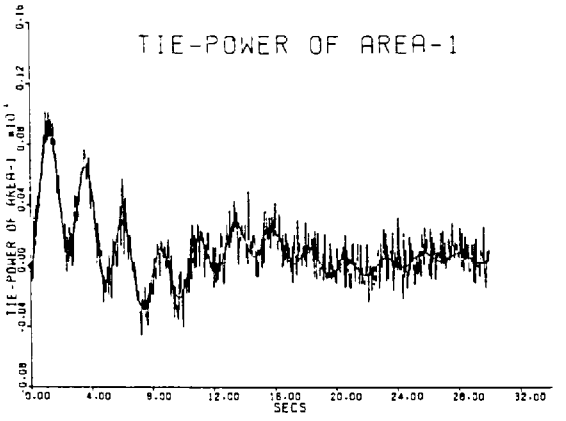

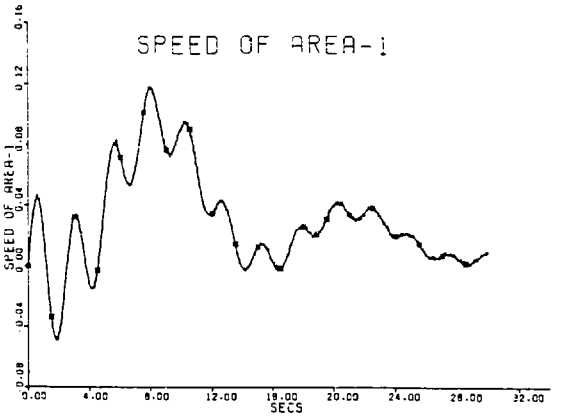

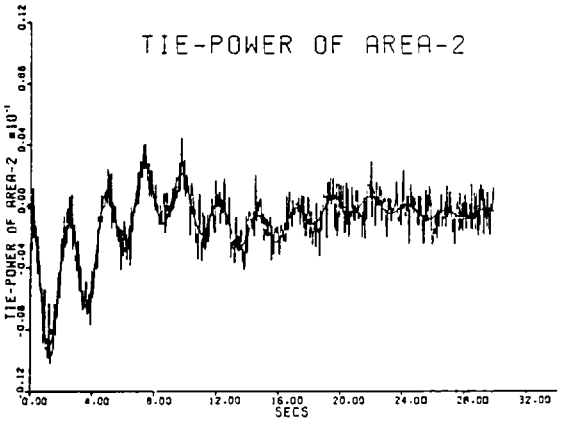

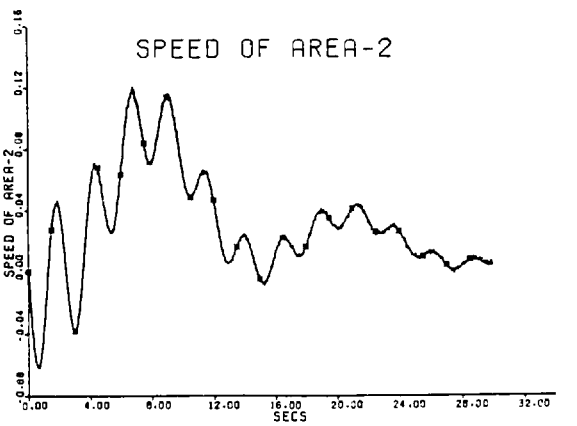

FIGURE 5.7: NOISY MEASUREMENTS OF TIE-LINE POWER AND AREA SPEED DEVIATION FOR TESTS 3

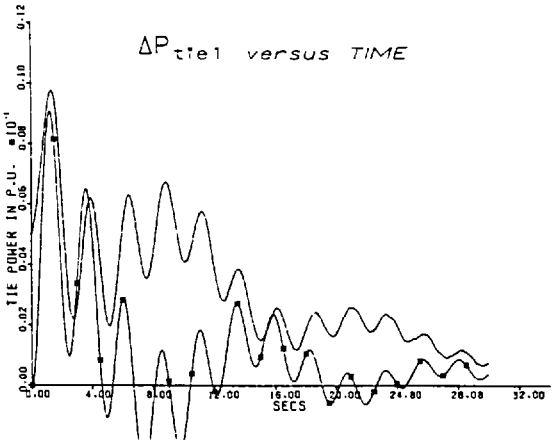

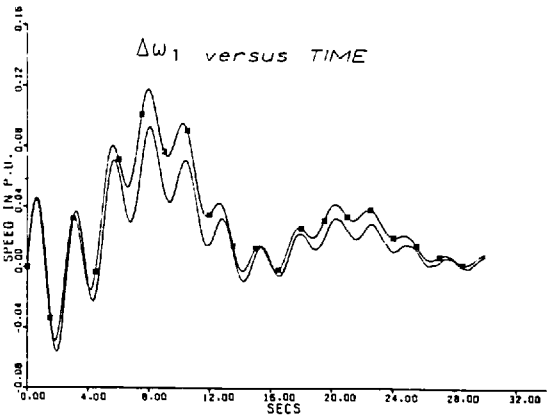

——*—*—— true system response

———— system state estimates

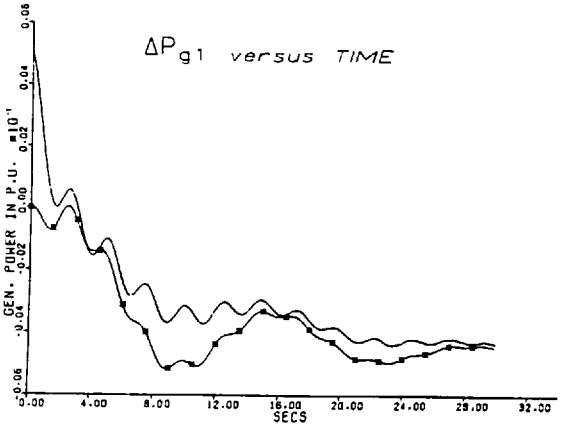

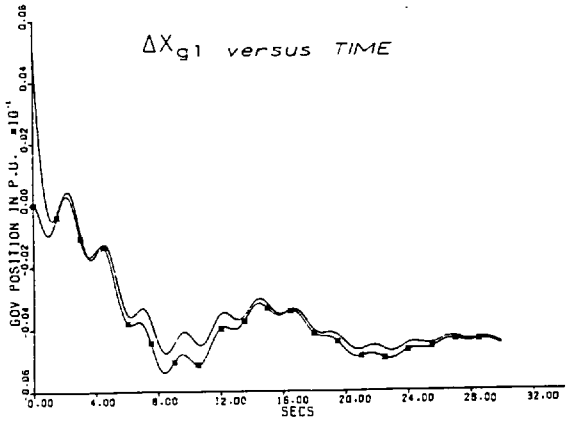

FIGURE 5.8: COMPLETELY DECOUPLED ESTIMATOR AT INCREASED TIE-LINE STRENGTH:
a. STEAM PLANT ESTIMATES

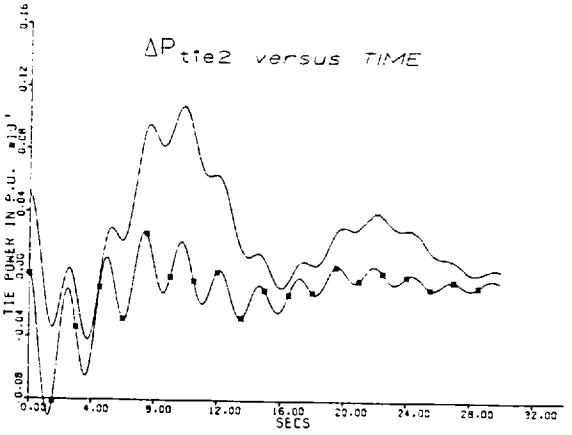

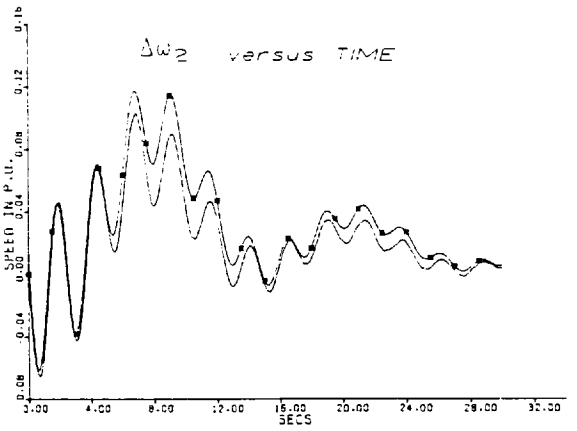

true system response

system state estimates

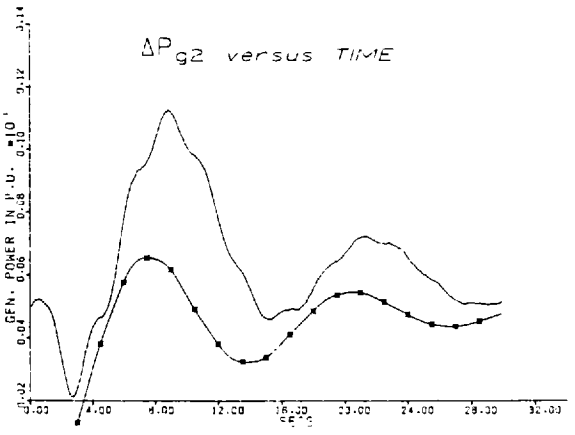

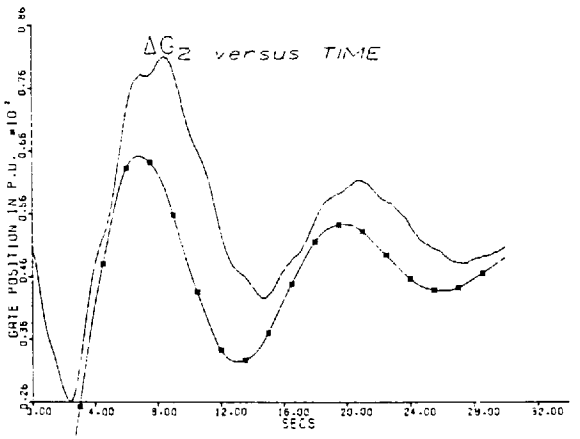

FIGURE 5.8: b. HYDRO PLANT ESTIMATES

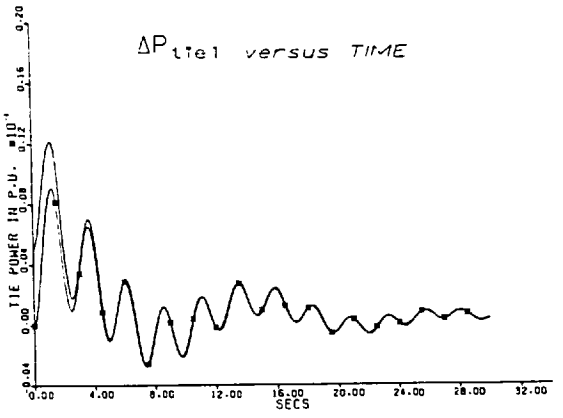

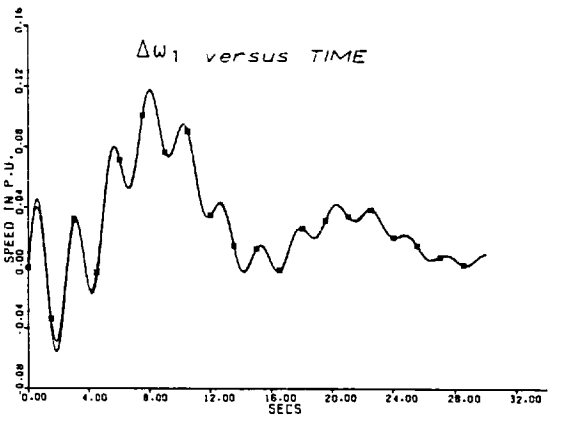

—*—*— true system response

——— system state estimates

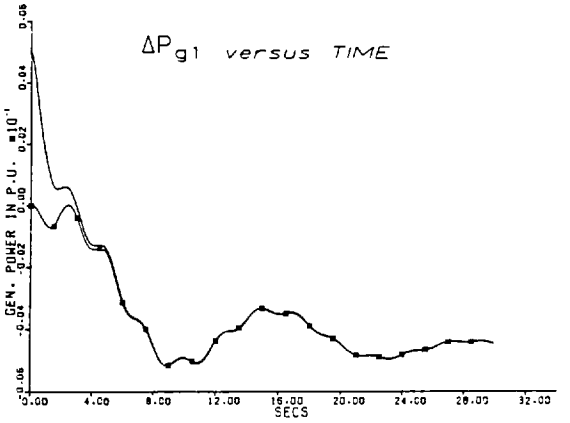

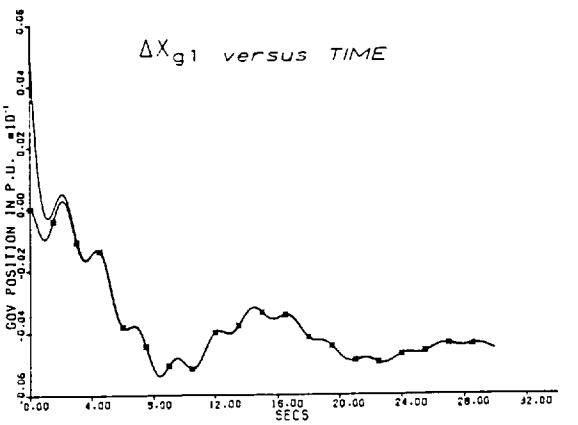

FIGURE 5.9: DECENTRALISED ESTIMATOR WITH $\underline{x}_j$ SIGNALS AT INCREASED TIE-LINE STRENGTH:
a. STEAM PLANT ESTIMATES

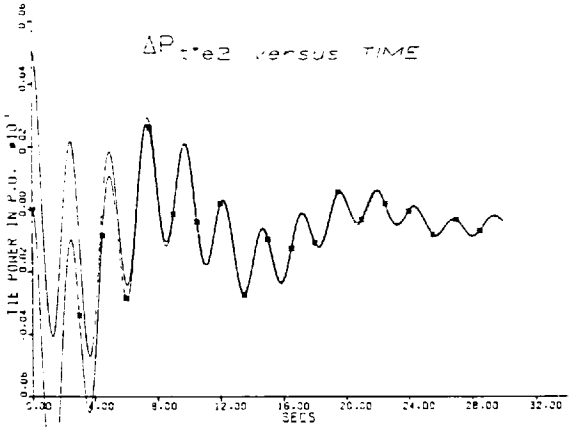

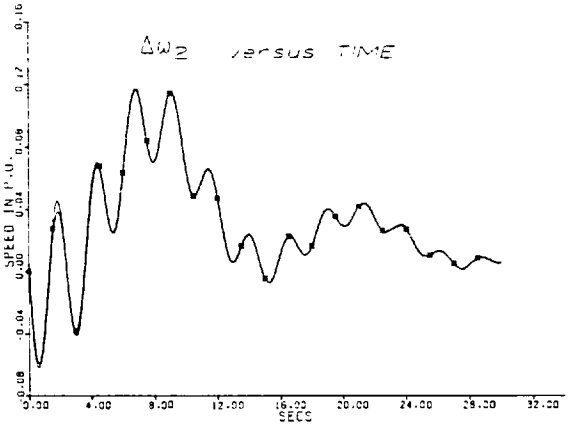

—*—*— true system response

——— system state estimates

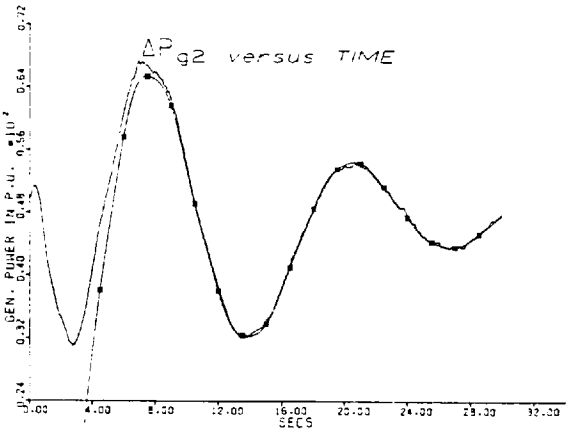

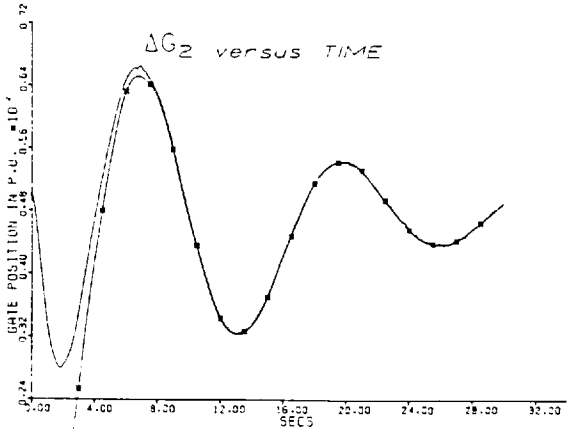

FIGURE 5.9: b. HYDRO PLANT ESTIMATES

CHAPTER VI

CONTINUOUS-TIME DYNAMIC ESTIMATION OF THE STATES OF A SYNCHRONOUS MACHINE

6.1 Introduction

Most multi-variable feedback control techniques employed in the design of optimal control strategies for synchronous machine operation assume that the machine state variables are either known a-priori or available for direct and accurate measurement[21,22,77]. This assumption is questionable since it is known that certain machine state variables are difficult to measure directly, for example, the machine angle with respect to a given reference.

To circumvent this assumption, Takata et al.[25,78] derived the machine states through non-linear sequential observer techniques. This method fails to consider the inevitable presence of measurement noise.

Arumugam et al.[24] considered a linearised version of the essentially highly non-linear estimation problem by deriving its extended Kalman-filter equivalent.

The two approaches proposed in the above methods both yield degenerate state estimates as a result of the assumptions made in deriving the machine state estimates.

In this chapter, the non-linear synchronous machine dynamic state estimation problem is described and solved via the invariant imbedding technique[26,27,80]. The assumptions of perfect instrumentation of Takata et al.[25,78] is relaxed whilst the linearisation of Arumugam et al.[24] is removed by using the exact non-linear synchronous machine equations.

6.2 General theory and problem statement

Consider the class of n-th order non-linear continuous-time systems given by:

$$\dot{\underline{x}}(t) = \underline{f}\left\{\underline{x}(t),t\right\} + G(t)\underline{\omega}(t) \qquad (6.2.1)$$

with its associated r-th order state observation given by:

$$\underline{z}(t) = \underline{h}\left\{\underline{x}(t),t\right\} + \underline{\nu}(t) \qquad (6.2.2)$$

Equation (6.2.1) represents the plant state variable differential equations and equation (6.2.2) represents the state observations where:

$\underline{x}(t)$ is the n-dimensional system state vector

$\underline{f}\left\{\underline{x}(t),t\right\}$ is the n-dimensional vector-valued non-linear function describing the plant structure and includes any known inputs

$\underline{\omega}(t)$ is the n-dimensional plant noise vector

$\underline{z}(t)$ is the r-dimensional observation vector

$\underline{h}\left\{\underline{x}(t),\ t\right\}$ is the r-dimensional vector-valued non-linear function describing the relation between the system states and observations

$\underline{\nu}(t)$ is the r-dimensional measurement noise vector.

The initial system state $\underline{x}(t_o)$ is assumed to be Gaussian and uncorrelated with the plant and measurement noise processes so that:

$$\text{cov}\left\{\underline{x}(t_o),\underline{\omega}(t)\right\} = \underline{0} = \text{cov}\left\{\underline{x}(t_o),\ \underline{\nu}(t)\right\} \qquad (6.2.3)$$

with the following a-priori statistics

$$E\left\{\underline{x}(t_o)\right\} = \mu_{xo} \quad \text{and} \quad \text{Var}\left\{\underline{x}(t_o)\right\} = P_{xo}$$

It is also further assumed that the plant and measurement noise processes are both white and Gaussian with zero means, uncorrelated and with the following covariances:

$$\text{cov}\left\{\omega(t),\omega(\tau)\right\} = Q(t)\,\delta(t-\tau) \qquad (6.2.4)$$

$$\text{cov}\left\{\nu(t),\nu(\tau)\right\} = R(t)\,\delta(t-\tau) \qquad (6.2.5)$$

where δ is the Dirac delta function. The (nxn) covariance matrix Q(t) is assumed positive semi-definite and symmetric whilst the (rxr) covariance

matrix R(t) is assumed to be positive definite and symmetric. In equation (6.2.1) it is assumed that any unknown vector of system parameters has been adjoined to the original system state vector as additional states.

In the system state and parameter estimation problem, least-squares estimates of $\underline{x}(t)$ are to be determined such that the cost functional J is minimised, where:

$$J = \tfrac{1}{2} \int_{t_o}^{t_f} \left[\hat{\underline{V}}^T(t)\, R^{-1}(t)\, \hat{\underline{V}}(t) + \hat{\underline{\omega}}^T(t)\, Q^{-1}(t)\, \hat{\underline{\omega}}(t) \right] dt \qquad (6.2.6)$$

$\hat{\underline{V}}(t)$ and $\hat{\underline{\omega}}(t)$ being the estimates of the system observation noise and system excitation noise respectively. The state and parameter estimator problem therefore leads to a sequential minimisation of J of equation (6.2.6) subject to the dynamical differential constraint:

$$\dot{\hat{\underline{x}}}(t) = \underline{f}\left\{\hat{\underline{x}}(t), t\right\} + G(t)\hat{\underline{\omega}}(t) \qquad (6.2.7)$$

where

$$\hat{\underline{V}}(t) = \underline{z}(t) - \underline{h}\left\{\hat{\underline{x}}(t), t\right\} \qquad (6.2.8)$$

$\hat{\underline{x}}(t)$ is the estimated system state and t_o to t_f is the time interval over which the estimates are to be generated. Equations (6.2.6) and (6.2.7) represent a minimisation problem of the Euler-Lagrange type in the Calculus of Variations[81].

The solution to the optimisation problem defined by equations (6.2.6) and (6.2.7) may be obtained by applying the Pontryagin Maximum Principle[82]. The Hamiltonian[82] for this optimisation problem is:

$$H = \tfrac{1}{2} \left\| \underline{z}(t) - \underline{h}\left\{\underline{x}(t), t\right\} \right\|^2_{R^{-1}(t)} + \tfrac{1}{2} \left\| \underline{\omega}(t) \right\|^2_{Q^{-1}(t)}$$

$$+ \Lambda^T(t) \left[\underline{f}\left\{\underline{x}(t), t\right\} + G(t)\underline{\omega}(t) \right] \qquad (6.2.9)$$

where $\| \cdot \|$ are Euclidean vector norms of the enclosed arguments and $\Lambda(t)$

is an n-dimensional vector Lagrange multiplier. The necessary conditions for a minimum of J follow directly by application of the Euler-Lagrange technique, yielding:

$$\frac{\partial H}{\partial \Lambda} = \dot{\hat{\underline{x}}}(t) = \underline{f}\{\hat{\underline{x}}(t),t\} + G(t)\hat{\underline{\omega}}(t) \tag{6.2.10}$$

$$-\frac{\partial H}{\partial \hat{\underline{x}}} = \dot{\Lambda}(t) = \frac{\partial \underline{h}^T\{\hat{\underline{x}}(t),t\}}{\partial \hat{\underline{x}}} R^{-1}(t)\left[\underline{z}(t)-\underline{h}\{\hat{\underline{x}}(t),t\}\right]$$

$$- \frac{\partial \underline{f}^T\{\hat{\underline{x}}(t),t\}}{\partial \hat{\underline{x}}} \Lambda(t) \tag{6.2.11}$$

$$\frac{\partial H}{\partial \hat{\omega}} = 0 = Q^{-1}(t)\hat{\underline{\omega}}(t) + G^T(t)\Lambda(t) \tag{6.2.12}$$

From equation (6.2.12),

$$\hat{\underline{\omega}}(t) = -Q(t)\, G^T(t)\Lambda(t) \tag{6.2.13}$$

Substitution of $\hat{\underline{\omega}}(t)$ into equation (6.2.10) yields the following equation:

$$\frac{\partial H}{\partial \Lambda} = \dot{\hat{\underline{x}}}(t) = \underline{f}\{\hat{\underline{x}}(t),t\} - G(t)\, Q(t)\, G^T(t)\, \Lambda(t) \tag{6.2.14}$$

The initial and final state estimates, $\hat{\underline{x}}(t_o)$ and $\hat{\underline{x}}(t_f)$ are in general unknown; however, the transversality condition[28] associated with the minimisation of H leads to the following boundary conditions for $\Lambda(t)$:

$$\Lambda(t_o) = \Lambda(t_f) = \underline{0} \tag{6.2.15}$$

Equations (6.2.11), (6.2.14) and (6.2.15) define a Two-Point Boundary-Value Problem, TPBVP, the solution of which determines the least-squares estimate, $\hat{\underline{x}}(t_f)$, of $\underline{x}(t_f)$. The solution to the TPBVP described above can be obtained by the method of continuous-time invariant imbedding[26,27,80].

6.3 Continuous-time invariant imbedding solution

It is easier to obtain a solution to the TPBVP of the last section as a specific or degenerate case of a more general problem by imbedding the specific problem into a more general one. The procedure for this generalisation of the variational problem of section 6.2 is as follows:

The boundary conditions of $\Lambda(t)$ given by equation (6.2.15) can be imbedded into the more general class of conditions:

$$\Lambda(t_f) = \underline{C}$$

where $\underline{C}$ is an n-vector that can assume any value, including $\underline{C} = \underline{0}$. t_f may now be assumed to be variable rather than fixed. For any trajectory that satisfies $\Lambda(t_f) = \underline{C}$, the terminal value of $\hat{\underline{x}}(t_f)$ can be expressed as a function of $\underline{C}$ and t_f by:

$$\hat{\underline{x}}(t_f) = \underline{F}(\underline{C}, t_f) \tag{6.3.1}$$

If the right-hand-sides of equations (6.2.14) and (6.2.11) are replaced by the functions $\underline{\alpha}(\hat{\underline{x}}, \underline{C}, t_f)$ and $\underline{\beta}(\hat{\underline{x}}, \underline{C}, t_f)$ where t is now t_f and $\Lambda(t)$ is now $\underline{C}$, it follows that:

$$\dot{\hat{\underline{x}}}(t_f) = \underline{\alpha}(\underline{F}, \underline{C}, t_f) \tag{6.3.2}$$

and

$$\dot{\Lambda}(t_f) = \underline{\beta}(\underline{F}, \underline{C}, t_f) \tag{6.3.3}$$

where:

$$\underline{\alpha}(\underline{F}, \underline{C}, t_f) = \underline{f}(\underline{F}, \underline{C}, t_f) - G(t)Q(t)G^T(t)\underline{C}$$

$$\underline{\beta}(\underline{F}, \underline{C}, t_f) = \frac{\partial \underline{h}^T(\underline{F}, \underline{C}, t_f)}{\partial \hat{\underline{x}}} R^{-1}(t) \left[\underline{z}(t) - \underline{h}(\underline{F}, \underline{C}, t_f) \right] - \frac{\partial \underline{f}^T(\underline{F}, \underline{C}, t_f)}{\partial \hat{\underline{x}}} \underline{C}$$

It follows from equation (6.3.1) that:

$$\hat{\underline{x}}(t_f + \Delta t_f) = \hat{\underline{x}}(t_f) + \dot{\hat{\underline{x}}}(t_f) \Delta t_f$$

$$= \underline{F}(\underline{C}, t_f) + \underline{\alpha}(\underline{F}, \underline{C}, t_f) \Delta t_f$$

But since $\hat{\underline{x}}(t_f + \Delta t_f) = \underline{F}(\underline{C} + \Delta \underline{C}, t_f + \Delta t_f)$ this implies:

$$\underline{F}(\underline{C} + \Delta \underline{C}, t_f + \Delta t_f) = \underline{F}(\underline{C}, t_f) + \underline{\alpha}(\underline{F}, \underline{C}, t_f) \Delta t_f \tag{6.3.4}$$

A first order Taylor series expansion of $\underline{F}(\underline{C} + \Delta \underline{C}, t_f + \Delta t_f)$ results in the approximate expression:

$$\underline{F}(\underline{C} + \Delta\underline{C}, t_f + \Delta t_f) = \underline{F}(\underline{C}, t_f) + \frac{\partial \underline{F}(\underline{C}, t_f)}{\partial \underline{C}} \Delta \underline{C}$$

$$+ \frac{\partial \underline{F}(\underline{C}, t_f)}{\partial t_f} \Delta t_f \qquad (6.3.5)$$

In a similar way, since:

$$\Lambda(t_f) = \underline{C}(t_f)$$

it follows that $\Delta \underline{C} = \Delta \Lambda$

But because:

$$\Delta \Lambda = \frac{\partial \Lambda(t_f)}{\partial t_f} \Delta t_f = \underline{\beta}(\underline{F}, \underline{C}, t_f) \Delta t_f$$

it also follows that:

$$\Delta \underline{C} = \underline{\beta}(\underline{F}, \underline{C}, t_f) \Delta t_f \qquad (6.3.6)$$

Equation (6.3.5) therefore becomes:

$$\underline{F}(\underline{C} + \Delta \underline{C}, t_f + \Delta t_f) = \underline{F}(\underline{C}, t_f) + \frac{\partial \underline{F}(\underline{C}, t_f)}{\partial \underline{C}} \underline{\beta}(\underline{F}, \underline{C}, t_f) \Delta t_f$$

$$+ \frac{\partial \underline{F}(\underline{C}, t_f)}{\partial t_f} \Delta t_f \qquad (6.3.7)$$

Equating the right-hand-sides of equations (6.3.4) and (6.3.7) gives:

$$\underline{F}(\underline{C}, t_f) + \underline{\alpha}(\underline{F}, \underline{C}, t_f) \Delta t_f = \underline{F}(\underline{C}, t_f) + \frac{\partial \underline{F}(\underline{C}, t_f)}{\partial t_f} \Delta t_f$$

$$+ \frac{\partial \underline{F}(\underline{C}, t_f)}{\partial \underline{C}} \underline{\beta}(\underline{F}, \underline{C}, t_f) \Delta t_f$$

or, after simplification,

$$\frac{\partial \underline{F}(\underline{C}, t_f)}{\partial t_f} + \frac{\partial \underline{F}(\underline{C}, t_f)}{\partial \underline{C}} \underline{\beta}(\underline{F}, \underline{C}, t_f) = \underline{\alpha}(\underline{F}, \underline{C}, t_f) \qquad (6.3.8)$$

There is no general closed form solution to the partial differential equation (6.3.8), however a solution of the form:

$$\underline{F}(\underline{C}, t_f) = \hat{\underline{x}}(t_f) - P(t_f)\, \underline{C} \qquad (6.3.9)$$

may be assumed which leads to an approximate expression for the filtered estimate, $\hat{\underline{x}}(t)$. Substitution of equation (6.3.9) into equation (6.3.8) yields:

$$\dot{\hat{\underline{x}}}(t_f) - \dot{P}(t_f)\underline{C} - P(t_f)\,|\underline{\beta}(\hat{\underline{x}}-P\underline{C},\,\underline{C},t_f) = \underline{\alpha}\,(\hat{\underline{x}}-P\underline{C},\underline{C},t_f) \qquad (6.3.10)$$

Expansion of $\underline{\alpha}$ and $|\underline{\beta}$ in Taylor series about the point $\underline{C} = \underline{0}$ with terms of order two or higher neglected leads to the approximate expression:

$$\dot{\hat{\underline{x}}}(t)-\dot{P}(t)\underline{C}-P(t)|\underline{\beta}(\hat{\underline{x}},\underline{0},t)-P(t)\frac{\partial}{\partial \underline{C}}\left\{|\underline{\beta}(\hat{\underline{x}}-P\underline{C},\underline{C},t)\right\}\Big|_{\underline{C}=\underline{0}}\underline{C}$$

$$= \underline{\alpha}\,(\hat{\underline{x}},\underline{0},t)+\frac{\partial}{\partial \underline{C}}\left\{\underline{\alpha}(\hat{\underline{x}}-P\underline{C},\,\underline{C},\,t)\right\}\Big|_{\underline{C}=\underline{0}}\underline{C} \qquad (6.3.11)$$

t_f has been replaced by the general time variable t, and P is an unknown (nxn) symmetric, positive definite matrix.

Collecting and equating like powers of $\underline{C}$ in equation (6.3.11) yields the following two sets of differential equations:

$$\dot{\hat{\underline{x}}}(t) = \underline{\alpha}\,(\hat{\underline{x}},\underline{0},t) + P(t)\,|\underline{\beta}(\hat{\underline{x}},\underline{0},t) \qquad (6.3.12)$$

$$\dot{P}(t) = -P(t)\,\frac{\partial}{\partial \underline{C}}\left\{|\underline{\beta}(\hat{\underline{x}}-P\underline{C},\underline{C},t)\right\}\Big|_{\underline{C}=0} - \frac{\partial}{\partial \underline{C}}\left\{\underline{\alpha}(\hat{\underline{x}}-P\underline{C},\underline{C},t)\right\}\Big|_{\underline{C}=0} \qquad (6.3.13)$$

From the expressions for $\underline{\alpha}(\cdot)$ and $|\underline{\beta}(\cdot)$, it follows that:

$$\underline{\alpha}\,(\hat{\underline{x}},\underline{0},t) = \underline{\alpha}\,(\hat{\underline{x}},t) = \underline{f}(\hat{\underline{x}},t) \qquad (6.3.14)$$

$$|\underline{\beta}(\hat{\underline{x}},\underline{0},t) = |\underline{\beta}(\hat{\underline{x}},t) = \frac{\partial \underline{h}^T\{(\hat{\underline{x}},t)\}}{\partial \hat{\underline{x}}}\;R^{-1}(t)\left\{\underline{z}(t)-\underline{h}(\hat{\underline{x}},t)\right\} \qquad (6.3.15)$$

In general the chain rule of differentiation gives for any function ψ :

$$\frac{\partial \psi}{\partial \underline{C}} = \frac{\partial}{\partial \hat{\underline{x}}}(\psi) * \frac{\partial \hat{\underline{x}}}{\partial \underline{F}} * \frac{\partial \underline{F}}{\partial \underline{C}}$$

This, together with the fact that $\frac{\partial \hat{\underline{x}}}{\partial \underline{F}} = 1$ and $\frac{\partial \underline{F}}{\partial \underline{C}} = -P(t)$ yields:

$$\frac{\partial}{\partial \underline{C}}\left\{\underline{\alpha}\,(\hat{\underline{x}}-P\underline{C},\underline{C},t)\right\} = \frac{\partial}{\partial \hat{\underline{x}}}\left\{\underline{f}(\hat{\underline{x}}-P\underline{C},\underline{C},t)\right\}\Big|_{\underline{C}=\underline{0}} * \left(-P(t)\right) - G(t)Q(t)G^T(t)$$

$$= - \frac{\partial \underline{f}(\hat{\underline{x}},t)}{\partial \hat{\underline{x}}} \; P(t) - G(t)\, Q(t) G^T(t) \qquad (6.3.16)$$

and

$$\frac{\partial}{\partial \underline{c}} \left\{ \underline{\beta}(\hat{\underline{x}}-P\underline{c},\underline{c},t) \right\} = - \frac{\partial \underline{f}^T(\hat{\underline{x}},t)}{\partial \hat{\underline{x}}}$$
$$+ \frac{\partial}{\partial \hat{\underline{x}}} \left[\frac{\partial \underline{h}^T(\hat{\underline{x}}-P\underline{c},\underline{c},t)}{\partial \hat{\underline{x}}} \; R^{-1}(t) \left\{ \underline{z}(t) - \underline{h}(\hat{\underline{x}}-P\underline{c},\underline{c},t) \right\} \right] \Bigg|_{\underline{c}=\underline{0}} * \left[-P(t) \right]$$
$$= - \frac{\partial \underline{f}^T(\hat{\underline{x}},t)}{\partial \hat{\underline{x}}} - \frac{\partial}{\partial \hat{\underline{x}}} \left[\frac{\partial \underline{h}^T(\hat{\underline{x}},t)}{\partial \hat{\underline{x}}} \; R^{-1}(t) \left\{ \underline{z}(t) - \underline{h}(\hat{\underline{x}},t) \right\} \right] P(t) \qquad (6.3.17)$$

Substitution of equations (6.3.14) and (6.3.15) into equation (6.3.12) yields:

$$\dot{\hat{\underline{x}}}(t) = \underline{f}(\hat{\underline{x}},t) + P(t) \frac{\partial \underline{h}^T(\hat{\underline{x}},t)}{\partial \hat{\underline{x}}} R^{-1}(t) \left[\underline{z}(t) - \underline{h}(\hat{\underline{x}},t) \right] \qquad (6.3.18)$$

whilst substitution of equations (6.3.16) and (6.3.17) into equation (6.3.13) gives:

$$\dot{P}(t) = P(t) \frac{\partial \underline{f}^T(\hat{\underline{x}},t)}{\partial \hat{\underline{x}}} + \frac{\partial \underline{f}(\hat{\underline{x}},t)}{\partial \hat{\underline{x}}} \; P(t) + P(t) \frac{\partial}{\partial \hat{\underline{x}}} \left[\frac{\partial \underline{h}^T(\hat{\underline{x}},t)}{\partial \hat{\underline{x}}} R^{-1}(t) \left\{ \underline{z}(t) - \underline{h}(\hat{\underline{x}},t) \right\} \right] P(t) + G(t)\, Q(t)\, G^T(t) \qquad (6.3.19)$$

The initial conditions for the two coupled differential equations, (6.3.18) and (6.3.19) are respectively:

$$\underline{x}(t_o) = \mu_{xo}$$

$$P(t_o) = P_{xo}$$

Implementation of equations (6.3.18) and (6.3.19) generate the optimal filtered estimate of the system state, $\hat{\underline{x}}(t)$. Although the statistics of $\underline{x}(t_o)$ and $\underline{\omega}(t), \underline{\nu}(t)$ were initially assumed, the derivations have not explicitly made use of these properties. In fact μ_{xo}, P_{xo}, $Q(t)$ and $R(t)$ could have been arbitrarily selected.

6.4 Non-linear machine and measurement equations

6.4.1 Machine state equations

The state of a single machine infinite busbar power system may be described by four non-linear differential equations [25,78] as follows:

$$\dot{e}_d = -A_1 e_d + A_2 \dot{\delta} \cos\delta + A_3 \sin\delta - A_4 \tag{6.4.1}$$

$$\dot{e}_q = -A_1 e_q - A_2 \dot{\delta} \sin\delta + A_3 \cos\delta + A_5 \tag{6.4.2}$$

$$\ddot{\delta} = A_7 \dot{\delta} + A_8(e_q \sin\delta - e_d \cos\delta) + A_6 \tag{6.4.3}$$

If the machine state vector is defined as

$$\underline{x}^T = (e_d \; e_q \; \delta \; \dot{\delta}) \tag{6.4.4}$$

then

$$\dot{x}_1 = -A_1 x_1 + A_2 x_4 \cos x_3 + A_3 \sin x_3 - A_4 \tag{6.4.5}$$

$$\dot{x}_2 = -A_1 x_2 - A_2 x_4 \sin x_3 + A_3 \cos x_3 + A_5 \tag{6.4.6}$$

$$\dot{x}_3 = x_4 \tag{6.4.7}$$

$$\dot{x}_4 = A_7 x_4 + A_8(x_2 \sin x_3 - x_1 \cos x_3) + A_6 \tag{6.4.8}$$

where x_1, x_2, x_3 and x_4 are the components of $\underline{x}$. For the machine model and the derivation of the machine dynamical equations and expressions for the system constants A_o, A_1,...,A_8 refer to Appendix B.

A more general representation of equations (6.4.5) to (6.4.8) in a vector differential equation form is:

$$\dot{\underline{x}}(t) = \underline{f}(\underline{x},t) \tag{6.4.9}$$

To account for system modelling errors and unknown disturbance inputs, equation (6.4.9) is corrupted by the finite-valued stochastic noise vector term $\underline{\omega}(t)$, to give a stochastic description of the machine behaviour as:

$$\dot{\underline{x}}(t) = \underline{f}(\underline{x},t) + \underline{\omega}(t) \qquad (6.4.10)$$

6.4.2 Machine measurement equations

It is very difficult to measure the physical machine state variables directly, either because the state variables are inaccessible for direct measurement (for example e_d, e_q the direct-and quadrature-axis stator voltages are not accessible for direct measurement) and/or their direct measurement is, economically, infeasible (for example δ the machine rotor angle). Although it is theoretically possible to select a host of quantities as suitable measurement variables, only the following were chosen for measurement because of their ease of measurement and accessibility.

1. Machine terminal voltage, V_t
2. Machine real-power output, P
3. Machine speed deviation, S

V_t, P and S may all be expressed in terms of the machine state variables as non-linear algebraic expressions:

$$V_t = (e_d^2 + e_q^2)^{\frac{1}{2}} \qquad (6.4.11)$$

$$P = \frac{e_s}{x_1} (e_q \sin\delta - e_d \cos\delta) \qquad (6.4.12)$$

$$S = \dot{\delta} \qquad (6.4.13)$$

If the measurement state vector is defined by:

$$\underline{z}^T = (V_t \; P \; S) \qquad (6.4.14)$$

then

$$z_1 = (x_1^2 + x_2^2)^{\frac{1}{2}} \qquad (6.4.15)$$

$$z_2 = \frac{e_s}{x_1} (x_2 \sin x_3 - x_1 \cos x_3) \qquad (6.4.16)$$

$$z_3 = x_4 \qquad (6.4.17)$$

where z_1, z_2 and z_3 are the components of $\underline{z}$. As in the case of the state equation a more general vector representation of the measurement variables is possible, namely:

$$\underline{z}(t) = \underline{h}(\underline{x},t) \tag{6.4.18}$$

A practical measurement model will always account for meter inaccuracies, instrumentation and telemetery errors as well as meter biases. For this reason, another stochastic disturbance vector term, $\underline{v}(t)$ of finite value is added to equation (6.4.18) to represent the real-time measurement situation:-

$$\underline{z}(t) = \underline{h}\ (\underline{x},t) + \ \underline{v}(t) \tag{6.4.19}$$

The dynamic power system state estimation problem has therefore been successfully transformed into its equivalent general state estimation problem (as described in the general theory of section 6.2) by suitably defining the non-linear vector functions $\underline{f}(\bullet)$ and $\underline{h}(\bullet)$. Comparison of equations (6.2.1) and (6.4.10) reveals that in the power system case, the input noise distribution matrix is the (nxn) identity matrix.

6.5 Estimation of machine states

By directly invoking the results of dynamic state estimation via the invariant imbedding technique (equations (6.3.18) and (6.3.19)), the state of the power system may be obtained from a sequential solution of the following set of non-linear differential equations:

$$\dot{\hat{\underline{x}}}(t) = \underline{f}(\hat{\underline{x}},t) + P(t)\ H^T(\hat{\underline{x}},t)\ R^{-1}(t) \left[\underline{z}-\underline{h}(\hat{\underline{x}},t)\right] \tag{6.5.1}$$

$$\dot{P}(t) = P(t)\ F^T(\hat{\underline{x}},t) + F(\hat{\underline{x}},t)\ P(t) + Q(t) + P(t) \frac{\partial}{\partial \hat{\underline{x}}} \Big\{ H^T(\hat{\underline{x}},t)\ R^{-1}(t) \left[\underline{z}(t) - \underline{h}(\hat{\underline{x}},t)\right] \Big\} P(t) \tag{6.5.2}$$

where $H(\hat{\underline{x}},t) = \dfrac{\partial \underline{h}(\hat{\underline{x}},t)}{\partial \hat{\underline{x}}}$

and $$F(\hat{\underline{x}},t) = \frac{\partial \underline{f}(\hat{\underline{x}},t)}{\partial \hat{\underline{x}}}$$

with the initial conditions:

$\hat{\underline{x}}(t_o) = \underline{x}_o$

and

$P(t_o) = P_o$

A subtle difference exists between this type of estimator and its corresponding extended Kalman-Bucy filter equivalent [28,83,84].

a. In the extended Kalman-filter, the Hessian of $\underline{h}(\hat{\underline{x}},t)$ that is $\frac{\partial^2 \underline{h}(\hat{\underline{x}},t)}{\partial \hat{\underline{x}}^2}$ is generally ignored leading to a simplified expression for the last term of equation (6.5.2) which is:

$-P(t)\ H^T(\hat{\underline{x}},t)\ R^{-1}(t)\ H(\hat{\underline{x}},t)\ P(t)$

Because no such assumptions are made in the method of this chapter better filtered estimates than any form of extended Kalman filter are obtained.

b. All Kalman filtering techniques require precise prior statistical information about the noise processes $\underline{w}(t)$ and $\underline{v}(t)$ as well as the initial state estimate $\hat{\underline{x}}(t_o)$

It is clear from the derivations that the covariance matrices $Q(t)$, $R(t)$ and P_{xo} need not be precisely known a-priori utilising the technique of this chapter, since $Q(t)$, $R(t)$, P_{xo} can all be arbitrarily chosen.

6.6 Solution technique

To solve the power system dynamical state estimation problem, the unknown initial conditions of $\hat{\underline{x}}(t_o)$ and $P(t_o)$ must be prescribed together with the noise intensity matrices $Q(t)$ and $R(t)$. It is obvious from the estimator equations that the performance of the estimation scheme in terms of accuracy of estimates and its rate of convergence to

the true power system states both depend on the choice of the parameters $\hat{\underline{x}}(t_o)$, $P(t_o)$, $Q(t)$ and $R(t)$. Since in a power system the steady-state values of the machine states are always known, $\hat{\underline{x}}(t_o)$ is chosen as the steady-state solution of $\dot{\underline{x}}(t) = \underline{f}(\underline{x}, t)$. $P(t_o)$ and $R(t)$ are assumed to be both identity matrices. For a system with accurately known initial state estimates, $P(t_o)$ set equal to the null-matrix provides the best initial estimate of P. If the statistics of $\underline{v}(t)$ is exactly known, then the best value of $R(t) = E\left\{ \underline{v}\, \underline{v}^T \right\}$
Matrix $Q(t)$ is the only unspecified one and it is simulated as a variable positive semi-definite matrix of the form $Q(t) = \alpha\,(I)$, where α is a variable parameter.

Since $P(t)$ is an (nxn) symmetric positive-definite matrix, $n(n+1)/2$ differential equations arise from the $\dot{P}(t)$ equation. As the $\dot{\hat{\underline{x}}}(t)$ equation is n-dimensional, the overall total number of non-linear differential equations to be solved is $n(n+3)/2$. For a fourth-order synchronous machine model this leads to the solution of 14 non-linear, coupled differential equations. The solution of these 14 equations by means of a suitable integration routine generates the estimates of the machine state variables, $\underline{x}^T = (e_d\ e_q\ \delta\ \dot{\delta})$

6.7 Numerical simulations and tests

6.7.1 Simulation of measurements

Errors from instrumentation and metering equipment were simulated as normally distributed random variables of zero mean and known variance, σ^2. In deriving the true measurement vector, the true trajectory of the system state $\underline{x}(t)$ was initially generated and $\underline{z}(t)$, was then obtained by using the functional relationship between it and $\underline{x}(t)$, namely $\underline{h}(\underline{x},t)$. The practical measurement was then obtained by adding

normally distributed pseudo-random numbers to $\underline{h}(\underline{x},t)$. The variance σ_i^2 of each measurement was considered as a parameter γ % of the true measurement function $\underline{h}(\underline{x},t)$, that is $\sigma_i^2 = \left\{\gamma \% \, h_i(\underline{x},t)\right\}^2$

6.7.2 Performance assessment

For qualitatively assessing the performance of the estimation scheme, an index of performance, PI, was defined as follows:

$$PI = \frac{1}{t_f - t_o} \sum_{t_i=t_o}^{t_f} \left\{\Delta \underline{x}(t_i)\right\}^T \left\{\Delta \underline{x}(t_i)\right\} \qquad (6.7.1)$$

where

$$\Delta\underline{x}(t_i) = \underline{x}(t_i) - \hat{\underline{x}}(t_i)$$

the estimation error.

The index of performance PI was calculated over the entire integration period in all regimes of operation of the synchronous machine at various measurement standard deviations and values of the parameter α.

6.7.3 Sets of measurement variables considered

Three distinct measurement situations may be considered for the estimator, namely:

i. When all three measurements of terminal voltage, V_t, real-power, P, and machine speed deviation, S, are available.

ii. When only any two of the three measurements are available, that is, $\left\{V_t, P\right\}$, $\left\{V_t, S\right\}$ or $\left\{P, S\right\}$

iii. When only one of the measurements is available, $[P]$, $[V_t]$ or $[S]$

These three distinct measurement situations were all tested. Table 6.1 lists the values of the constants used [25,78].

TABLE 6.1

POWER SYSTEM CONSTANTS

Constant	Value in pu
x_s	1.0
x_l	0.6
T_{do}	3.0 s
T_{d1}	1.0 s
H	5.0 s
D	0.005
$e_s=e_{fd}=e_{fq}$	1.0
P_{in}	0.76923
f	50.0 Hz
$\omega=2\pi f$	314.7 rad/s

Two operating regimes of the synchronous machine were considered, hunting and step-out, with the following initial states:

$\underline{x}^T(t_o)$ = (-0.48593 0.86149 0.50763 2.15710) in hunting region

$\underline{x}^T(t_o)$ = (-0.49367 0.85013 0.76809 8.18410) in step-out region

The initial estimates of the synchronous machine states were chosen to be the steady-state values;

$\hat{\underline{x}}^T(t_o)$ = (-0.20944 0.97767 0.26809 0.00000)

6.7.4 Discussion of results

Tables 6.2 and 6.3 list the values of PI against the parameter α and Figs. 6.1 and 6.2 present the system dynamical response as well as the estimator results when all three measurements are available. Fig. 6.3 refers to the case when only the measurement set $[P, V_t]$ is available.

TABLE 6.2

PERFORMANCE INDEX PI AS A FUNCTION OF VARIABLE PARAMETER α IN HUNTING REGION

α	PI
0.0	0.359
50.0	0.113
100.0	0.038
200.0	0.036
400.0	0.033
750.0	0.030
1000.0	0.028

TABLE 6.3

PERFORMANCE INDEX PI AS A FUNCTION OF VARIABLE PARAMETER α IN STEP-OUT REGION

α	PI
0.0	3.030
0.2	2.996
0.5	2.985
0.8	2.984
1.0	2.985
100.0	13.633
500.0	73.904

In all the figures, the machine state estimates are illustrated with asterisks, *.

With P, R and $\underline{\hat{x}}(t_o)$ pre-selected as mentioned earlier, the non-linear dynamical power system state estimation equations were implemented with γ in the range 1% to 5% and the system excitation noise intensity matrix parameter α assuming a sequence of values. Both the system and estimation differential equations were solved by means of a simple 4th-order Runge-Kutta integration routine [85,86] with a time-step of 0.005 sec. The choice of this time step was not just arbitrary but based on the realisation that stable integration results if the time-step is at most equal to 20% of the lowest power system time constant [35].

With all three measurements available (Figs. 6.1 and 6.2) all the estimates of the power system states were acceptable after a period of approximately 0.2 secs. In the simulations involving two measurements or less (not all indicated) the algorithm either failed to converge altogether or yielded estimates which were grossly erroneous. This observation is not surprising when one considers the need to establish system observability in all estimation problems before implementation. Unfortunately, observability cannot be established in non-linear dynamical estimation problems a-priori; it is only after the success of the estimation process that observability is deemed established under the measurement conditions assumed. It was observed that successful estimation was possible with fewer than three measurements provided at least one mechanical and one electrical state variable appears in the measurement defining equation $\underline{h}(\underline{x},t)$ as well as in the

measurement Jacobian matrix $H(\underline{x},t)$. This assertion is substantiated by the highly acceptable results indicated in Fig. 6.3 where the measurement set $\left\{P,\ V_t\right\}$ was considered available.

Tables 6.2 and 6.3 show that high values of α yield low PIs in the hunting region whilst low values of α yield $|\dot{\omega}|$ PIs in the step-out region. It may be inferred from these apparently contradictory observations that the design of non-linear dynamical power system estimators requires careful consideration of the operating regime of the machine.

6.8 Conclusions

The present study illustrates the feasibility of designing a continuous-time non-linear state estimator for a synchronous machine. The restrictive assumptions made by Messrs Takata et al.[25,78] and Arumugan et al.[24], namely the absence of system and measurement noise and the linearisation of the highly non-linear machine equations, have all been avoided. The resulting algorithm is shown to be of a similar nature to the extended Kalman-filter[83,84] except for the inclusion of terms arising from the measurement Hessian matrix and the lack of statistical assumptions about the noise processes.

The principal revelations of the study are:

i. Choice of α and hence Q is intimately related to the operating regime of the machine. In the hunting region of operation high α values must be prescribed whilst in the step-out regime low α values are mandatory.

ii. Successful estimation of the machine states is only possible if at least one mechanical and one electrical state variable appear

in both the measurement equation and its Jacobian matrix.

iii. The use of only a single measurement fails to yield reliable estimates even with high values of α .

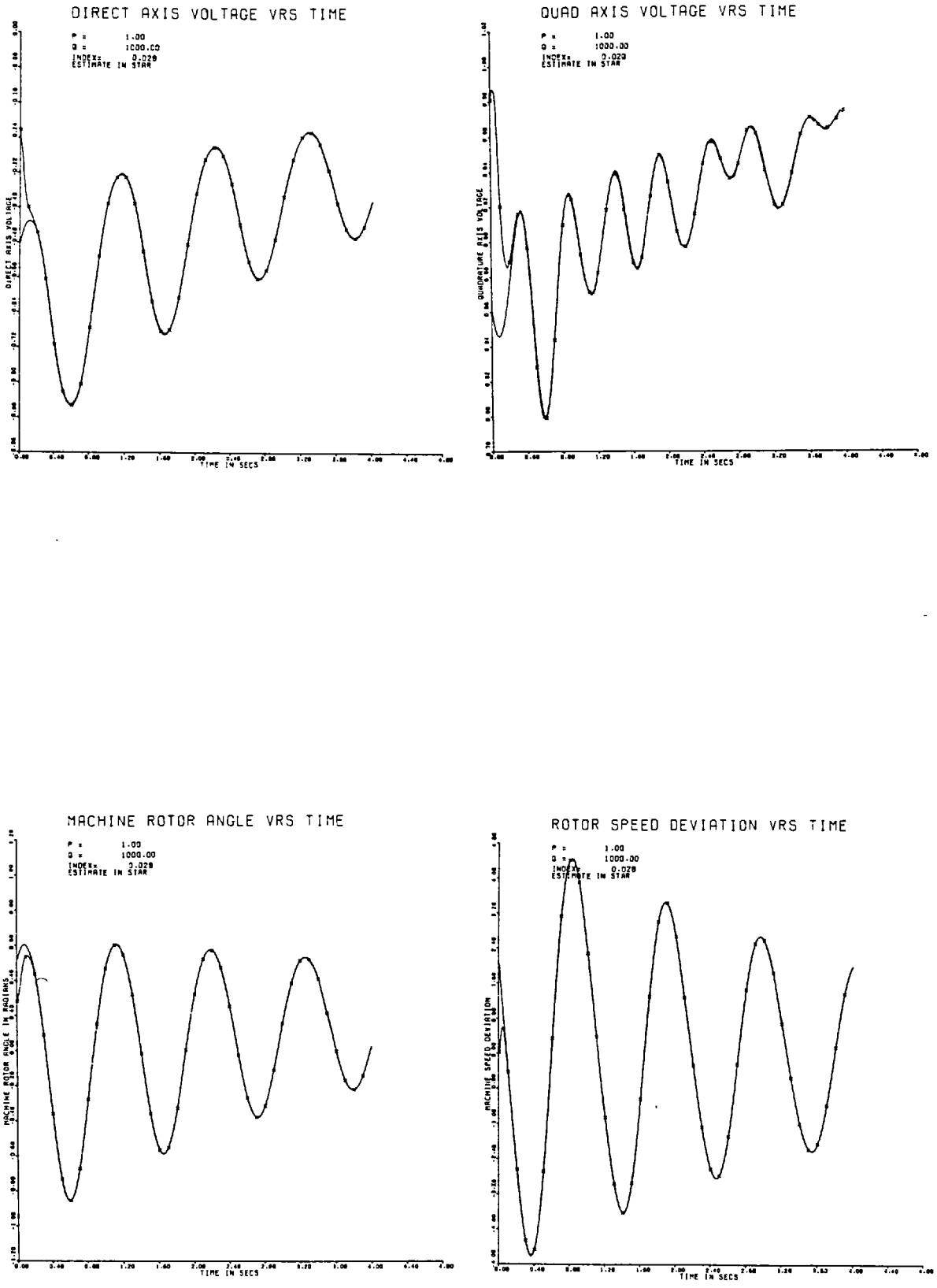

FIGURE 6.1: HUNTING REGION MACHINE STATE ESTIMATES WITH ALL THREE MEASUREMENTS (P, V_t, S)

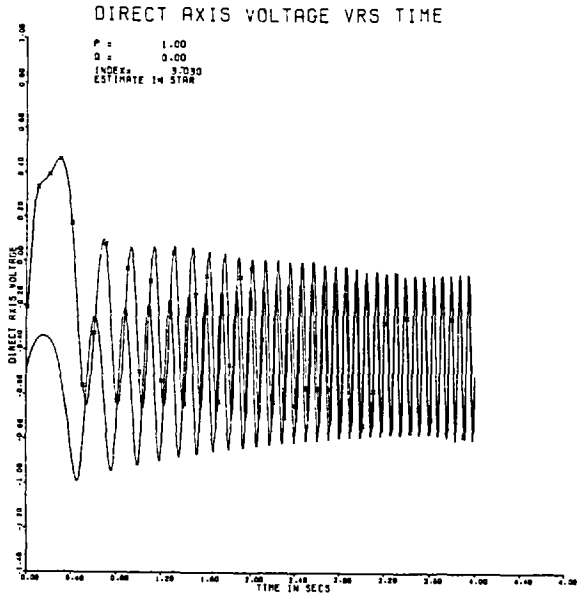

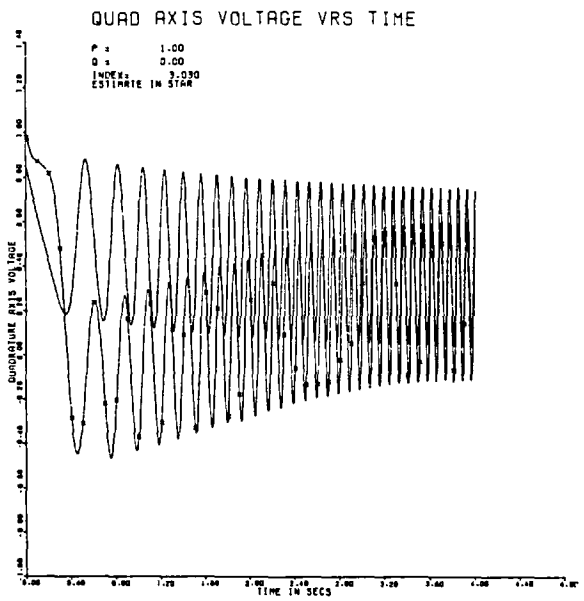

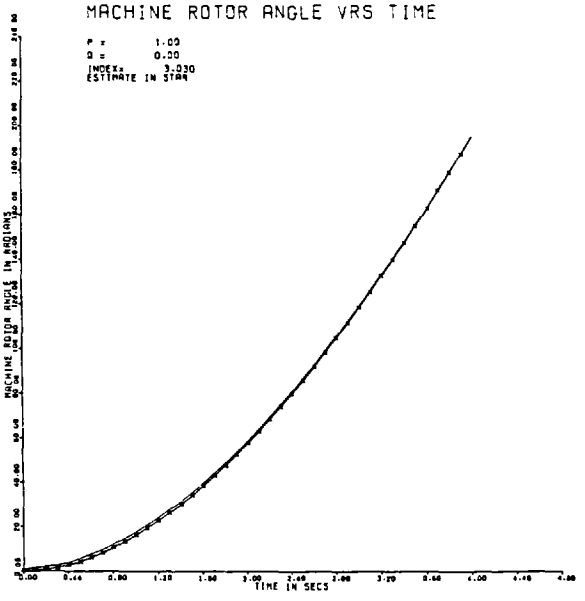

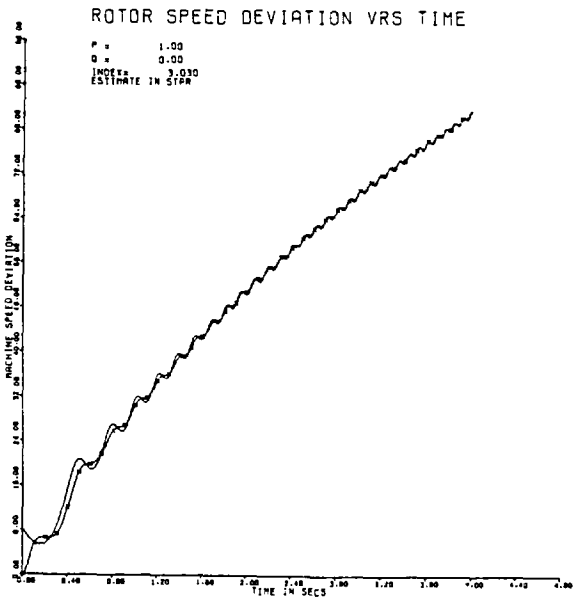

FIGURE 6.2: STEP-OUT REGION MACHINE STATE ESTIMATES WITH ALL THREE MEASUREMENTS (P, V_t, S)

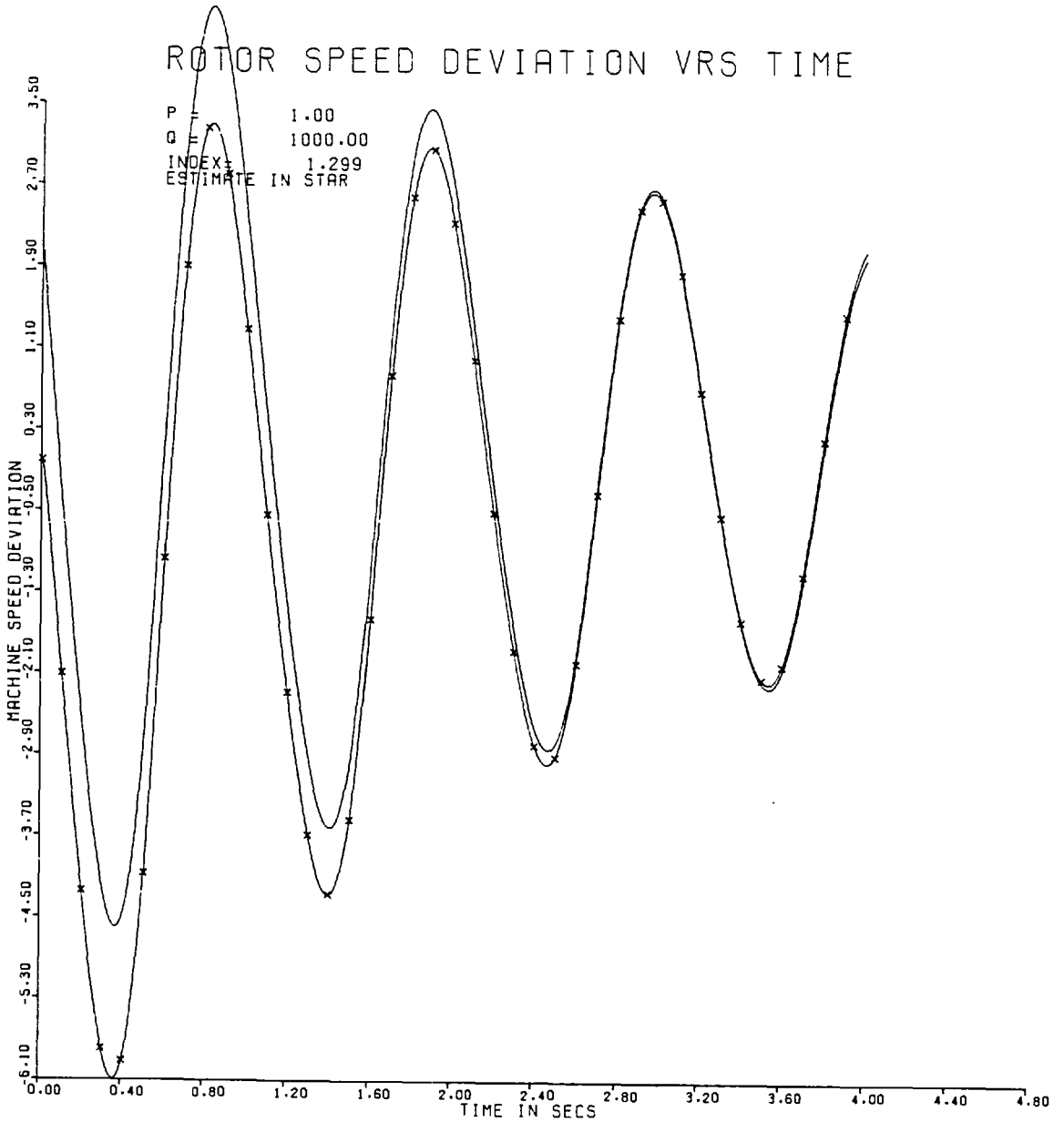

FIGURE 6.3: HUNTING REGION MACHINE STATE ESTIMATES WITH MEASUREMENT SET (P,V_t)

CHAPTER VII

CONCLUSIONS

7.1 Static power systems state estimation

Two basic estimation techniques, LWLS and GWLS, applicable to a power system in a static operating state have been presented and studied both in the presence of normal observation errors and when grossly erroneous input measurement information exists. Approximations concerning the physical network characteristics used in the conventional fast decoupled load flow technique led to the derivation of two enhanced estimation methods P-δ, Q-E estimator and FDE, for the GWLS scheme.

From the simulation tests it is concluded that, except for the constant gain-matrix algorithm, all the estimators described successfully filter normal errors of measurement at different levels of measurement redundancy and are capable of detecting and identifying sources of gross measurement error at reasonable levels of measurement redundancy.

Although all the estimators converged reliably in a finite number of iterations, they required widely differing execution times. Indeed a comparison of Tables 2.5 and 3.13 shows the superiority of the AEP and FDE methods in terms of solution time requirements, where the AEP technique is the fastest of them all, and the full GWLS method the slowest Before any single estimation technique is deemed best suited for on-line implementation on small process control computers, its core requirements must be appreciably low. The exact comparison of the absolute core requirements of the methods described in this thesis is not directly possible; however the storage locations taken up by the largest matrices (A for LWLS and H for GWLS) offer a rough guide to the core used. For a

power network consisting of N-nodes and L-lines where only complex branch power flow measurements at all line and transformer ends are taken, the dimensions of A and H are 2L(N-1) and 4L(2N-2) respectively. The core size ratio is therefore approximately 1 to 4 for the LWLS and GWLS methods. By re-using the storage space (overlaying) of the active measurements Jacobian for the reactive measurements Jacobian in the FDE method, its core requirements are then comparable to that of the AEP technique. In the light of the discussions on the solution times and storage space it is concluded that, except in applications involving very small-sized power systems, the direct on-line implementation of the GWLS estimation algorithm is not recommended. The FDE algorithm clearly possesses the same attractive computational speed and core requirements as the AEP method. Coupled with its versatility in handling not only branch power flow measurements but injection measurements as well, the FDE technique's computational superiority has been ascertained in the off-line studies of this thesis giving it immense prospects for on-line implementation studies.

Finally it ought to be stressed that because of the linearising transformation and load flow approximations made in deriving the AEP and FDE techniques, they do not exhibit the statistical optimal properties of least square estimators possessed by the GWLS method.

7.2 Dynamic power systems state estimation

The estimation of the dynamic state variables of power systems was studied by considering a linear multi-area load frequency control model and a non-linear single machine infinite busbar model.

In the multi-area case it has been shown that global estimator, although superior, presents problems in dealing with the solution of the highly dimensional matrix Ricatti equation. The results of the simulations show that provided supplementary signals from other areas are available in a given location, it is feasible to design dynamic linear estimators on a local basis. The decentralized estimation scheme offers the following advantages over the global scheme:

i. estimation involving large power system areas can be handled in smaller decentralised forms

ii. computer core requirements are much lower when solving the algebraic matrix Ricatti equation

iii. only a minimal amount of information need be exchanged between areas.

For the non-linear synchronous machine model, the machine state variables were reliably estimated from noisy measurements of speed deviation, terminal voltage and generator output power. The simulations established that for reliable estimation the measurement Jacobian and measurement defining equations must contain at least one mechanical and one electrical state variable. The results indicated that successful estimation can only be achieved by a careful choice of the input disturbance noise covariance matrix Q, which depends on the operating regime of the synchronous machine, that is whether in the step-out region or hunting region. Low Q values are recommended for the step-out region and high Q values for the hunting region.

7.3 Suggestions for further research work

i. The static state estimation algorithms need to be assessed in a real-time situation to provide a meaningful comparison of their

on-line capabilities. Arriola-Valdes assessed the on-line behaviour of the AEP (LWLS) estimation technique on the Power System Simulator at Imperial College. A further investigation ought to be carried out on the simulator to compare the on-line operational characteristics of the LWLS, GWLS technique and its enhanced approximations, P-δ, Q-E and FDE methods. The comparative results of these on-line tests would, hopefully, provide a more reliable and tried basis for prescribing general rules for choosing static state estimation algorithms for on-line power system operation.

ii. To obtain further computational gains in speed of solution and computer core storage in the GWLS static state estimation method efforts should be directed towards the provision of the same constant coefficient matrix for both the active and the reactive power loop solutions for the state estimate mismatch vector $(\Delta\delta_k, \Delta E_k)$. Such a constant coefficient matrix will need to be stored once only at the beginning of the estimation process and will require only one factorisation per iteration for both power loops to yield a still faster and lower core storage technique.

iii. The linear LFC decentralised dynamic estimation scheme described in Chapter V of the thesis used a simple two-area power system model, where the normally unknown time varying load power demand $\Delta P_d(t)$ term was assumed constant in magnitude and time invariant. By considering a power system LFC model consisting of a mixture of hydro-, thermal- and nuclear-power plants in a multi-area situation, a better and far more reaching conclusions may be

reached concerning the viability of the decentralised dynamic estimation scheme. For a large area the dimensions of the matrix Ricatti equations needed to be solved to obtain the measurement feedback gain matrices K_i (Kalman filter gain) are also correspondingly high. It may therefore be necessary to search for more efficient methods of solving for the filter gain matrices.

As the load demand pattern ΔP_d of a power system is continually changing, the assumption of constant ΔP_d is not strictly true. One way of considering this unknown load demand situation in estimation is to assume that ΔP_d has a known mean value with a known stochastic variation about this mean value or to identify the load demand $\Delta P_d(t)$ before implementing the estimator. A useful research may therefore be conducted to estimate $\Delta P_d(t)$ using mathematical identification techniques. Since the identification of $\Delta P_d(t)$ is then a subproblem of the overall estimation process, the amount of computations to be performed becomes formidable and the challenge is to be able to solve the two problems concurrently.

iv. The model which was used to investigate the performance of the non-linear dynamic power system estimator involved only four basic machine state variables namely, the direct and quadrature axes voltages e_d and e_q, the machine speed $\dot{\delta}$ and the machine rotor angle δ. By including the state variables of the associated control equipment i.e. Automatic Voltage Regulator (AVR) and Governor, the order of the non-linear machine differential equations may be suitably increased to give a fuller, more complete

machine representation, and consequently better machine state estimates may be derived. With such an enlarged state vector, the associated machine differential equations will become highly dimensional and increase the computational effort required to solve the non-linear machine estimation problem. The large size of the enlarged state vector requires more efficient numerical integration techniques for solving the estimation equations, especially if the non-linear system of equations happens to be stiff. Stochastic control algorithms should be designed to investigate the reliability of the derived state estimates. Their effectiveness may be measured in terms of the success of the feedback control laws used to augment the transient stability behaviour of the machine.

v. Other areas worth further investigation are:

   a. the non-linear dynamic estimation scheme applied to a multi-machine power system model

   b. possible design of decentralized estimation schemes for the multi-machine, non-linear dynamic estimator

   c. derivation of stochastic optimal control strategies with the system states determined from the above schemes.

APPENDIX A

THEORY OF WEIGHTED LEAST SQUARES ESTIMATION

A.1 Introduction

As a prelude to power systems static state estimation, the theory of least-squares is developed. It is an application of minimum variance estimators to multivariable problems in situations where a known functional relationship exists between a system's observed variables and the system's state and/or parameter vector that needs to be estimated. The functional form is often derived on the basis of a known theoretical or deterministic model of the system behaviour arising from the natural physical laws governing the operation of the system. Normally, mathematical descriptions of most physical processes and phenomena are, in general, non-linear in nature; however from the point of view of problem tractability, equivalent linear approximations to the essentially non-linear system equations may be derived either by a mathematical transformation or through a mathematical linearisation. Weighted least squares estimation may therefore be performed with two distinct system models, the linear system model and the non-linear system model yielding respectively the Linear Weighted Least Squares estimator (LWLS) and the Generalized Weighted Least Squares estimator (GWLS)

A.2 Problem statement and formulation

Consider a vector $\underline{z}_m$ of the raw system observations that is functionally related to the system state and/or parameter vector $\underline{x}_t$. The state estimation problem entails the determination of a vector $\hat{\underline{x}}$ that is the best approximation to $\underline{x}_t$ according to a chosen criterion. Often, the number of system measurements exceeds the number of states

to be determined (redundancy) leading to the determination of $\hat{\underline{x}}$ from a mathematically over-determined yet independent system of equations. Multiple solutions for $\hat{\underline{x}}$ may be obtained but subject to the choice of a particular criterion of best-fit, a specific best solution for $\hat{\underline{x}}$ can be derived.

The relation between the raw system measurements and the system state and/or parameter vector can be qualitatively described by[38]:

Raw measurement = True-but-unknown measurement + measurement errors and uncertainties (A.2.1)

Equation (A.2.1) is mathematically written as:

$$\underline{Z}_m = \underline{Z}_t + \underline{V} \qquad \text{(A.2.2.)}$$

where:

$\underline{Z}_m$: is an m-dimensional vector of the raw system measurements which are of different mean-values and have unequal variances and are uncorrelated in pairs.

$\underline{Z}_t$: is an m-dimensional vector of the true-but-unknown values of the exact system measurements, it may be either a linear or a non-linear function of the system state and/or parameter vector.

$\underline{V}$: is an m-dimensional vector of stochastic random variables that represents spurious system observation errors and uncertainties.

The first- and second-order central moments of the random variable $\underline{V}$ are assumed to be:

$$E(\underline{V}) = \underline{0} \qquad \text{(A.2.3)}$$

$$E(\underline{V}\ \underline{V}^T) = R \qquad \text{(A.2.4)}$$

where:

R: is an (mxm)-dimensional diagonal matrix of the individual measurement error variances. The diagonal property specifies that the measurement errors are uncorrelated in pairs and the i-th measurement has variance $\sigma_i^2 = R_{ii}$.

E is the statistical expectation operator.

The weighted least squares estimate of $\underline{x}_t$ is defined as the value of $\underline{x}_t$, denoted by $\hat{\underline{x}}$, that yields a minimum of the sum of the squares of weighted differences between the actual, raw measurement ($\underline{Z}_m$) and its true-but-unknown value ($\underline{Z}_t$). The criterion for this best-fit situation is given by the minimisation of the quadratic cost functional expression[36-39,46,88]:

$$J(\underline{x}_t) = (\underline{Z}_m - \underline{Z}_t)^T P(\underline{Z}_m - Z_t) \qquad \text{(A.2.5a)}$$

$$= \underline{V}^T P \underline{V} \qquad \text{(A.2.5b)}$$

P is a weighting-matrix that is always restricted to being symmetric and positive-definite.

In a number of practical situations, certain components of the measurement vector $\underline{Z}_m$ may be known to be more accurate (low σ_i^2) than others (high σ_i^2). To lend more credence and importance to the more accurate and hence more reliable measurements, the matrix P, which is present in $J(\underline{x}_t)$ to reflect exactly this situation, is chosen[46] to be R^{-1}. The quadratic index of fit is then:

$$J(\underline{x}_t) = (\underline{Z}_m - \underline{Z}_t)^T R^{-1}(\underline{Z}_m - Z_t) \qquad \text{(A.2.5c)}$$

A.3 Linear weighted least squares estimation (LWLS)

For a linear description of the observation equation, the raw measurement is expressed as:

$$\underline{Z}_m = A\underline{x}_t + \underline{V} \qquad \text{(A.3.1)}$$

and the quadratic cost functional to be minimised as

$$J(\underline{x}_t) = (\underline{Z}_m - A\underline{x}_t)^T R^{-1} (\underline{Z}_m - A\underline{x}_t) \qquad (A.3.2)$$

A is an (mxn)-dimensional coefficient matrix which establishes the linear relationship between the true measurement and the state and/or parameter vector $\underline{x}_t$.

$\underline{x}_t$ is the true-but-unknown n-dimensional vector of system states and/or parameters which is to be estimated.

At the minimum of $J(\underline{x}_t)$, the following orthogonality condition holds:

$$\frac{\partial}{\partial \underline{x}_t} \left[J(\underline{x}_t) \right] \Bigg|_{\hat{\underline{x}} = \underline{x}_t} = -2A^T R^{-1} (\underline{Z}_m - A\hat{\underline{x}}) = 0 \qquad (A.3.3)$$

or:

$$A^T R^{-1} (\underline{Z}_m - A\hat{\underline{x}}) = 0 \qquad (A.3.4)$$

from the above equation, the best estimate of $\underline{x}_t$, which is $\hat{\underline{x}}$, is given by:

$$(A^T R^{-1} A)\, \hat{\underline{x}} = A^T R^{-1} \underline{Z}_m \qquad (A.3.5)$$

Defining:

$$\Sigma_x^A = (A^T R^{-1} A)^{-1} \qquad (A.3.6)$$

then it follows from equation (A.3.5) that:

$$\hat{\underline{x}} = \Sigma_x^A \, A^T R^{-1} \underline{Z}_m \qquad (A.3.7)$$

The quantities derived from $\underline{x}_t$ and $\hat{\underline{x}}$ may be defined as follows:

a. the true-but-unknown measurement $\underline{Z}_t$:

$$\underline{Z}_t = A\underline{x}_t \qquad (A.3.8)$$

b. the estimated value of the measurement $\hat{\underline{z}}$:

$$\hat{\underline{Z}} = A\hat{\underline{x}} \qquad (A.3.9)$$

c. the measurement residual $\underline{r}$ being the difference between the raw measurement and its estimated value

$$\underline{r} = \underline{Z}_m - \hat{\underline{Z}}$$

$$= A(\underline{x}_t - \hat{\underline{x}}) + \underline{V} \qquad (A.3.10)$$

It is now necessary to determine the first-and second order central moments of the estimated variables for post estimation reliability and error analysis.

A.3.1 Expectations and covariances of the estimated variables $E(\hat{\underline{x}})$, $E(\hat{\underline{z}})$, $E(\underline{r})$, $cov(\hat{\underline{x}})$, $cov(\hat{\underline{z}})$, $cov(\underline{r})$, $E\{J(\underline{x})\}$

i. Expectation $E(\hat{\underline{x}})$ and covariance $cov(\hat{\underline{x}})$ of $\hat{\underline{x}}$

From equations (A.3.7) and A.3.1):

$$\hat{\underline{x}} = \Sigma_x^A A^T R^{-1} (A\underline{x}_t + \underline{v})$$

$$= \underline{x}_t + \Sigma_x^A A^T R^{-1} \underline{v} \qquad (A.3.11)$$

The expectation of the system state estimate $\hat{\underline{x}}$ is then:

$$E(\hat{\underline{x}}) = E(\underline{x}_t) + \Sigma_x^A A^T R^{-1} E(\underline{v})$$

$$= \underline{x}_t \qquad (A.3.12)$$

The expected value of $\hat{\underline{x}}$ is therefore $\underline{x}_t$ which is the true value of the system state vector that we initially set out to estimate. The LWLS estimate $\hat{\underline{x}}$ of $\underline{x}_t$ is therefore unbiased[36,37].

The goodness of the state estimate $\hat{\underline{x}}$ is measured in terms of its variability about its expected value and is calculated as its covariance matrix which is defined as[36,37]:

$$cov(\hat{\underline{x}}) = E\left(\hat{\underline{x}} - E(\hat{\underline{x}})\right)\left(\hat{\underline{x}} - E(\hat{\underline{x}})\right)^T$$

$$= E(\hat{\underline{x}} - \underline{x}_t)(\hat{\underline{x}} - \underline{x}_t)^T$$

From equation (A.3.11)

$$\hat{\underline{x}} - \underline{x}_t = \Sigma_x^A A^T R^{-1} \underline{v}$$

Hence

$$cov(\hat{\underline{x}}) = E(\Sigma_x^A A^T R^{-1} \underline{v}\ \underline{v}^T R^{-1} A\ \Sigma_x^A)$$

$$= \Sigma_x^A A^T R^{-1} E(\underline{v}\ \underline{v}^T) R^{-1} A\ \Sigma_x^A$$

$$= \Sigma_x^A A^T R^{-1} R R^{-1} A\ \Sigma_x^A$$

$$= \Sigma_x^A A^T R^{-1} A\ \Sigma_x^A$$

$$= \Sigma_x^A \qquad (A.3.13)$$

The variances of the individual components of the system state estimates, σ^2_{xi}, are given by the diagonal elements of the covariance matrix $\sum_x$.

$$\sigma^2_{xi} = (\sum_x^A)_{ii} \qquad i = 1,2,\ldots,n \qquad (A.3.14)$$

The matrix $\sum_x^A = (A^T R^{-1} A)^{-1}$ is referred to in the literature as the system information matrix[29,47,48,89]

ii. Expectation $E(\hat{\underline{z}})$ and covariance $cov(\hat{\underline{z}})$ of $\hat{\underline{z}}$

Since the estimated measurement $\hat{\underline{z}}$ is given in equation (A.3.9), its expectation is given by:

$$E(\hat{\underline{z}}) = E(A\hat{\underline{x}})$$
$$= AE(\hat{\underline{x}})$$

and by virtue of equation (A.3.12)

$$E(\hat{\underline{z}}) = A\underline{x}_t$$
$$= \underline{z}_t \qquad (A.3.15)$$

The estimator for $\hat{\underline{z}}$ is therefore also unbiased, yielding the true value of $\underline{z}_t$.

The covariance of $\hat{\underline{z}}$ is similarly defined as for $\hat{\underline{x}}$, namely:

$$\begin{aligned} cov(\hat{\underline{z}}) &= E\left(\hat{\underline{z}}-E(\hat{\underline{z}})\right)\left(\hat{\underline{z}}-E(\hat{\underline{z}})\right)^T \\ &= E(\hat{\underline{z}}-\underline{z}_t)(\hat{\underline{z}}-\underline{z}_t)^T \\ &= E(A\hat{\underline{x}}-A\underline{x}_t)(A\hat{\underline{x}}-A\underline{x}_t)^T \\ &= AE(\hat{\underline{x}}-\underline{x}_t)(\hat{\underline{x}}-\underline{x}_t)^T A^T \\ &= A \sum_x^A A^T \qquad (A.3.16) \end{aligned}$$

The variances of the individual components of $\hat{\underline{z}}$, σ^2_{zi} are given by the diagonal elements of its covariance matrix

$$\sigma^2_{zi} = (A \sum_x^A A^T)_{ii} \qquad i = 1,2,\ldots,m \qquad (A.3.17)$$

iii. Expectation $E(\underline{r})$ and covariance $cov(\underline{r})$ of $\underline{r}$

The residual vector of measurement errors $\underline{r}$ is as given in equation

(A.3.10). Thus:

$$\underline{r} = \underline{Z}_m - \underline{Z} = A(\underline{x}_t - \hat{\underline{x}}) + \underline{V}$$

$$= -A(\hat{\underline{x}} - \underline{x}_t) + \underline{V}$$

From equation (A.3.11),

$$\hat{\underline{x}} - \underline{x}_t = -\Sigma_x^A A^T R^{-1} \underline{V} \qquad \text{(A.3.18)}$$

Therefore:

$$\underline{r} = \underline{Z}_m - \hat{\underline{Z}} = -A \Sigma_x^A A^T R^{-1} \underline{V} + \underline{V}$$

$$= \left(I_m - A\Sigma_x^A A^T R^{-1}\right) \underline{V} \qquad \text{(A.3.19)}$$

where I_m is the (mxm)-dimensional identity matrix.

Defining $W^A = I_m - A\Sigma_x^A A^T R^{-1}$ then

$$\underline{r} = W^A \underline{V} \qquad \text{(A.3.20)}$$

It follows that:

$$E(\underline{r}) = W^A E(\underline{V})$$

$$= \underline{0} \qquad \text{(A.3.21)}$$

W^A is known as the residual sensitivity matrix[29,47,48,89]. The measurement residual is therefore also unbiased.

The covariance of the measurement residual is expressible as:

$$\text{cov}(\underline{r}) = E(\underline{r}\,\underline{r}^T) = E\left[W^A \underline{V}\,\underline{V}^T (W^A)^T\right]$$

$$= W^A R (W^A)^T$$

$$= \left(I_m - A\Sigma_x^A A^T R^{-1}\right) R \left(I_m - A\,\Sigma_x^A A^T R^{-1}\right)$$

$$= R - A\Sigma_x^A A^T \qquad \text{(A.3.22)}$$

$$= WR \qquad \text{(A.3.23)}$$

The variance of the i-th component of the measurement residual $\sigma^2_{r_i}$ is therefore equal to i-th diagonal element of $\text{cov}(\underline{r}) = \Sigma_r^A$ and

$$\sigma^2_{r_i} = (R - A\Sigma_x^A A^T)_{ii} \qquad i = 1,2,\ldots,m \qquad \text{(A.3.24)}$$

iv. Expectation of the minimum value of the quadratic performance index, $E\left\{J(\hat{\underline{x}})\right\}$

At the minimum, $\underline{Z}_m - A\underline{x}_t = \underline{Z}_m - A\hat{\underline{x}} = W^A \underline{\nu}$.

In other words:

$$J(\hat{\underline{x}}) = \left(\underline{Z}_m - A\hat{\underline{x}}\right)^T R^{-1} \left(\underline{Z}_m - A\hat{\underline{x}}\right) = (W^A \underline{\nu})^T R^{-1} (W^A \underline{\nu})$$

$$= \underline{\nu}^T (W^A)^T R^{-1} W^A \underline{\nu}$$

$$= \underline{\nu}^T (I_m - R^{-1} A \Sigma_x^A A^T) R^{-1} (I_m - A \Sigma_x^A A^T R^{-1}) \underline{\nu}$$

$$= \underline{\nu}^T (R^{-1} - R^{-1} A \Sigma_x^A A^T R^{-1})(I_m - A \Sigma_x^A A^T R^{-1} \underline{\nu}$$

$$= \underline{\nu}^T (R^{-1} - R^{-1} A \Sigma_x^A A^T R^{-1} - R^{-1} A \Sigma_x^A A^T R^{-1} + R^{-1} A \Sigma_x^A A^T R^{-1} A \Sigma_x^A A^T R^{-1}) \underline{\nu}$$

$$= \underline{\nu}^T (R^{-1} - R^{-1} A \Sigma_x^A A^T R^{-1}) \underline{\nu}$$

$$= \underline{\nu}^T R^{-1} (I_m - A \Sigma_x^A A^T R^{-1}) \underline{\nu}$$

$$= \underline{\nu}^T R^{-1} W^A \underline{\nu} \qquad \text{(A.3.25)}$$

$$= \underline{\nu}^T R^{-1} (R - A \Sigma_x^A A^T) R^{-1} \underline{\nu}$$

$$= (R^{-1} \underline{\nu})^T \Sigma_r^A (R^{-1} \underline{\nu}) \qquad \text{(A.3.26)}$$

The expected value of $J(\hat{\underline{x}})$ is therefore from (A.3.25)

$$E\left\{J(\hat{\underline{x}})\right\} = E(\underline{\nu}^T R^{-1} W^A \underline{\nu}) \qquad \text{(A.3.27)}$$

Now any weighted quadratic form $\underline{\varepsilon}^T B \underline{\varepsilon}$ is a scalar sum which is identical with its trace, $tr(\underline{\varepsilon}^T B \underline{\varepsilon})$. Moreover, matrices may be commuted under the trace operator[37], yielding:

$$E(\underline{\varepsilon}^T B \underline{\varepsilon}) = E\{tr(\underline{\varepsilon}^T B \underline{\varepsilon})\}$$

$$= E\{tr(B \underline{\varepsilon} \underline{\varepsilon}^T)\}$$

$$= tr\{B E(\underline{\varepsilon} \underline{\varepsilon}^T)\}$$

Therefore

$$E\left\{J(\hat{\underline{x}})\right\} = tr\left\{R^{-1} W^A E(\underline{\nu} \underline{\nu}^T)\right\}$$

$$= \text{tr}\,(R^{-1}W^{A}R)$$

$$= \text{tr}\,(W^{A}RR^{-1}) \;=\; \text{tr}\,(W^{A})$$

$$= \text{tr}\,(I_m - A\,\Sigma_x^A A^T R^{-1})$$

$$= \text{tr}(I_m) - \text{tr}\,(\Sigma_x^A\, A^T R^{-1} A) \qquad \text{(A.3.28)}$$

The matrices $A^T R^{-1} A$ and $\Sigma_x^A = (A^T R^{-1} A)^{-1}$ are both (nxn)-dimensional. Hence $\Sigma_x^A\, A^T R^{-1} A$ is the (nxn)-dimensional identity matrix, I_n.

Therefore

$$E\left\{ J(\hat{\underline{x}})\right\} = \text{tr}(I_m) - \text{tr}(I_n)$$

$$= m - n \qquad \text{(A.3.29)}$$

It is interesting to observe from all the derivations so far that regardless of the probability distribution of the assumed measurement model, all the system parameters and variables have been estimated without bias. In particular we have stayed clear of any probabilistic distributional assumptions about the measurement errors, $\underline{V}$ and the measurement residuals, $\underline{r}$. The analysis has, despite these assumptions, led to least-squares point estimates of $\hat{\underline{x}}$, $\hat{\underline{z}}$ and $\underline{r} = \underline{z}_m - \hat{\underline{z}}$. In normal practice point estimation alone is not enough. It is also necessary to supply some statement about the error on the estimate and more importantly to ascribe a certain amount of confidence to the point estimate of each particular variable. To do this requires probabilistic distributional assumptions about the measurement model. Usually, it is justifiable to assume that the stochastic vector of measurement errors $\underline{V}$ is a normally distributed random vector on the basis of the Central Limit Theorem[53]. That is:

$\underline{V} \sim N(0, R)$

with the probability distribution function[36,37,88]:

$$p(\underline{v}_i) = \frac{1}{(2\pi R_{ii})^{\frac{1}{2}}} \exp\left[-\tfrac{1}{2} * \frac{\{\underline{v}_i - E(\underline{v}_i)\}^2}{R_{ii}}\right] \qquad (A.3.30)$$

$$i = 1,2,\ldots,m$$

where

$p(\underline{v}_i)$ = probability density function of $\underline{v}_i$

$E(\underline{v}_i) = 0$

$E(\underline{v}\,\underline{v}^T) = R$

and R_{ii} = variance of the i-th component of $\underline{v}$

v. Probability distribution of $J(\hat{\underline{x}})$

From equation (A.3.26)

$$J(\hat{\underline{x}}) = (R^{-1}\underline{v})^T \Sigma_r^A (R^{-1}\underline{v})$$

and since

$\underline{r} = W\underline{v}$ from equation (A.3.20)

$= (R - A\Sigma_x^A A^T) R^{-1}\underline{v}$

$= \Sigma_r^A R^{-1}\underline{v}$

it follows that provided Σ_r^A is invertible,

$$R^{-1}\underline{v} = (\Sigma_r^A)^{-1}\underline{r}$$

giving

$$J(\hat{\underline{x}}) = \underline{r}^T (\Sigma_r^A)^{-1} \Sigma_r^A (\Sigma_r^A)^{-1}\underline{r}$$

$$= \underline{r}^T (\Sigma_r^A)^{-1}\underline{r}$$

$$= \sum_{i=1}^{m} \left[\frac{r_i}{\sqrt{\text{diag}(\Sigma_r^A)_{ii}}}\right]^2 \qquad (A.3.31)$$

Because it has already been established that:

$E(\underline{r}) = \underline{0}$

$\text{cov}(\underline{r}) = \Sigma_r^A$

$\underline{r} = W\underline{v}$

and by virtue of the latter linear relationship between $\underline{r}$ and $\underline{V}$, and the fact that $\underline{V}$ is a normally distributed random variable, it can be proved that $\underline{r}$ is also a normally distributed random variable whose distribution is given by[88]:

$$\underline{r} \sim N(0,\ R\text{-}A\ \Sigma_x^A\ A^T) \qquad (A.3.32)$$

$\dfrac{r_i}{\sqrt{diag(\Sigma_r^A)_{ii}}}$ is therefore a standardised unit normal random variable[36,37], that is:

$$\frac{r_i}{\sqrt{diag(\Sigma_r^A)_{ii}}} \sim N(0,\ 1) \qquad (A.3.33)$$

Equation (A.3.31) which represents $J(\hat{\underline{x}})$ is therefore the sum of the squares of independently distributed unit normal random variables yielding a chi-square (χ^2) distributed random variate with degrees of freedom equal to the rank of the quadratic form for $J(\hat{\underline{x}})$, that is m-n[37]. Or:

$$J(\hat{\underline{x}}) \sim \chi^2_{df=m-n} \qquad (A.3.34)$$

where df stands for degrees of freedom.

A.4 Generalized or non-linear weighted least squares estimation (GWLS)

In the case of a non-linear measurement model, the observation defining equation is a non-linear vector function of the true-but-unknown system state and/or parameter vector $\underline{x}_t$.

$$\underline{Z}_m = \underline{h}(\underline{x}_t) + \underline{V} \qquad (A.4.1)$$

where

$\underline{h}(\underline{x}_t)$ is an m-dimensional non-linear vector function of $\underline{x}_t$ that determines the true-but-unknown exact measurement vector.

As in the linear case, GWLS estimation produces the minimum-mean-squared unbiased estimate $\hat{\underline{x}}$ of $\underline{x}_t$ by minimising the corresponding weighted quadratic performance index, $J(\underline{x}_t)$, where:

$$J(\underline{x}_t) = \left[\underline{Z}_m - \underline{h}(\underline{x}_t)\right]^T R^{-1} \left[\underline{Z}_m - \underline{h}(\underline{x}_t)\right] \qquad (A.4.2)$$

Differentiating $J(\underline{x}_t)$ with respect to $\underline{x}_t$ and setting the result to zero leads to a set of non-linear simultaneous equations, which is practically difficult to solve directly. However, $J(\underline{x}_t)$ can be minimised directly by an iterative process that involves a linearisation of the non-linear system equations.

The Gauss-Newton method[53] is applied by replacing the non-linear observation equation of (A.4.1) by the terms of its Taylor series expansion about $\hat{\underline{x}}$:

$$\underline{Z}_m = \underline{h}(\hat{\underline{x}}) + H(\hat{\underline{x}})(\underline{x}_t - \hat{\underline{x}}) + \underline{V} + \text{H.O.T.} \qquad (A.4.3)$$

The higher order terms, HOT, may be neglected to a first order approximation to give $\underline{Z}_m = H(\hat{\underline{x}})\ (\underline{x}_t - \hat{\underline{x}}) + \underline{V}$ (A.4.4)

where:

$$H(\hat{\underline{x}}) = \left.\frac{\partial \underline{h}(\underline{x}_t)}{\partial \underline{x}_t}\right|_{\underline{x}_t = \hat{\underline{x}}}$$

is an (mxn)-dimensional Jacobian matrix that relates changes in the measurements to the changes in the state $\underline{x}_t$.

Minimisation of $J(x_t)$ by setting its first derivative with respect to $\underline{x}_t$ to zero yields the optimality condition

$$\left.\frac{\partial}{\partial \underline{x}_t}\left\{J(\underline{x}_t)\right\}\right|_{\underline{x}_t = \hat{\underline{x}}} = -2H^T(\hat{\underline{x}})\ R^{-1}\left[\underline{Z}_m - \underline{h}(\hat{\underline{x}})\right] = 0 \qquad (A.4.5)$$

From equation (A.4.4) we get:

$$H^T(\hat{\underline{x}})\ R^{-1}\left[\underline{h}(\hat{\underline{x}}) + H(\hat{\underline{x}})(\underline{x}_t - \hat{\underline{x}}) + \underline{V} - \underline{h}(\hat{\underline{x}})\right] = 0$$

or:

$$H^T(\hat{\underline{x}})\ R^{-1}H(\hat{\underline{x}})\ (\underline{x}_t-\hat{\underline{x}}) = -H^T(\hat{\underline{x}})\ R^{-1}\ \underline{v} \qquad (A.4.6)$$

Defining:

$$\Sigma_x^H = \left(H^T(\hat{\underline{x}})\ R^{-1}\ H(\hat{\underline{x}})\right)^{-1} \qquad (A.4.7)$$

it follows that:

$$\underline{x}_t - \hat{\underline{x}} = -\Sigma_x^H\ H^T(\hat{\underline{x}})\ R^{-1}\ \underline{v} \qquad (A.4.8)$$

The equivalent derived quantities based on $\underline{x}_t$ and $\hat{\underline{x}}$ may be similarly defined as:

i. $\underline{Z}_t = \underline{h}(\underline{x}_t)$

ii. $\hat{\underline{Z}} = \underline{h}(\hat{\underline{x}})$

iii. $\underline{r} = \underline{Z}_m - \hat{\underline{Z}}$

$= \underline{h}(\underline{x}_t) + \underline{v} - \underline{h}(\hat{\underline{x}})$

It is necessary to show that the non-linear technique also yields estimates of system states and variables with the same properties as those obtained with the linear technique.

A.4.1 Expectations $E(\hat{\underline{x}})$, $E(\hat{\underline{z}})$, $E(\underline{r})$, $E\{J(\hat{\underline{x}})\}$ and covariances $cov(\hat{\underline{x}})$, $cov(\hat{\underline{z}})$, $cov(\underline{r})$ of the estimated variables

i. $E(\hat{\underline{x}})$ and $cov(\hat{\underline{x}})$

From equation (A.4.8) the expectation of $\hat{\underline{x}}$ is derived as:

$$E(\underline{x}_t - \hat{\underline{x}}) = -\Sigma_x^H\ H^T(\hat{\underline{x}})\ R^{-1}E(\ \underline{v})$$

implying that

$$E(\hat{\underline{x}}) = \underline{x}_t \qquad (A.4.9)$$

The GWLS estimator therefore also yields an unbiased estimate $\hat{\underline{x}}$ of $\underline{x}_t$. The covariance matrix of $\hat{\underline{x}}$ is also given by:

$$cov(\hat{\underline{x}}) = E\{\hat{\underline{x}} - E(\hat{\underline{x}})\}\ \{\hat{\underline{x}} - E(\hat{\underline{x}})\}^T$$

$$= E\ (\hat{\underline{x}} - \underline{x}_t)\ (\hat{\underline{x}} - \underline{x}_t)^T$$

$$= E\left\{ \Sigma_x^H H^T(\underline{x})\ R^{-1}\ \underline{\nu}\ \underline{\nu}^T\ R^{-1} H(\underline{x})\ \Sigma_x^H \right\}$$

$$= \Sigma_x^H \qquad \text{(A.4.10)}$$

ii. $E(\hat{\underline{z}})$ and $\text{cov}(\hat{\underline{z}})$

To derive $E(\hat{\underline{z}})$, consider the measurement mismatch vector term:

$$\underline{z}_t - \hat{\underline{z}} = \underline{h}(\underline{x}_t) - \underline{h}(\hat{\underline{x}})$$

$$\simeq \underline{h}(\hat{\underline{x}}) + H(\hat{\underline{x}})(\underline{x}_t - \hat{\underline{x}}) - h(\hat{\underline{x}})$$

that is:

$$\underline{z}_t - \hat{\underline{z}} = -H(\hat{\underline{x}})\ \Sigma_x^H H^T(\hat{\underline{x}})\ R^{-1}\ \underline{\nu} \qquad \text{(A.4.11)}$$

Thus:

$$E(\underline{z}_t - \hat{\underline{z}}) = -H(\hat{\underline{x}})\ \Sigma_x^H H^T(\hat{\underline{x}})\ R^{-1} E(\ \underline{\nu}\ )$$

$$= \underline{0}$$

Therefore:

$$E(\hat{\underline{z}}) = \underline{z}_t \qquad \text{(A.4.12)}$$

yielding similarly an unbiased estimate $\hat{\underline{z}}$ for $\underline{z}_t$

$$\text{cov}(\hat{\underline{z}}) = E\left\{ \hat{\underline{z}} - E(\hat{\underline{z}}) \quad \hat{\underline{z}} - E(\hat{\underline{z}}) \right\}^T$$

$$= E\ (\hat{\underline{z}} - \underline{z}_t)(\hat{\underline{z}} - \underline{z}_t)^T$$

$$= E\left\{ H(\hat{\underline{x}})\ \Sigma_x^H H^T(\hat{\underline{x}})\ R^{-1}\ \underline{\nu}\ \underline{\nu}^T R^{-1} H(\hat{\underline{x}})\ \Sigma_x^H H^T(\hat{\underline{x}}) \right\}$$

$$= H(\hat{\underline{x}})\ \Sigma_x^H H^T(\hat{\underline{x}}) \qquad \text{(A.4.13)}$$

iii. $E(\underline{r})$ and $\text{cov}(\underline{r})$

The residual vector is given by:

$$\underline{r} = \underline{z}_m - \hat{\underline{z}}$$

$$\simeq h(\underline{x}) + H(\hat{\underline{x}})(\underline{x}_t - \hat{\underline{x}}) + \underline{\nu} - \underline{h}(\hat{\underline{x}})$$

$$\simeq -H(\hat{\underline{x}})\ \Sigma_x^H H^T(\hat{\underline{x}})\ R^{-1}\ \underline{\nu} + \underline{\nu}$$

$$\simeq \left\{ I_m - H(\hat{\underline{x}})\ \Sigma_x^H H^T(\hat{\underline{x}})\ R^{-1} \right\} \underline{\nu} \qquad \text{(A.4.14)}$$

Similarly defining:

$$W^H = \left\{ I_m - H(\hat{\underline{x}})\ \Sigma_x^H H^T(\hat{\underline{x}})\ R^{-1} \right\}$$

$$\underline{r} = W^H \underline{V} \tag{A.4.15}$$

then it follows that:

$$E(\underline{r}) = W^H E(\underline{V})$$

$$= \underline{0}$$

The GWLS measurement residual $\underline{r}$ is also unbiased.

$$\text{cov}(\underline{r}) = E(\underline{r}\,\underline{r}^T) = E\left\{ W^H \underline{V}\,\underline{V}^T (W^H)^T \right\}$$

$$= W^H R$$

$$= R - H(\hat{\underline{x}})\, \Sigma_x^H\, H^T(\hat{\underline{x}}) \tag{A.4.16}$$

Defining $\Sigma_r^H = R - H(\hat{\underline{x}})\, \Sigma_x^H\, H^T(\hat{\underline{x}})$

iv. $E\{ J(\hat{\underline{x}}) \}$

At the minimum, the quadratic performance index is:

$$J(\hat{\underline{x}}) = \underline{r}^T R^{-1} \underline{r}$$

$$= \underline{V}^T R^{-1} W^H \underline{V} \tag{A.4.17}$$

$$= (R^{-1} \underline{V})^T \Sigma_r^H R^{-1} \underline{V} \tag{A.4.18}$$

By comparing the expressions for $J(\hat{\underline{x}})$ in equations (A.4.17) and (A.4.18) with those of equations (A.3.25) and (A.3.26) respectively, subject to the same probabilistic distributional assumptions for $\underline{V}$, it may be similarly established that:

$$E\{ J(\hat{\underline{x}}) \} = m-n \tag{A.4.19}$$

with

$$J(\hat{\underline{x}}) \sim \chi^2_{m-n} \tag{A.4.20}$$

Table A.1 present a tabulated summary of the salient features of the LWLS and GWLS estimators. It is clearly borne-out that the two techniques are at variance only in respect of the two (mxn)-dimensional matrices A and $H(\hat{\underline{x}})$. These two matrices establish a one-to-one equivalence between the LWLS and GWLS estimation processes.

TABLE A.1

COMPARISON OF LWLS AND GWLS EXPRESSIONS

System Variable	LWLS	GWLS
Objective function $J(\underline{x})$	$(\underline{z}_m - A\underline{x}_t)^T R^{-1} (\underline{z}_m - A\underline{x}_t)$	$\left[\underline{z}_m - \underline{h}(\underline{x}_t)\right]^T R^{-1} \left[\underline{z}_m - \underline{h}(\underline{x}_t)\right]$
Raw measurement $\underline{z}_m$	$A\underline{x}_t + \underline{v}$	$\underline{h}(\underline{x}_t) + \underline{v}$
Estimation Error $\underline{x}_t - \hat{\underline{x}}$	$-(A^T R^{-1} A)^{-1} A^T R^{-1} \underline{v}$	$-(H^T R^{-1} H)^{-1} H^T R^{-1} \underline{v}$
Measurement residual $\underline{r} = \underline{z}_m - \hat{\underline{z}}$	$\left[I_m - A(A^T R^{-1} A)^{-1} A^T R^{-1}\right]\underline{v}$	$\left[I_m - H(H^T R^{-1} H)^{-1} H^T R^{-1}\right] \underline{v}$
Measurement prediction error $\underline{z}_t - \hat{\underline{z}}$	$-A(A^T R^{-1} A)^{-1} A^T R^{-1} \underline{v}$	$-H(H^T R^{-1} H)^{-1} H^T R^{-1} \underline{v}$
Expectation of $\hat{\underline{x}}$ $E(\hat{\underline{x}})$	$\underline{x}_t$	$\underline{x}_t$
Expectation of $\hat{\underline{z}}$ $E(\hat{\underline{z}})$	$\underline{z}_t (= A\underline{x}_t)$	$\underline{z}_t \{= \underline{h}(\underline{x}_t)\}$
Expection of $\underline{r}$ $E(\underline{r})$	$\underline{0}$	$\underline{0}$
Covariance of $\hat{\underline{x}}$ $\text{cov}(\hat{\underline{x}}) = \Sigma_x$	$\Sigma_x^A = (A^T R^{-1} A)^{-1}$	$\Sigma_x^H = (H^T R^{-1} H)^{-1}$
Covariance of $\hat{\underline{z}}$ $\text{cov}(\hat{\underline{z}}) = \Sigma_z$	$\Sigma_z^A = A \Sigma_x^A A^T$	$\Sigma_z^H = H \Sigma_x^H H^T$
Covariance of $\underline{r}$ $\text{cov}(\underline{r}) = \Sigma_r$	$\Sigma_r^A = R - A \Sigma_x^A A^T$	$\Sigma_r^H = R - H \Sigma_x^H H^T$
Expectation of $J(\hat{\underline{x}})$ $E\left[J(\hat{\underline{x}})\right]$	$m - n$	$m - n$
Distribution of $\underline{v}$	$N(0, R)$	$N(0, R)$
Distribution of $\underline{r}$	$N(0, \Sigma_r^A)$	$N(0, \Sigma_r^H)$
Distribution of $J(\hat{\underline{x}})$	$\chi^2_{df=m-n}$	$\chi^2_{df=m-n}$

Although it has been possible to derive estimates of the covariances $\sum_x$, $\sum_z$ and $\sum_r$ of the system quantities, it is realised that these covariances being a posteriori estimates are determined only after the results of the estimation process have been accepted. For this reason, the individual normalised random variables defined by

$$\frac{\hat{\underline{x}} - E(\hat{\underline{x}})}{\sqrt{\Sigma_x}} \quad , \quad \frac{\hat{\underline{z}} - E(\hat{\underline{z}})}{\sqrt{\Sigma_z}} \quad , \quad \frac{\underline{r} - E(\underline{r})}{\sqrt{\Sigma_r}}$$

are strictly not independently distributed unit normal random variates. They are actually t-distributed random variables. The impact this property has on the intervals (confidence limits) in which the values of the estimated variables lie will be described when the theory is applied to the power systems problem.

TABLE A.3.1

5-NODES, 7-LINES NETWORK: LOAD FLOW VOLTAGE PROFILE AND LOAD CONDITIONS

BUS	ETRUE, e_i	FTRUE, f_i	PTRUE, P_i	QTRUE, Q_i
1	1.06000	0	1.29598	-.07465
2	1.04620	-.05130	.19915	.20040
3	1.02030	-.08920	-.44907	-.15179
4	1.01920	-.09510	-.40105	-.04771
5	1.01216	-.10900	-.59917	-.10055

TABLE A.3.2

23-NODES, 30-LINES NETWORK: LOAD FLOW VOLTAGE PROFILE AND LOAD CONDITIONS

BUS	ETRUE, e_i	FTRUE, f_i	PTRUE, P_i	QTRUE, Q_i
1	1.01860	0	-.12133	.51134
2	1.02140	-.02900	.24177	.35838
3	1.03130	.09020	1.02799	.56477
4	1.03600	.17070	.20280	.58174
5	1.00530	.30320	9.02678	1.66655
6	.98950	.35130	8.50714	1.18523
7	.99540	.00600	-.48116	-.12011
8	.98630	.16790	-.03599	-.00190
9	1.00370	.03990	-1.49627	-.38006
10	.98240	.04800	-1.76855	-.45118
11	1.01000	.02280	-.00018	-.01030
12	1.02560	.14740	-.04382	.00259
13	1.01830	.18600	.04794	.00318
14	1.00100	.00550	-.47034	-.12962
15	1.00710	.14280	-2.00887	-.50242
16	.98880	.25310	-1.31018	-.33990
17	.98900	.21570	-3.44976	-.85737
18	.99700	.19590	-1.03706	-.24993
19	.99410	.18820	-3.75679	-.94816
20	.98700	-.06760	-.51020	-.13054
21	1.00090	.24200	-3.74937	-.94161
22	1.00220	.23990	2.09813	.51878
23	.98090	.08460	-.40996	-.09972

All values are in per unit form on 100-MVA base

TABLE A.3.3

10-NODES, 13-LINES NETWORK: LOAD FLOW VOLTAGE PROFILE AND LOAD CONDITIONS

Bus	ETRUE, e_i	FTRUE, f_i	PTRUE, P_i	QTRUE, Q_i
1	1.04000	0	4.21462	.47894
2	1.04840	.03450	3.83853	-.24743
3	1.04258	-.11630	-.38130	.50053
4	1.03410	-.11050	-4.66122	1.76510
5	.99270	-.18580	.06049	.08040
6	1.02820	-.15620	-.19445	.57995
7	1.02040	-.13750	-.89883	-.39907
8	.94570	-.12770	-2.59948	-1.55075
9	.97950	-.18620	-1.00121	-.49997
10	1.02990	-.07050	1.92165	-.80006

TABLE A.3.4

14-NODES, 20-LINES NETWORK: LOAD FLOW VOLTAGE PROFILE AND LOAD CONDITIONS

Bus	ETRUE, e_i	FTRUE, f_i	PTRUE, P_i	QTRUE, Q_i
1	1.06000	0	2.32339	-.16708
2	1.04100	-.09070	.18326	.29705
3	1.03690	-.26280	-.11264	.04641
4	.98510	-.22230	-.94214	.04370
5	1.06020	-.25190	.00052	.17346
6	1.00200	-.18250	-.47857	.03898
7	1.03290	-.24550	-.06285	-.01388
8	1.00820	-.15570	-.07481	-.01551
9	1.02040	-.27240	-.23217	.05858
10	1.01470	-.27390	-.09124	-.05895
11	1.02180	-.26980	-.03399	-.01790
12	1.01860	-.27440	-.06097	-.01597
13	1.01360	-.27460	-.13491	-.05796
14	.99520	-.28610	-.14903	-.05019

All values are in per unit form on 100-MVA base

TABLE A.3.5

5-NODES, 7-LINES NETWORK: LINE PARAMETERS

Line		Branch Impedance		Shunt Admittance
SB	EB	R(P.U)	X(P.U)	YS(P.U)
1	2	.0200	.0600	.0300
1	3	.0800	.2400	.0250
2	3	.0600	.1800	.0200
2	4	.0600	.1800	.0200
2	5	.0400	.1200	.0150
3	4	.0100	.0300	.0100
4	5	.0800	.2400	.0250

TABLE A.3.6

10-NODES, 13-LINES NETWORK: LINE PARAMETERS

Line		Branch Impedance		Shunt Admittance
SB	EB	R(P.U)	X(P.U)	YS(P.U)
1	2	.0099	.0484	.0506
1	3	.0450	.1236	.0506
1	4	.0118	.0780	.0759
1	8	.0114	.0553	.0506
2	4	.0099	.0484	.0253
3	7	.0163	.0638	.0759
4	6	.0074	.0489	.0253
4	7	.0163	.0652	.0759
4	8	.0488	.1916	.0506
4	10	.0039	.0197	.0506
5	9	.0118	.0780	.0759
6	9	.0188	.0628	.0506
8	9	.0488	.1916	.0506

All values are in per unit form on 100-MVA base

TABLE A.3.7

14-NODES, 20-LINES NETWORK: LINE PARAMETERS

Line		Branch Impedance		Shunt Admittance	
SB	EB	R(P.U)	X(P.U)	YS(P.U)	
1	2	.0194	.0592	.0264	
8	1	.0540	.2230	.0244	
2	4	.0470	.1979	.0219	
2	6	.0581	.1763	.0187	
2	8	.0569	.1739	.0170	
3	8	0	.2349	.2895	(-.3106)
3	11	.0950	.1989	0	
3	12	.1229	.2558	0	
3	13	.0661	.1303	0	
4	6	.0670	.1710	.0173	
5	7	0	.1761	0	
6	7	0	.2045	-.1100	(0.1076)
6	8	.0133	.0421	.0064	
6	9	0	.5389	-.0594	(0.0575)
7	9	0	.1410	0	
9	10	.0318	.0845	0	
9	14	.1271	.2704	0	
10	11	.0821	.1921	0	
12	13	.2209	.1999	0	
13	14	.1709	.3480	0	

All values are in per unit form on 100-MVA base
Other line end shunt admittances in brackets

TABLE A.3.8

23-NODES, 30-LINES NETWORK: LINE PARAMETERS

Line		Branch Impedance		Shunt Admittance	
SB	EB	R(P.U)	X(P.U)	YS(P.U)	
1	2	.0025	.2000	0	
1	11	.0242	.0540	.0059	
1	14	.0309	.0693	.0076	
2	20	.0404	.0888	.0099	
2	7	.0615	.1620	.0171	
3	10	.0233	.0514	.0228	
4	12	.0043	.0351	.1187	
4	13	.0043	.0351	.1187	
5	19	.0045	.0362	.1226	
5	21	.0019	.0156	.0528	
5	8	.0325	.0709	.0079	
6	16	.0020	.0164	.0555	
6	13	.0089	.0720	.2436	
7	9	.0229	.0504	.0056	
8	23	.0446	.1003	.0109	
8	10	.0597	.1315	.0146	
8	12	.0024	.0867	-.3805	(0.3683)
8	13	.0024	.0881	-.5671	(0.5401)
9	14	.0266	.0700	.0074	
9	10	.0597	.1315	.0146	
9	12	.0019	.1365	-.3662	(0.3488)
9	13	.0022	.0819	.2904	(-.2975)
11	23	.0576	.1520	.0160	
12	15	.0038	.0307	.1039	
15	18	.0035	.0288	.0976	
16	17	.0010	.0080	.0272	
17	18	.0021	.0167	.0567	
18	19	.0016	.0127	.0431	
18	22	.0024	.0192	.0649	
21	22	.0014	.0114	.0385	

All values are in per unit form on 100-MVA base
Other line end shunt admittances in brackets

APPENDIX B

SINGLE-MACHINE INFINITE BUSBAR POWER SYSTEM MODEL

Nomenclature

L_s	synchronous inductance
x_s	synchronous reactance
L_{af}	mutual inductance
x_{af}	mutual reactance
L_{ff}	field winding inductance
x_{ff}	field winding reactance
r_f	field winding resistance
r_a	armature winding resistance
T_{do}	field open-circuit time constant
T_{d1}	field short-circuit time constant
H	inertia time constant (sec)
M	moment of inertia
D	damping coefficient
x_l	transmission line inductance
r_l	transmission line resistance
e_s	infinite bus voltage
e	armature terminal voltage
i	armature current
e_f	field excitation voltage
i_f	field current
λ	armature flux linkage
λ_f	field flux linkage
P_e	real machine output power
T_e	electromechanical torgue
δ	machine rotor angle

$\dot{\delta}$ machine speed deviation

ω_r instantaneous machine rotor velocity

ω_o synchronous speed of machine

Subscripts

d refers to direct-axis components

q refers to quadrature-axis components

Power system model

The power system considered consists of a doubly-excited synchronous machine (i.e. provided with field windings on both the direct and quadrature axes) connected to an infinite busbar through a transmission line (Fig. B.1). Park's representation of the machine in d-q form[87] is utilised subject to the assumptions:

i. The machine rotor is cylindrical or non-salient pole with no damper windings.

ii. Saturation is negligible

iii. Transformer voltage, armature resistance and line resistance are negligible.

The system equations are then as follows:

Synchronous machine equations

Voltage:

$$e_d = -\omega_o \lambda_q \qquad \text{(B1)}$$

$$e_q = \omega_o \lambda_d \qquad \text{(B2)}$$

$$e_{fd} = \dot{\lambda}_{fd} + r_f i_{fd} \qquad \text{(B3)}$$

$$e_{fq} = \dot{\lambda}_{fq} + r_f i_{fq} \qquad \text{(B4)}$$

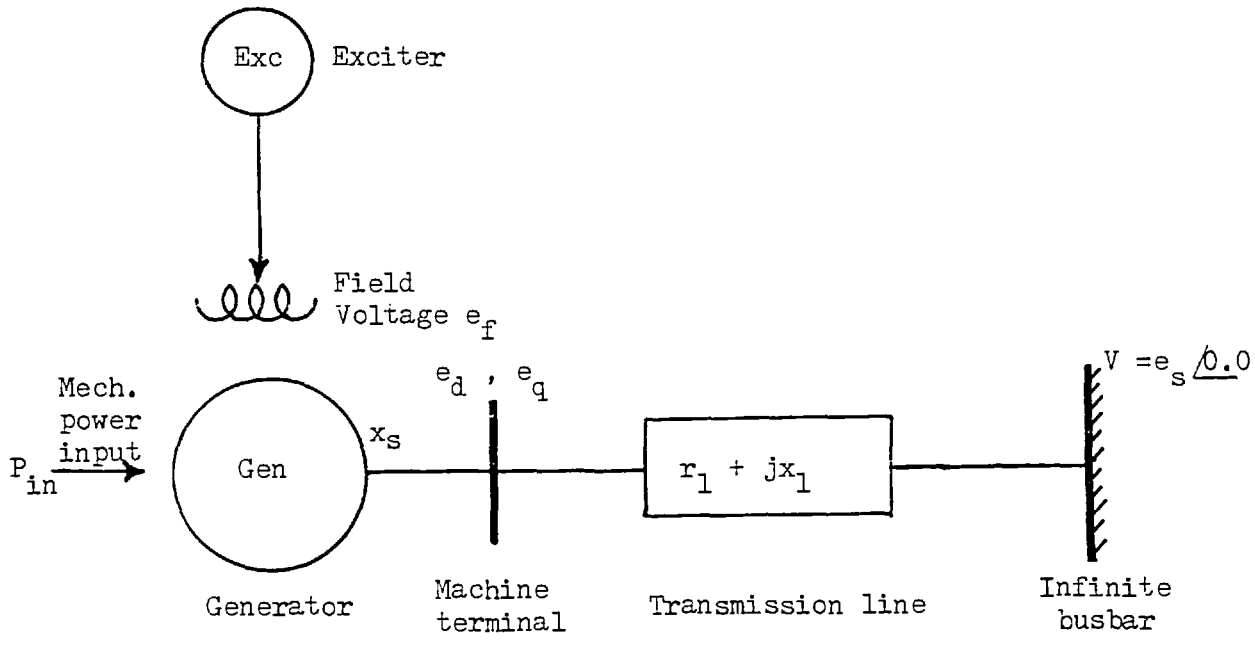

FIGURE B.1: SINGLE-MACHINE INFINITE BUSBAR POWER SYSTEM MODEL

Flux linkage:

$$\lambda_d = -L_s i_d + L_{af} i_{fd} \tag{B5}$$

$$\lambda_q = -L_s i_q + L_{af} i_{fq} \tag{B6}$$

$$\lambda_{fd} = -L_{af} i_d + L_{ff} i_{fd} \tag{B7}$$

$$\lambda_{fq} = -L_{af} i_q + L_{ff} i_{fq} \tag{B8}$$

Output power:

$$P_e = e_d i_d + e_q i_q \tag{B9}$$

Mechanical Motion:

$$M\ddot{\delta} + D\dot{\delta} + P_e = P_{in} \tag{B10}$$

Transmission line:

$$e_d = e_s \sin\delta - x_l i_q \tag{B11}$$

$$e_q = e_s \cos\delta + x_l i_d \tag{B12}$$

From equations (B1) and (B5)

$$e_d = -\omega_o \lambda_q = \omega L_s i_q - \omega L_{af} i_{fq}$$

or:

$$i_{fq} = -\frac{1}{x_{af}} (e_d - x_s i_q) \tag{B13}$$

and

$$\dot{i}_{fq} = -\frac{1}{x_{af}} (\dot{e}_d - x_s \dot{i}_q) \tag{B14}$$

Similarly, equations (B2) and (B6) give

$$i_{fd} = \frac{1}{x_{af}} (e_q + x_s i_d) \tag{B15}$$

$$\dot{i}_{fd} = \frac{1}{x_{af}} (\dot{e}_q + x_s \dot{i}_d) \tag{B16}$$

From equations (B3) and (B7)

$$e_{fd} = -L_{af} \dot{i}_d + L_{ff} \dot{i}_{fd} + r_f i_{fd} \tag{B17}$$

Similarly, equations (B4) and (B8) give

$$e_{fq} = -L_{af}\dot{i}_q + L_{ff}\dot{i}_{fq} + r_f i_{fq} \qquad (B18)$$

Substituting i_{fd} and $\dot{i}_{fd}$ from equations (B15) and (B16) respectively in (B17) yields:

$$e_{fd} = -L_{af}\dot{i}_d + \frac{L_{ff}}{x_{af}}(\dot{e}_q + x_s\dot{i}_d) + \frac{r_f}{x_{af}}(e_q + x_s i_d) \qquad (B19)$$

Similarly

$$e_{fq} = -L_{af}\dot{i}_q - \frac{L_{ff}}{x_{af}}(\dot{e}_d - x_s\dot{i}_q) - \frac{r_f}{x_{af}}(e_d - x_s i_q) \qquad (B20)$$

Therefore:

$$\frac{x_{af}}{L_{ff}} e_{fd} = (x_s - \frac{x^2_{af}}{x_{ff}})\dot{i}_d + \dot{e}_q + \frac{r_f}{L_{ff}}(e_q + x_s i_d) \qquad (B21)$$

$$\frac{x_{af}}{L_{ff}} e_{fq} = -(x_s - \frac{x^2_{af}}{x_{ff}})\dot{i}_q - \dot{e}_d - \frac{r_f}{L_{ff}}(e_d - x_s i_q) \qquad (B22)$$

However the transmission line equations (B11), (B12) give the following equalities

$$i_d = \frac{1}{x_1}(e_q - e_s \cos\delta) \qquad (B23)$$

$$i_q = \frac{-1}{x_1}(e_d - e_s \sin\delta) \qquad (B24)$$

$$\dot{i}_d = \frac{1}{x_1}(\dot{e}_q + e_s\dot{\delta}\sin\delta) \qquad (B25)$$

$$\dot{i}_q = -\frac{1}{x_1}(\dot{e}_d - e_s\dot{\delta}\cos\delta) \qquad (B26)$$

Substitution of (B23) and (B25) in (B21) and (B24) and (B26) (B22) results in:

$$\frac{x_{af}}{L_{ff}} e_{fd} = \frac{x'_d}{x_1}(\dot{e}_q + e_s\dot{\delta}\sin\delta) + \dot{e}_q + \frac{1}{T_{do}}\left[e_q + \frac{x_s}{x_1}(e_q - e_s\cos\delta)\right]$$

and (B27)

$$\frac{x_{af}}{L_{ff}} e_{fq} = -\frac{x'_d}{x_1}(\dot{e}_d - e_s\dot{\delta}\cos\delta) - \dot{e}_d - \frac{1}{T_{do}}\left[e_d + \frac{x_s}{x_1}(e_d - e_s\sin\delta)\right]$$

(B28)

where:

T_{do} = field winding open circuit time constant, $\frac{L_{ff}}{r_f}$

x_d' = direct-axis transient reactance, $x_s - \frac{x_{af}^2}{x_{ff}}$

Grouping like terms together in equations (B27) and (B28) respectively yields:

$$\frac{x_{af}}{L_{ff}} e_{fd} = \left(1 + \frac{x_d'}{x_l} \right) \dot{e}_q + \frac{1 + x_s / x_l}{T_{do}} e_q - \frac{e_s x_s}{T_{do} x_l} \cos\delta + \frac{x_d'}{x_l} e_s \dot{\delta} \sin\delta$$

$$\frac{x_{af}}{L_{ff}} e_{fq} = - \left(1 + \frac{x_d'}{x_l} \right) \dot{e}_d - \frac{1 + x_s / x_l}{T_{do}} e_d + \frac{e_s x_s}{T_{do} x_l} \sin\delta + \frac{x_d'}{x_l} e_s \dot{\delta} \cos\delta$$

which on further simplification give:

$$\dot{e}_d = \frac{1}{1 + x_d' / x_l} \left\{ - \frac{1}{T_{do}} (1 + x_s / x_l) e_d + \frac{x_d'}{x_l} e_s \dot{\delta} \cos\delta + \frac{e_s x_s}{T_{do} x_l} \sin\delta - \frac{x_{af}}{L_{ff}} e_{fq} \right\} \qquad (B.29)$$

$$\dot{e}_q = \frac{1}{1 + x_d' / x_l} \left\{ - \frac{1}{T_{do}} (1 + x_s / x_l) e_q - \frac{x_d'}{x_l} e_s \dot{\delta} \sin\delta + \frac{e_s x_s}{T_{do} x_l} \cos\delta + \frac{x_{af}}{L_{ff}} e_{fd} \right\} \qquad (B.30)$$

or

$$\dot{e}_d = \frac{1}{T_{do} + x_d' / x_l T_{do}} \left\{ - (1 + x_s / x_l) e_d + \frac{x_d'}{x_l} T_{do} e_s \dot{\delta} \cos\delta + \frac{x_s}{x_l} e_s \sin\delta - \frac{x_{af}}{L_{ff}} T_{do} e_{fq} \right\}$$

and

$$\dot{e}_q = \frac{1}{T_{do} + x_d' / x_l T_{do}} \left\{ - (1 + x_s / x_l) e_q - \frac{x_d'}{x_l} T_{do} e_s \dot{\delta} \sin\delta + \frac{x_s}{x_l} e_s \cos\delta + \frac{x_{af}}{L_{ff}} T_{do} e_{fd} \right\}$$

However because $\frac{T_{do}}{x_d} = \frac{T_{do}}{x_s} = \frac{T_{d1}}{x'_d}$

$$\dot{e}_d = \frac{1}{T_{do} + x_s / x_1 T_{d1}} \left\{ - (1 + x_s/x_1)\, e + \frac{x_s}{x_1} T_{d1}\, e_s \dot{\delta} \cos\delta + \frac{x_s}{x_1} e_s \sin\delta - \frac{x_{af}}{r_f} e_{fq} \right\}$$

$$\dot{e}_q + \frac{1}{T_{do} + x_s/x_1 T_{d1}} \left\{ - (1 + x_s / x_1)\, e_q - \frac{x_s}{x_1} T_{d1}\, e_s \dot{\delta} \sin\delta + \frac{x_s}{x_1} e_s \cos\delta + \frac{x_{af}}{r_f} e_{fd} \right\}$$

which may be more generally expressed by:

$$\dot{e}_d = - A_1 e_d + A_2 \dot{\delta} \cos\delta + A_3 \sin\delta - A_4 \qquad \text{(B31)}$$

$$\dot{e}_q = - A_1 e_q - A_2 \dot{\delta} \sin\delta + A_3 \cos\delta + A_5 \qquad \text{(B32)}$$

where:

$$A_1 = (1 + \frac{x_s}{x_1}) / A_o \,, \quad A_o = T_{do} + \frac{x_s}{x_1} T_{d1}$$

$$A_2 = \frac{x_s}{x_1} e_s T_{d1} / A_o \qquad A_3 = \frac{x_s}{x_1} e_s / A_o$$

$$A_4 = B\, e_{fq} / A_o \qquad A_5 = B\, e_{fd} / A_o$$

$$B = \frac{x_{af}}{r_f}$$

$\ddot{\delta}$ may be obtained from equation (B10) as:

$$\ddot{\delta} = \frac{1}{M} \left\{ P_{in} - D\dot{\delta} - P_e \right\} \qquad \text{(B33)}$$

Now $P_e = e_d i_d + e_q i_q$

$$= \frac{e_d}{x_1} (e_q - e_s \cos\delta) - \frac{e_q}{x_1} (e_d - e_s \sin\delta)$$

$$= \frac{e_s e_q}{x_1} \sin\delta - \frac{e_s e_d}{x_1} \cos\delta$$

Thus:

$$\ddot{\delta} = -\frac{D}{M}\dot{\delta} - \frac{e_s}{x_1 M}\left(e_q \sin\delta - e_d \cos\delta \right) + \frac{P_{in}}{M} \qquad \text{(B34)}$$

which may be more generally expressed by:

$$\ddot{\delta} = A_7\dot{\delta} + A_8 \left(e_q \sin\delta - e_d \cos\delta \right) + A_6 \qquad \text{(B35)}$$

with:

$$A_7 = -\frac{D}{M} \qquad A_8 = -\frac{e_s}{x_1 M}$$

$$A_6 = \frac{P_{in}}{M}$$

Equations (B31), (B32) and (B35) define the non-linear machine equations used for the non-linear dynamic estimator of the synchronous machine power system model of chapter six.

REFERENCES

1. TOMAS E. DY LIACCO:
"System security: the computer's role" IEEE Spectrum, Volume 15, No. 6, June 1978, pp 43-50.

2. G.W. STAGG, J.F. DOPAZO, O.A. KLITIN, L.S. VAN SLYCK:
"Techniques for the real-time monitoring of Power System operations" IEEE Transactions on Power Apparatus and Systems, Vol. PAS-89, April 1970, pp 545-555.

3. J.F. DOPAZO, O.A. KLITIN, G.W. STAGG, L.S. VAN SLYCK:
"State calculation of Power Systems from line flow measurements" IEEE Transactions on Power Apparatus and Systems, Vol.PAS-89, September/October 1970, pp 1698-1708.

4. J.F. DOPAZO, O.A. KLITIN, L.S. VAN SLYCK:
"State calculation of Power Systems from line flow measurements, Part II" IEEE Transactions on Power Apparatus and Systems, Vol. PAS-91, January/February 1972, pp 145-151.

5. J.F. DOPAZO, O.A. KLITIN, A.M. SASSON, L.S. VAN SLYCK:
"Real-time load flow for the AEP system" 4th PSCC proceedings, Paper No. 3.3/8, September 1972.

6. J.F. DOPAZO, S.T. EHRMANN, O.A. KLITIN, A.M. SASSON:
"Justification of the AEP real-time load flow project" IEEE Power Engineering Society Winter Meeting, New York, 1973 Paper No.T73 108-8.

7. J.F. DOPAZO, O.A. KLITIN, A.M. SASSON:
"State estimation for Power Systems: Detection and identification of gross measurement errors" Proceedings of the 8th PICA Conference, June 1973.

8. F.C. SCHWEPPE, J. WILDES:
"Power System static state estimation, Part I: exact model" IEEE Transactions on Power Apparatus and Systems, Vol.PAS-89 January 1970 pp 120-125.

9. F.C. SCHWEPPE, D.B. ROM:
"Power System static state estimation, Part II: approximate model" IEEE Transaction on Power Apparatus and Systems, Vol. PAS-89, January 1970 pp 125-130.

10. F.C. SCHWEPPE:
"Power System Static State Estimation, Part III: implementation" IEEE Transactions on Power Apparatus and Systems, Vol. PAS-89, January 1970 pp 130-135.

11. H.M. MERRILL, F.C. SCHWEPPE:
"Bad Data Suppression in Power System Static State Estimation" IEEE Transactions on Power Apparatus and Systems, Vol. PAS-90, November/December 1971, pp 2718-2725.

12. H.M. MERRILL, F.C. SCHWEPPE:
"On-line System Model Error Correction" IEEE Power Engineering Society Winter Meeting, New York, 1973, Paper No. T73 106-2.

13. R.D. MASIELLO, F.C. SCHWEPPE:
"A Tracking Static State Estimator" IEEE Transactions on Power Apparatus and Systems, Vol. PAS-90, May/June 1971, pp 1025-1033.

14. H.P. HORISBERGER, J.C. RICHARD, C. ROSIER:
"Fast Decoupled Static Least-Square Estimator" IEEE Transactions on Power Apparatus and Systems, Vol. PAS-76, January/February 1976, pp 208-215.

15. J.S. HORTON, R.D. MASIELLO:
"On-line Decoupled Observability Processing" IEEE PICA Conference, 1977 pp 420-426.

16. G.H. COUCH:
"Improved Power System State Estimation with Constant Gain Matrices" Proceedings of the IEEE, November 1976 pp 1641-1642.

17. K. UEMURA:
"State Estimation of Large Electric Power Systems by Decomposition Methods" Proceedings of the 5th IFAC World Congress, Paris, France, 1972 Paper No. 7.5.

18. G.H. COUCH, A.C. SULLIVAN, J.A. DEMBECKI:
"Results from a Decoupled State Estimator with Transformer Ratio Estimation for a 5GW Power System in the presence of bad-data" 5th PSCC, 1975 Paper No. 2.3/3.

19. A. GARCIA and P. ABREU:
"Fast Decoupled State Estimation and Bad Data Processing"
IEEE Power Engineering Society Summer Meeting, Los Angeles, CA. July 16-21 1978. Paper No. F78 687-6.

20. C.E. FOSHA Jr. and O.J. ELGERD:
"The Megawatt Frequency Control Problem: a New Approach via Optimal Control Theory" IEEE Trans. Power Apparatus and Systems, Vol. PAS-89, pp 563-578, April 1970.

21. YAO-NAN YU, KHIEN VONGSURIYA, LEONARD N. WEDMAN:
"Application of an Optimal Control Theory to a Power System"
IEEE Transactions on Power Apparatus and Systems, Vol. PAS-89, No. 1, January 1970 pp 55-62.

22. J.H. ANDERSON:
"The Control of a Synchronous Machine using Optimal Control Theory"
Proceedings of IEEE, Vol. 59, No. 1, January 1971 pp 25-35.

23. R.E. KALMAN and R.S. BUCY:
"New results in Linear Filtering and Prediction Theory"
Journal of Basic Engineering, Trans. ASME, Series D, Vol. 83, No. 1, March 1961, pp 96-108.

24. M. ARUMUGAN and M. RAMAMOORTY:
"A Dynamic Observer for a Synchronous Machine" International Journal of Control, Vol. 15, No. 6 1972 pp 1129-1136.

25. H. TAKATA, R. UEDA, T. FUJITA, S. TAKATA:
"An Iterative Sequential Observer for estimating the Transient States of a Power System". IEEE Transactions on Power Apparatus and Systems, Vol. PAS-96, No.2, March/April 1977 pp 673-680.

26. D.M. DETCHMENDY and R. SRIDHAR:
"Sequential Estimation of States and Parameters in Noisy non-linear Dynamical Systems" Journal of Basic Engineering, Transactions ASME, Series D, Vol. 88, No. 2 June 1966, pp 362-368.

27. HARIET H. KAGIWADA:
"System Identification Methods and Applications" (Book)
Addison-Wesley Publishing Company-Inc. 1974.

28. A.P. SAGE, C.C. WHITE III:
"Optimum systems control, 2nd Edition" Prentice Hall Inc.
1977 (Book).

29. FRED C. SCHWEPPE and EDMUND J. HANDSCHIN:
"Static state estimation in Electric Power Systems"
Proceedings of the IEEE, Vol. 62, No. 7, July 1974 pp 972-982.

30. P.H. HALEY and M. ENNS:
"Power system state estimation. Generalisation of the AEP
algorithm with improved bad data suppression" IEEE Power
Engineering Society 1973 Summer Power Meeting, Vancouver.
Paper No. T73 479-3.

31. B. PORETTA and R.S. DHILLON:
"Performance evaluation of state estimation from line flow
measurements on Ontario Hydro power system" IEEE Transactions
on Power Apparatus and Systems, Vol. PAS-92, September/October 1973
pp 1702-1712.

32. K. SRINIVASAN and Y. ROBICHAUD:
"A dynamic estimator for complex bus voltage determination"
IEEE Power Engineering Society 1974 Winter Power Meeting, New York,
Paper No. T74 153-3.

33. K. SRINIVASAN:
"State estimation from line flows and bus injections in the
absence of reference voltage" IEEE Power Engineering Society
1976 Summer Power Meeting, Portland, Paper No. A76 414-3.

34. J.F. DOPAZO, S.T. EHRMANN, O.A. KLITIN, A.M. SASSON, L.S. VAN SLYCK:
"Implementation of the AEP real-time monitoring system" IEEE
transactions on Power Apparatus and Systems, Vol. PAS-95, No.5
September/October 1976 pp 1618-1629.

35. E.J. HANDSCHIN:
"Real-time data processing using state estimation in Electric Power Systems" in Real-time control of Electric Power Systems (Book) Amsterdam, Elsevier, 1972 Chapter 2.

36. B.R. MARTIN:
"Statistics for Physicists" (Book)
Academic Press Inc.(London) Ltd 1971.

37. M.G. KENDALL, A. STUART:
"The advanced theory of statistics: Vol. 2 Inference and Relationship" (Book) 3rd Edition.

38. RALPH DEUTSCH:
"Estimation theory" (Book)
Prentice-Hall, New Jersey, 1965.

39. S.R. SEARLE:
"Linear Models" (Book)
John Wiley & Sons Inc., 1971.

40. N.D. REPPEN, R.J. RINGLEE, B.F. WOLLENBERG, A.J. WOOD, K.A. CLEMENTS:
"Probabilistic Methodologies - A critical review" in Systems Engineering for Power: Status and prospects, Henniker, New Hampshire August 17-22 1975 pp 290-310.

41. A.S. DEBS and A.R. BENSON:
"Security Assessment of Power Systems" in Systems Engineering for power: Status and Prospects, Henniker, New Hampshire August 17-22 1975 pp 144-176.

42. HOMER E. BROWN:
"Solutions of large networks by matrix methods" (Book)
John Wiley and Sons, Inc. New York, London, Sydney, Toronto 1975 Chapters 6 and 7.

43. REGINALD T. TEWARSON:
"Sparse Matrices" (Book)
Academic Press, New York, London 1973.

44. K. ZOLLENKOPF:
"Bi-Factorisation - Basic computational algorithm and programming techniques" in Large sparse sets of linear equations (Book) Editor, J.K. Reid, Academic Press, New York, London, 1971.

45. A. BRAMELLER, R.N. ALLAN, Y.M. HAMAM:
"Sparsity" (Book) Pitman Publishing, 1976.

46. YONATHAN BARD:
"Nonlinear Parameter Estimation" (Book)
Academic Press, New York, London 1974.

47. E. HANDSCHIN, F.C. SCHWEPPE, J. KOHLAS, A. FIECHTER
"Bad-data analysis for Power Systems State Estimation" IEEE Transactions on Power Apparatus and Systems Vol. PAS-94 March/April 1975 pp 329-33.

48. E. HANDSCHIN and C. BONGERS:
"Theoretical and practical considerations in the design of State Estimators for Electric Power Systems" in Computerized operation of Power Systems: Editor S.C. Savulescu, Elsevier, Amsterdam 1976.

49. F. ABOYTES and B.J. CORY:
"Identification of measurement, parameter and configuration errors in Static State Estimation" Proceedings of the 9th PICA Conference, June 1975.

50. G.W. STAGG and E.H. EL-ABIAD:
"Computer methods in Power Systems Analysis" (Book)
McGraw-Hill, New York 1968.

51. L.L. FRERIS and A.M. SASSON:
"Investigation of the load flow problem" Proceedings of the IEE, Vol. 115, No. 10 October 1968.

52. N. NABONA and L.L. FRERIS:
"New programming approach to the Newton-Raphson load flow" IEEE Power Engineering Society Winter Power Meeting, 1973 Paper No. C73 119-5 .

53. S.A. MOLINA:
"Decomposition and measurement optimisation in Electric Power System State Estimation" PhD Thesis, University of London, 1977.

54. B. STOTT and O. ALSAC:
"Fast Decoupled Load Flow" IEEE Power Engineering Society Summer Meeting July 1973 Paper No. T73 463-7.

55. S.C. TRIPATHY, N.D. RAO, A. KUMAR:
"Real-time monitoring of Power Systems using fast decoupled load flow" Proc of IEE, Vol. 124, No.7, July 1977 pp 602-606.

56. B.J. CORY and C.K. GHARBAN:
Discussion of "An on-line topological equivalent of a Power System" by T.E. Dyliacco et. al., in IEEE transactions on Power Apparatus and Systems, Vol. PAS-97, No.5, September/October 1978, pp 1550-1563.

57. F.C. ASCHMONEIT, D. DENZEL, R. GRAF, G. SCHELLSTEDE:
"Development of an optimal state estimator and implementation in a real-time computer system" CIGRE, 1976 25th August to 2nd September Paper No. 32-16.

58. F. ASCHMONEIT:
"Optimal power system static state estimation" 5th PSCC, Vol.1, 1975 Paper No. 2.3/9.

59. J.F. BERMUDEZ:
"Efficient static power system state estimation" PhD Thesis, University of Manchester Institute of Science and Technology, 1977.

60. P. JERVIS and J.N. PREWETT:
"State estimation for the CEGB Power System (Closing Report)" Central Electricity Research Laboratories, August 1977.

61. MICHAEL ATHANS:
"The role and use of the Stochastic Linear-Quadratic-Gaussian problem in control system design", IEEE Trans. (Automatic Control) Vol. AC-16, No.6, December 1971 pp 529-552.

62. R.H. CAVIN, M.C. BUDGE Jr., R. RASMUSSEN:
"An optimal linear systems approach to load frequency control" IEEE Trans. (Power Apparatus and Systems), Vol. PAS-90, No.6, November/December 1971, pp 2472-2482.

63. S.M. MINIESY and E.V. BOHN:
"Two-level control of interconnected power plants" IEEE Power Engineering Society 1971 Summer Meeting Paper No. 71 TP 624-PWR.

64. HUBERT KWAKERNAAK and RAPHAEL SIVAN:
"Linear Optimal Control Systems" (Book)
Wiley-Interscience, Inc. 1972.

65. ARTHUR E. BRYSON Jr., and YU-CHI HO:
"Applied optimal control: Optimisation, Estimation and Control" (Book) Blaisdell Publishing Company, Waltham, Massachusetts/ Toronto, London 1969.

66. M.M. ELMETWALLY and N.D. RAO:
"Decentralized optimal control of multi-area power systems" 1976 IEEE Power Engineering Society Winter Meeting, Paper No.A76 146-1.

67. MILAN CALOVIC:
"Linear regulator design for a load and frequency control" IEEE Trans. Power Apparatus and Systems , Vol-91, No.6, 1972 pp 2271-2285.

68. Y. KURIHARA, S. NARITA, Y. TAMURA:
"Modal control of multi-area power system with hierachical control structure" Paper No. 2.1/2, 5th PSCC, Cambridge, England, September, 1972.

69. J.J. O'DONNELL:
"Asymptotic solution of the matrix Riccati equation of optimal control" Proc. 4th Annual Allerton Conference on Circuits and Systems Theory, 1966 pp 577-586.

70. J.E. POTTER:
"Matrix Quadratic Solution"
J. SIAM, Vol. 14, May 1966 pp 496-501.

71. J.H. WILKINSON et al:
"Handbook for Automatic Computations: Linear Algebra"
Volume II (Book) 1970 pp 212-226 and pp 227-240.

72. NAG 4 Library Subroutine No. F02AAF, Imperial College
Computer Centre Fortran Library documentation.

73. M.K. SUNDARESHAN:
"Generation of Multilevel Control and Estimation Schemes for
Large-Scale Systems: A Perturbation Approach". IEEE Trans.
(Systems, Man and Cybernetics) Vol. SMC-7, No.3, March 1977
pp 144-152.

74. M.K. SUNDARESHAN:
"Decentralized observation in large-scale systems" IEEE Trans.
(Systems, Man and Cybernetics) Vol. SMC-7, No.12 December 1977
pp 863-867.

75. S.M. MINIESY and E.V. BOHN:
"Optimum load frequency continuous control with unknown
deterministic power demand" IEEE Trans. (Power Apparatus
and Systems) Vol. PAS-91, No. 5, 1972 pp 1910-1915.

76. B.J. CORY, C.K. GHARBAN, L. MOGRIDGE:
"Discussion of Paper F78 674-4: Real-time external system
equivalent for on-line contingency analysis: by J.F. Dopazo and
A.M. Sasson" Summer Power Meeting, Los Angeles, July 1978.

77. "Systems Engineering for Power: Status and Prospects"
Henniker, New Hampshire August 17th to 22nd 1975.

78. R. UEDA, H. TAKATA, S. YOSHIMURA, S. TAKATA
"Estimation of transient state of multi-machine power system by
extended linear observer" IEEE Transactions on Power Apparatus and
Systems, Vol. PAS-96, No. 2, March/April 1977 pp 681-687.

79. G. QUAZZA:
"Highlights on technological trends in the on-line optimisation of power system operation" International Conference on: On-line Operation and Optimisation of Transmission and Distribution Systems. 22nd-25th June 1976 IEE Conference Publication No. 140.

80. DANIEL GROUPE:
"Identification of Systems" (Book)
Van Nostrand Reinhold Company 1972 pp 160-168.

81. D.G. SCHULTZ and J.L. MELSA:
"State Functions and Linear Control Systems" (Book)
McGraw-Hill Book Company 1967 pp 197-253.

82. C.W. MERRIAM III:
"Optimisation Theory and the Design of Feedback Control Systems" (Book) McGraw-Hill Book Company 1964 pp 63-86.

83. R.K. MEHRA:
"A comparison of several non-linear filters for re-entry vehicle tracking" IEEE Transactions on Automatic Control, Vol. AC-16, 1971 pp 307-319.

84. H. COX:
"On the estimation of state variables and parameters for noisy dynamic systems" IEEE Transactions on Automatic Control, Vol. AC-9, No. 1, January 1964 pp 5-12.

85. ANTHONY RALSTON:
"A First Course in Numerical Analysis" (Book)
McGraw-Hill Book Company 1965 pp 159-216.

86. A. RALSTON, H.S. WILF:
"Mathematical Methods for Digital Computers, Vol.I" (Book) John Wiley and Sons Inc. 1962 pp 93-132.

87. E.W. KIMBARK:
"Power System Stability, Vol. II" (Book)
New York, John Wiley & Sons Inc., 1956.

88. C.R. RAO:
"Linear Statistical Inference and Its Applications"
(Book) 2nd Edition
John Wiley & Sons Inc., 1973.

89. S.C. SAVULESCU (EDITOR):
"Computerised Operation of Power Systems" (Book)
Elsevier Publishing, Amsterdam 1976.